ASSESSMENT OF GRAY WHALE FEEDING GROUNDS AND SEA FLOOR INTERACTION IN THE NORTHEASTERN BERING SEA

by

Kirk R. Johnson, C. Hans Nelson, and
Heidi-Lynn Mitchell

U.S. Geological Survey

Final Report
Outer Continental Shelf Environmental Assessment Program
Research Unit 634

July 1983

TABLE OF CONTENTS

LIST OF FIGURES

Figure 8. Histogram of Gray whale gape lengths compiled from Rice and Wolman (1971); Dale Rice, NMML, pers. comm., 1982; Steve Leatherwood, Hubbs-Seaworld Research Assoc., Pers. Comm. 1982. In cases in which only head length was known, gape length was computed as 75% of head length.

Figure 9. Water masses in the northeastern Bering Sea. The Alaskan Coastal Water (14-31.5 °/oo, 8° C) occupies the eastern portion of the map area, the Bering Shelf Water (sometimes called Modified Shelf Water, 31.5-33 °/00, 0-4° C) covers the central area, and the Anadyr Water (33 °/oo, 1-3° c) occurs on the western portion of the map area. From Nelson et al., 1981.

Figure 10. Offshore water circulation and maximum bottom current velocities from available measurements in the northeastern Bering and sourthern Chukchi Sea. From Nelson et al., 1981.

Figure 11. (A) Histogram of bottom current speeds from long-term current meter, LD-3A. July-Sept., 1978. (B) Cumulative frequency graph of bottom current speeds from long-term current meter LD-3A. (C) Daily bottom current speeds from long-term current meter, LD-3A. Location of current meter shown in Figure 5.

Figure 12. Preliminary map of the northeastern Bering shelf surficial geology (modified from Nelson, 1982).

Figure 13. Mean grain size (Folk and Ward) for surface sediment in Norton Basin, northeastern Bering Sea.

Figure 14. Percent sand in surface sediment of Norton Basin, northeastern Bering Sea.

Figure 15. Sorting values (Folk and Ward) for surface sediment in Norton Basin, northeastern Bering Sea.

Figure 16. Potentially hazardous areas of the northeastern Bering Sea. Current scour depressions occur in the area of intense current activity off the Yukon Delta. From Thor and Nelson (1981).

Figure 17. 105 kHz sonograph of (A) ice scour from Norton Sound, (B) current scour depressions from the Yukon Delta front, (C) circular gas expulsion craters from Norton. Sound. Arrows show location of features in B and C.

Figure 18. (A) Radiograph of a box core, showing the v-shaped burrows of the amphipod, Ampelisca macrocephala. The core was taken from the fine transgressive sand body in the center of Chirikov Basin at a water depth of 27 m. (B) Plan view photo of the box core top taken immediately after collection. Slit-like, mucus-lined burrows are typical of the amphipod Ampelisca macrocephala.

Figure 19. Distribution of ampeliscid amphipods in the northeastern Bering Sea. Compiled from USGS cruises 1960-1980, Stoker (1978), Nerini (1980), Feder and Jewett (1981), Thomson (1983).

Figure 20. (A) Distribution of gray whale sightings in the northeastern Bering Sea from June - August 1978 (From Consiglieri, Braham, and Jones, 1980). (B) Ship and aerial tracklines completed for whale observations during June - August 1978 (From Consiglieri, Braham, and Jones, 1980).

Figure 21. Sonograph of several long, narrow walrus feeding furrows, 100 kHz, eastern Chirikov Basin (see arrows).

Figure 22. Sonograph of a single walrus feeding furrow; note the large rocks on the record, northern Chirikov Basin (see arrows for furrow).

Figure 23. Sketches of three types of bottom pits, attributed to Gray whale feeding and subsequent current scour, based on observations from side scan sonar and by SCUBA divers in Chirikov basin and the nearshore areas of St. Lawrence Island. All drawings are to the scale shown for Type 1.

Figure 24. Sonograph of area near station Dog 7, 105 kHz, Type 1, close-up of a multiple suction feeding event (see arrow). Sonograph location is shown in Figure 7.

Figure 25. Sonograph of station Dog 8, 105 kHz, Type 1, current-scour enlarged and oriented pits with fresh multiple suction feeding events (see arrow). Sonograph location is shown in Figure 7.

Figure 26. Sonograph of station Dog 1, 105 kHz, Type 1, current-scour enlarged and oriented pits. Sonograph location is shown in Figure 7.

Figure 27. Sonograph of station Dog 14, 105 kHz, Type 1, current-scour enlarged pits. Sonograph location is shown in Figure 7.

Figure 28. Sonograph of station Dog 3, 105 kHz, Type 2, elongate pits pervasive throughout the record. Sonograph location is shown in Figure 7.

Figure 29. Sonograph of station Dog 4, 105 kHz, Type 2, elongate pits pervasive throughout the record. Sonograph location is shown in Figure 7.

Figure 30. Sonograph of station Dog 6, 105 kHz, Type 2, elongate pits pervasive throughout the record. Sonograph location is shown in Figure 7.

Figure 31. Sonograph of station Dog 12, 105 kHz, Type 2, dense fresh and partially modified pits. Sonograph location is shown in Figure 7.

Figure 32. Sonograph of station Dog 13, 105 kHz, Type 2, common elongate pits. Sonograph location is shown in Figure 7.

Figure 33. Sonograph of station Dog 2, 105 kHz, Type 3, scattered oval pits. Note elongate chain of pits in center of sonograph. Sonograph location is shown in Figure 7.

Figure 34. Sonograph of station Dog 5, 105 kHz, Type 3, dense oval pits. Note side-scan distortion which stretches pits that are near the margin of the record. Sonograph location is shown in Figure 7.

Figure 35. Sonograph of station Dog 9, 105 kHz, Type 3, scattered oval pits. Sonograph location is shown in Figure 7.

Figure 36. Sonograph of station Dog 10, 105 kHz, Type 3, dense oval pits. Sonograph location is shown in Figure 7.

Figure 37. Sonograph of station Dog 11, 105 kHz, Type 3, sparse oval pits. Sonograph location is shown in Figure 7.

Figure 38. Sonograph of station Dog 15, 105 kHz, Type 3, sparse oval pits. Sonograph location is shown in Figure 7.

Figure 39. Sonograph of station Dog 16, 105 kHz, Type 3, sparse oval pits. Sonograph location is shown in Figure 7.

Figure 40. Distribution of three types of bottom pits, mapped by side-scan sonar and attributed to gray whale feeding on the seafloor of Chirikov basin, northeastern Bering Sea.

Figure 41. Total percentage of area at each side-scan quantification station disturbed by all fresh and current-enlarged feeding pits.

Figure 42. Percentage of area at each side-scan sonar quantification station disturbed only by fresh feeding pits in the smallest size class (0-5.3 m^2).

Figure 43. Sonograph of station Dog 7, 105 kHz, Type 1, multiple suction feeding events. Sonograph location is shown in Figure 7.

Figure 44. Sonograph of station Tate 1, 10S kHz, Type 1, distinct groups of fresh elongate feeding pits from the Russian River area of the California coast. Upper and lower sets of arrows point out pit groups in right half of sonograph.

LIST OF TABLES

ABSTRACT

A dense ampeliscid amphipod community in Chirikov Basin and around St. Lawrence Island in the northeastern Bering Sea has been outlined by summarizing biological studies, analyzing bioturbation in sediment samples, and examining sea floor photos and videotapes. The amphipod population is associated with a homogeneous, relict fine-grained sand body 0.10-1.5 m thick that was deposited during the marine transgression over the Bering land bridge 8,000-10,000 yr B.P. Modern current and water mass movements and perhaps whale feeding activity prevent modern deposition in this area.

The distribution of the transgressive sand sheet, associated amphipod community and feeding gray whales mapped by aerial survey correlate closely with three types of sea-floor pits observed on high (500 kHz) and low (105 kHz) resolution side-scan sonar; they are attributed to gray whale feeding traces and their subsequent current scour modification. The fresh and modified feeding pits are present in 22,000 km^2 of the basin and they cover a total of 2 - 18% of the sea floor in different areas of the feeding region. The smallest size class of pits approximates whale mouth gape size and is assumed to represent fresh whale feeding pits. Fresh feeding disturbance of the sea floor is estimated to average about 5.7% for a full feeding season. Combined with information that 34% of the measured benthic biomass is amphipod prey species, and calculating the number of gray whale feeding days in the Alaskan waters plus amount consumed per day, it can be estimated that Chirikov Basin supplies a minimum of 5.3% of the gray whale's food resource in the Bering Sea and Arctic Ocean. If 100% of the Chirikov biomass is assumed to be utilized as a whale food source and a maximum of 50% of the fresh feeding features are assumed to be missed because they parallel side-scan beam paths, then a maximum whale food resource of 32 - 42% is possible in northeastern Bering Sea. Because of side-scan techniques and higher biomass estimates, a reasonable minimum estimate of the total whale food resource in northeastern Bering Sea is 10%.

These data show that side-scan sonar is a powerful new technique for analyzing marine mammal benthic feeding grounds. Monographs reveal that the gray whales profoundly disturb the substrate and initiate substantial further erosion by bottom currents, all of which enhances productivity of the prey species and results in a "farming of the sea floor". In turn, because of the high concentration of whale prey species in a prime feeding ground that is vulnerable to the development of petroleum and mining for sand, great care is required in the exploitation of these resources in the Chirikov Basin.

INTRODUCTION

The California Gray Whale (Eschrichtius robustus) is perhaps the most resilient and versatile of the great whales. Twice hunted to near-extinction levels (Gilmore, 1955), the gray whales have rebounded to near pre-exploitation levels. At present, approximately 18,000 gray whales exist in the eastern Pacific Ocean (Herzing and Mate, 1981; NMFS, 1981; Rugh, 1981; NMML, 1980; Reilly, Rice, and Wolman, 1980). An historic stock, the Korean Gray whales which inhabited the western Pacific Ocean are presumed extinct (Rice and Wolman, 1971) or at least highly depressed (Brownell, 1977). Subfossil remains and scanty whaling records verify the existence of an Atlantic stock which is also extinct (Mead and Mitchell, in press).

Each year the gray whales migrate from their winter breeding and calving lagoons in Baja California, Mexico to their summer feeding grounds in the Bering, Chukchi, and Beaufort Seas between Alaska and Siberia. For most of this 6000 km migration, the whales remain within sight of land. This coastal affinity, which at one time nearly spelled their doom by allowing easy access for whalers, now allows them to be thoroughly studied.

Approximately one million square kilometers in the Bering, Chukchi, and Beaufort Seas provide the major foraging grounds for the gray whales (Frost and Lowry, 1981; Votrogov and Bogoslavskaya, 1980; Rice and Wolman, 1971; Pike, 1962; Zenkovich, 1934; Scammon, 1874). Our study covers an important part of their summer feeding grounds, the Chirikov basin in the northeastern Bering Sea (Fig. 1).

The California Gray Whale is the only type of whale that relies predominantly on a benthic food source. Feeding on infaunal organisms, mainl

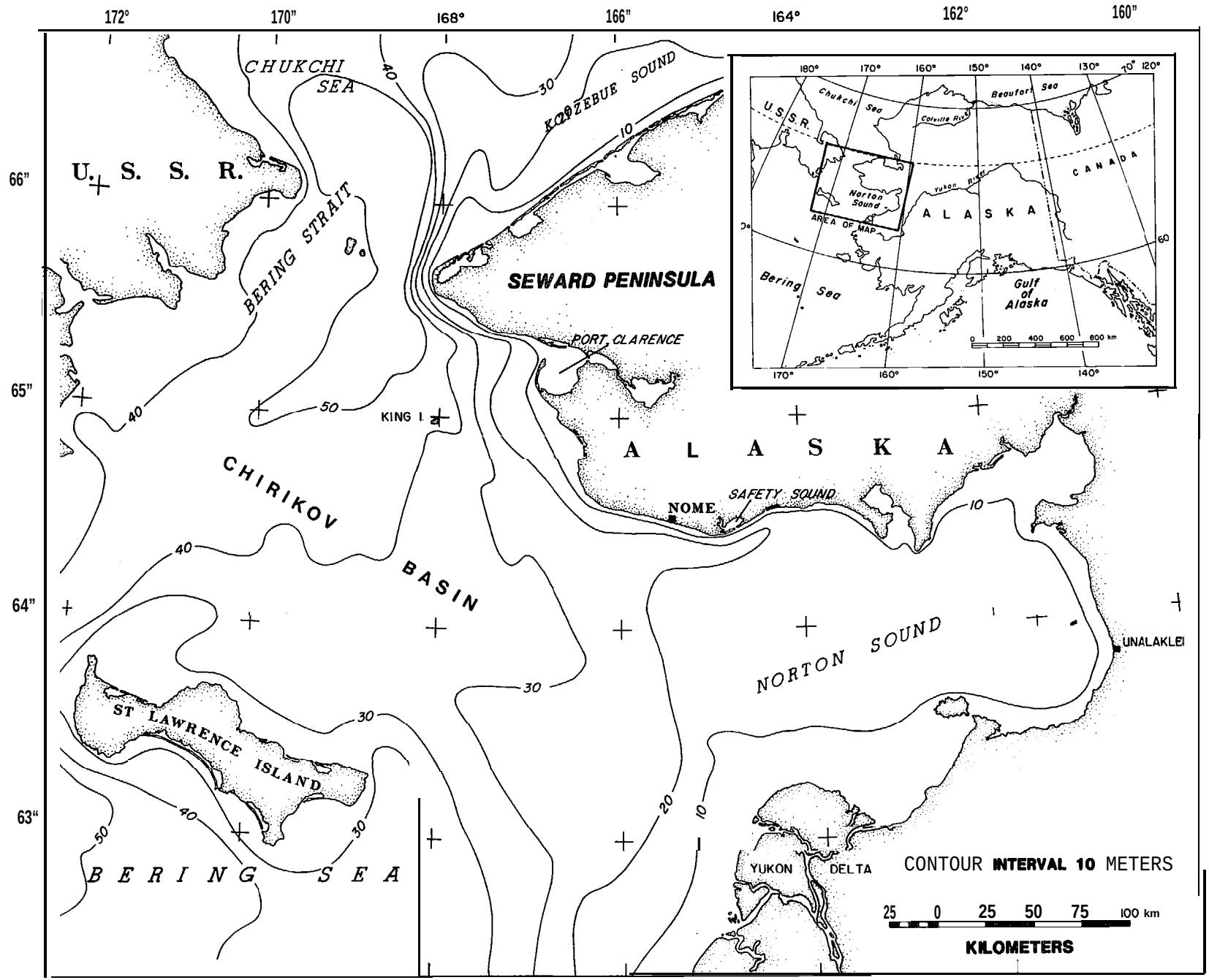

Figure 1 Generalized bathymetry of the northeastern Bering Sea in 10-m contour intervals.

Ampeliscid amphipods, disturbs the sediment surface and leaves a record preserved in the substrate. We use this record to map gray whale feeding grounds and understand the method of gray whale feeding.

To interpret this record we assess all of the main components of the system, including the distribution and feeding ecology of the gray whales, the distribution and ecology of the prey species, their oceanographic setting, the nature and extent of the surficial sediment types that are the habitat of the prey species, and, most importantly, the types and distribution of feeding traces left in the sea floor by foraging gray whales.

Physical processes also produce features on the sea floor such as ice gouges, current scour depressions, and biogenic gas expulsion craters (Larsen et al., 1979; Nelson et al., 1980; Thor and Nelson, 1981). These features have been mapped so they are not confused with whale feeding traces.

Both the physical features and the gray whale feeding traces have been inspected by underwater video, SCUBA divers, and side-scan sonar. The side-scan sonar is a planographic sea-floor mapping device which generates monographs of the sea floor that are analogous to aerial photographs of land areas (Fig. 2). The side-scan sonar allows the size, density, distribution, and modification histories of the whale feeding traces to be approximated. These approximations can then be used to estimate the extent and degree of utilization of the gray whale feeding grounds in Chirikov basin.

Through a more complete knowledge of gray whale feeding and potential hazards in their northern feeding grounds, ecologically sound decisions can be made concerning the exploitation of resources on the Alaskan continental shelf.

SIDE-SCAN SONAR SURVEY TECHNIQUE

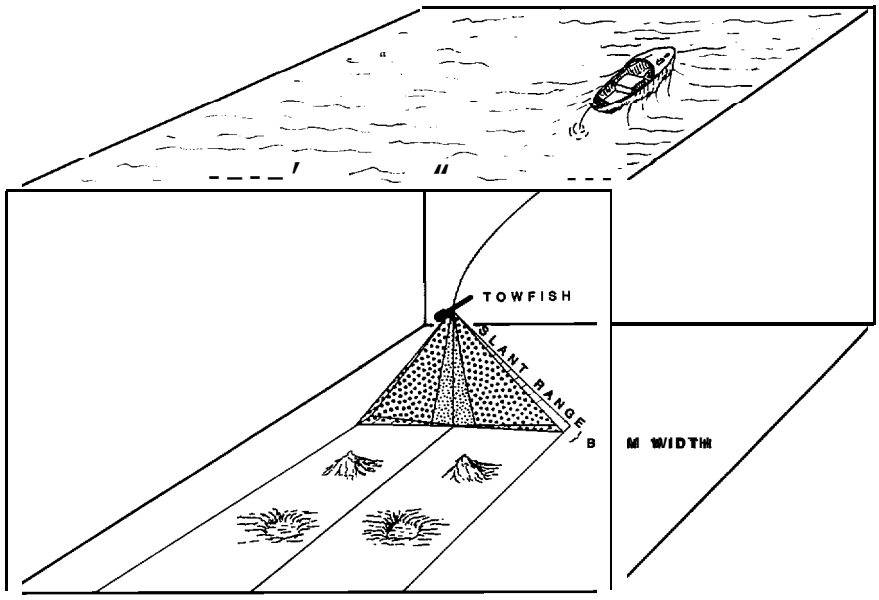

RESULTING MONOGRAPHS

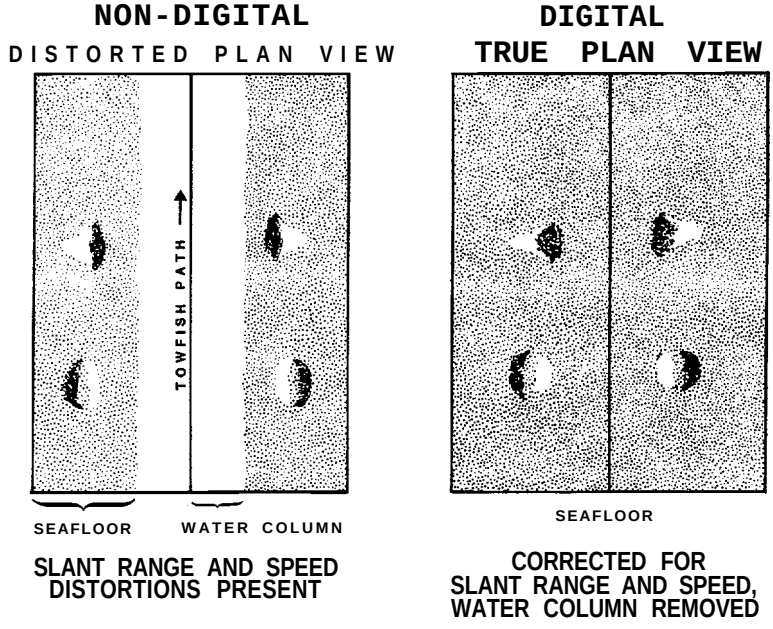

Figure 2 Schematic diagram of side-scan sonar survey technique.

TERMINOLOGY

A new terminology is required to define whale feeding features on the bottom. They may be called feeding features or feeding traces because these names have no implications as to the mechanism of their origin other than that they were caused by feeding. It is erroneous to call them feeding gouges or whale gouges for this implies direct scooping of sea-floor sediment. The term “whale bites” also suggests that the whales scoop up the sediment with their mouths, which is not likely. Also, it is erroneous to call them feeding furrows because this implies that the displaced sediment has been transferred to the side of the pit and not simply removed and dispersed in the water column as is the true case. The term “whale scour” implies some relationship to current or abrasive processes and does not accurately reflect the true process of sea-floor interaction by the whales. The terms “whale depressions”, “bottom depressions”, “sea-floor depressions”, or “feeding depressions” all imply compaction of the sediment instead of its excavation. The word “depression” can be used, however, to describe places where whale flukes or bodies have made contact with the sea floor during the act of feeding.

Since benthic suction is the postulated mode of feeding, “multiple suction feeding events”, “suction events” or "feeding pits" are all acceptable terms. For the description of these pits, the word “elongate” simply implies a length axis much greater than width axis. For specific definitions of shape, “wide elliptic” is used for pits whose L/W ratio is less than 2.3, “elliptic” for pits whose L/W ratio is between 2.3 and 3.0, and “narrow elliptic” for pits whose L/W ratio is greater than 3.0. These terms have been

modified from Hickey (1973) who used them to describe leaf blade shape for dicotyledonous plants.

The large pits caused by scour enlargement of fresh feeding pits are known as "current-scour-enlarged pits", "current-enlarged pits", "scour pits", "current modified features", or "modified whale feeding pits" because their origin is both whale- and current-related.

The combination of fresh whale feeding pits, partially modified whale pits and current-scour-enlarged pits (considerably modified pits) is known as "total bottom disturbance". For the purposes of this paper, other bottom features, such as ice scour are not included in the calculation of total bottom disturbance. "Percent total bottom disturbance" is the percentage of sea floor affected by fresh feeding pits and current-scour-enlarged pits.

METHODS

Substrate

The data utilized in this study can be grouped into two categories. In the first are data derived from direct sampling or observation of the sea floor. These include box cores, grab samples, SCUBA diver observations, underwater still photographs and underwater television (Appendix A-l). The second group is remote sensing data gathered almost entirely by side-scan sonar (Figs. 2, 3).

Substrate parameters such as grain-size distribution and sorting were compiled from bottom samples collected by University of Washington and USGS cruises from 1960-1980 (Hess et al., 1981). Box core radiographs of amphipod bioturbation (Nelson, et al., 1981) combined with observations of

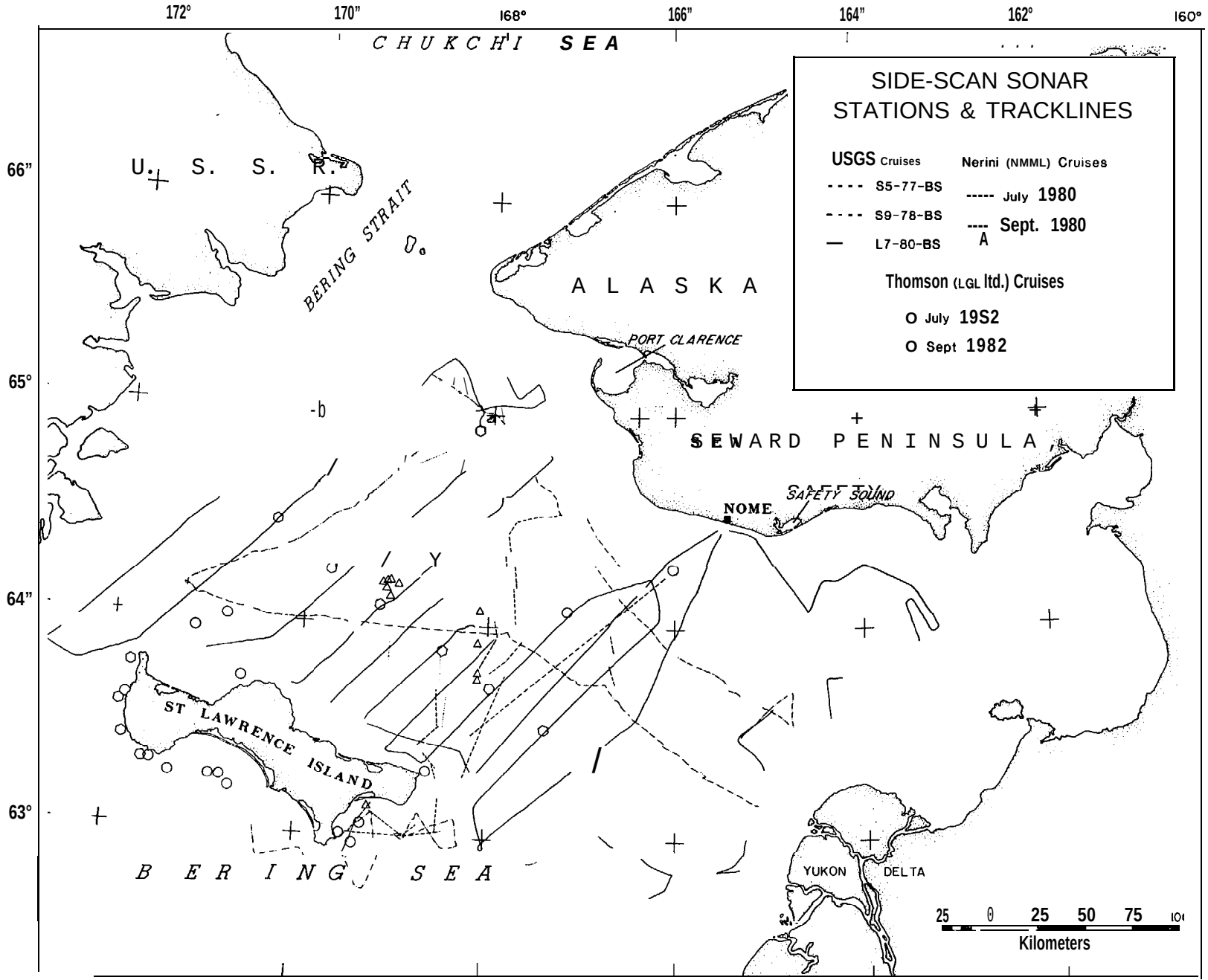

Figure 3 Location of 100, 105, and 500 kHz side-scan sonar tracklines and site survey stations from USGS cruises (S5-77-BS, S9-78-BS, L7-80-BS), NMML cruises (Mary Nerini, 2 cruises, 1980), LGL ltd. cruises (Denis Thomson, 2 cruises, 1982).

amphipods in bottom samples, sea-floor photographs; and underwater television qualitatively established the presence or absence of the amphipod community. Bottom samples with quantitative biological data available from Stoker (1978), Nerini et al. (1980), Feder and Jewett (1981), and Thomson (in press) were integrated with the USGS data base collected from 1968-1980. A total of 221 stations in Chirikov Basin were used in the assessment of the amphipod community, whereas 683 stations in Chirikov Basin and Norton Sound contributed to the substrate data base (Fig. 4) (Hess et al., 1981). Communication with divers from two cruises in 1980 led by Mary Nerini (NMML-NMFS-NOAA) and two cruises in 1982 led by Denis Thomson (L.G.L. Ltd.) provided insight as to the nature of the benthic biota and sea-floor depressions believed to be made by the gray whale.

Bottom current speed data from central Chirikov Basin were compiled from long-term current meters (Fig. 5) (J. Schumacher, NOAA-PMEL pers. comm., 1982; Cacchione and Drake, 1979) and bottom current measurements made during collection of substrate samples (Figs. 4, 5) (Larsen, Nelson, and Thor, 1979). The data were used to verify locations where current speeds are high enough to enlarge bottom features initiated by whale feeding.

Techniques and problems of side-scan analysis

The observation of whale feeding features on the sea floor of Chirikov Basin is best accomplished by SCUBA-diving. Unfortunately, harsh conditions, water depth, poor visibility (< 1 m), and size of the basin make it difficult for SCUBA divers to do extensive surveys. Though divers from the 1980 NMML cruise (Nerini et al., 1980) did dive in the central portion of the basin, most divers have kept to the shallower, inshore waters near St. Lawrence

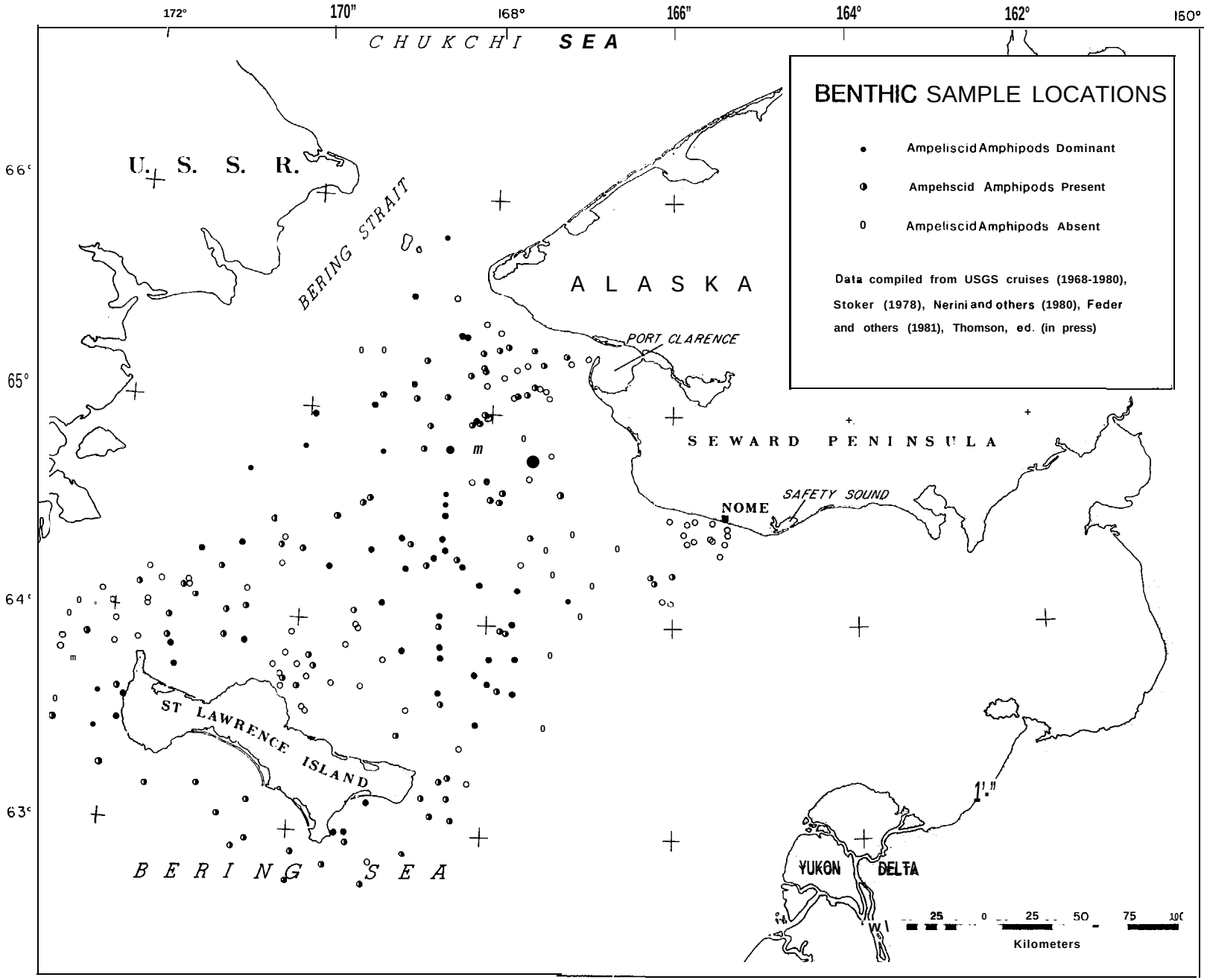

Figure 4 Location of benthic samples used to establish the extent of the Ampeliscid amphipod population in the northeastern Bering Sea.

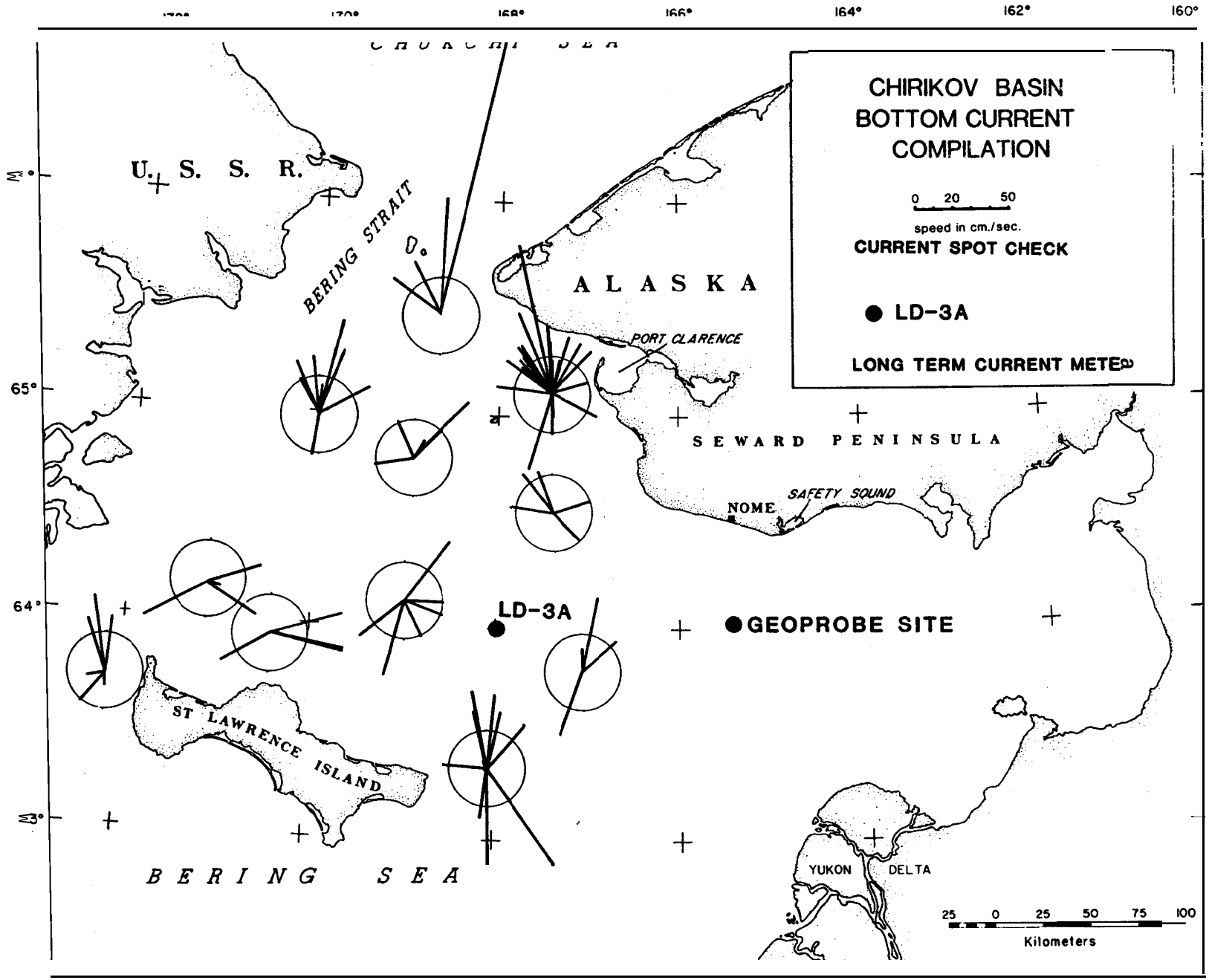

Figure 5 Compilation of spot check bottom current speeds in Chirikov Basin and location of long-term current meter, LD-3A. Each rose diagram has a radius of 20 cm/sec, the approximate current speed needed to initiate movement in a very fine sand. Compiled from USGS cruises, 1960-1980; Fleming and Heggarty, 1961; Husby, 1971; McManus and Smyth, 1970; Nelson and Hopkins, 1972; Nelson, Rowland, Stoker, and Larsen, 1981.

Island and Seward Peninsula (Oliver, Slattery, Silberstein and O'Connor, 1983; Thomson, in press; Nerini et. al., 1980; Nerini and Oliver, in press). It was this need for a regional but accurate bottom surveying device that suggested use of side-scan sonar. This study has placed an emphasis on the regional aspects of the whale feeding while interpreting the side-scan data. Site-specific work on pit morphology and the amount of prey consumed per pit has been undertaken by SCUBA divers who can directly measure and sample the pits (Oliver, Slattery, Silberstein and O'Connor, 1983, and writ. comm., 1983; Thomson, in press; Nerini, 1981; Nerini et al., 1980).

The possibility of side-scan sonar providing data on whale feeding traces was first noticed while Nelson was conducting OCSEAP geohazard surveys throughout Chirikov Basin. The appearance of long, sinuous furrows unlike any known physically created features suggested that marine mammal interaction with the sea floor was indeed discernible by side-scan sonar. Nerini (1980), cooperating with USGS scientists used side-scan sonar successfully on her two cruises studying gray whales. Since then, side-scan sonar has received more attention as a tool for the description and mapping of large-scale biological processes.

Three different degrees of resolution were utilized to obtain side-scan records. The vast majority of coverage was provided by the 105 kHz digital Seafloor Mapper produced by EG & G Environmental Equipment (Fig. 2). Additional 100 kHz non-digital data were gathered using a system manufactured by Klein Associates, Inc. Site-specific side-scans with a high-resolution (500 kHz) non-digital Klein system were undertaken by Nerini (NMML-NMFS-NOAA) on two cruises in 1980 and by Thomson (L.G.L. Ltd.) during two cruises in 1982. On the second Thomson cruise (September 1982), Kirk Johnson was

aboard and involved in all side-scan data collection. Both of these data bases were made available to the USGS. In all, roughly 4500 line-km of side-scan data were collected from the Chirikov Basin and nearshore areas of St. Lawrence Island (Fig. 3).

The side-scan systems were calibrated during the second Thomson cruise, (Sept. 1982) on the NOAA R/V Discoverer by towing the high-resolution 500 kHz system simultaneously with the low-resolution 100 kHz system. The systems were towed off opposite sides of the ship's fantail so that their inner channels overlapped. In this way the same bottom features were obtained on each record and could be compared. A further calibration was performed by towing the 500 kHz side-scan system behind a small boat and past a buoy which marked areas previously inspected by SCUBA divers. Thus, direct diver observations could be compared with the records to establish their accuracy. The 500 kHz system also was used to scout potential dive sites. In this manner, the 100 and 105 kHz systems were linked with actual bottom observations. This is an important calibration because the majority of the continuous line side scan was collected with a 1 05 kHz system. A more thorough treatment of these side-scan operations can be found in Thomson (in press) .

Side-scan sonar is a sonar device which produces a plan view of the sea floor by sending out a set of radiating sound beams which are gated to specify a certain lateral slant range (Fig. 2). The beams are sent out from a transducer known as the tow fish which is towed behind a ship. As the sound bounces off the sea floor it is picked up by the tow fish and transmitted up the tow cable to the recorder/printer aboard ship. A strong return signal caused by a strong reflector such as a rock or abrupt wall will be printed

dark. A weak return from a weak reflector such as fine-grained sediment or an acoustic shadow behind a strong reflector will print light. Thus, a boulder on the sea floor would print with a dark return (from the direct reflection of the boulder) adjacent to a light patch (the acoustic shadow of the boulder), the dark return being nearer the center of the record (and the tow-fish trace) than the light patches. Conversely, a hole in the sea floor would print as a light patch (the acoustic shadow of the lip of the hole) nearer the center of the record and a dark patch (the strong reflection of the far wall of the hole) adjacent to it. The whale feeding traces show up as pits of varying sizes in the sea floor.

It is important to review the limitations of side-scan. The description of features from the side-scan record remains subjective and sensitive to weather and instrument conditions at the time of data collection. In addition to recording the surface of the sea floor, the side-scan system measures tow-fish height above the sea floor, tow-fish depth below the sea surface, as well as the sometimes erratic motion of the tow fish itself. In rough weather, the ship motion from swells is transmitted down the cable as a series of jerks and slacks and results in uneven accelerations of the tow fish. This distortion bends otherwise straight features into S-shaped folds (Fig. 6). Because of these factors, all measurements of whale-related features in this report were made from records taken during calm seas to minimize distortions. Distorted records are still valid for the qualitative mapping of general feature type and density.

The lateral resolution of the side-scan system is generally considered to be l/400 of the lateral slant range (Klein Associates, Inc., 1982, EG & G Environmental Equipment, Inc.). Thus, with a slant range of 100 m, a feature

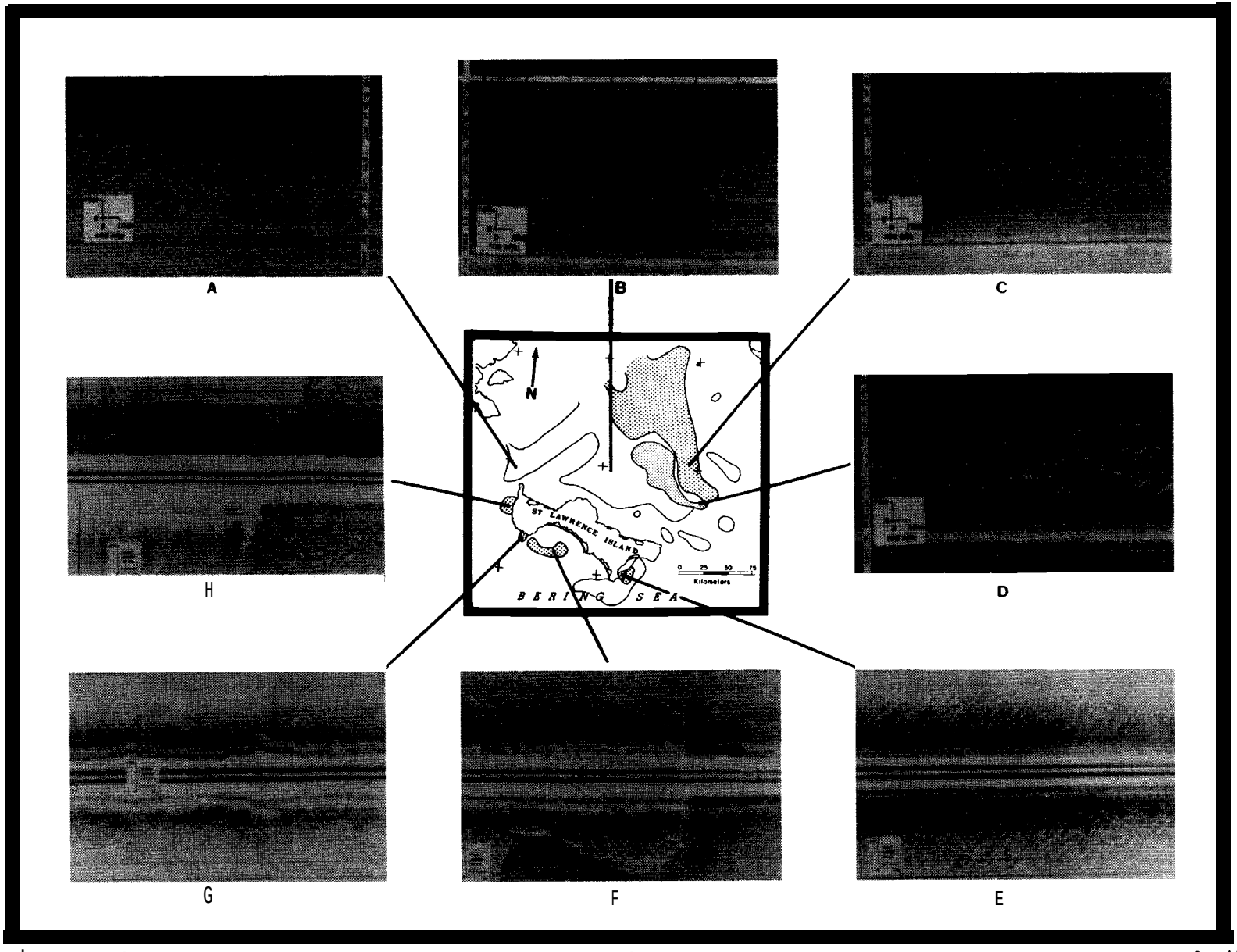

Figure 6 Locations and photographs of side-scan sonographs showing the three bottom pit types attributed to gray whale feeding and subsequent current scour. (A) 105 kHz, type 3, dense, wide elliptic pits (B) 105 kHz, type 3, sparse, wide elliptic pits (C) 105 kHz, type 2, dense, elongate (narrow elliptic) pits (D) 105 kHz, type 1, current enlarged pits showing regional lineation (E) 500 kHz, type 1, current enlarged pits showing regional lineation (F) 500 kHz, type 2, elongate (narrow elliptic) pits in inner shelf, fine-grained, transgressive sand adjacent to and overlying coarse basal transgressive sand which has been worked into sand waves. Note the sinuous distortion of sand waves and elongate pits due to wave swell effect on the side-scan sonar tow fish. (G) 500 kHz, type 1, current enlarged pits (H) 500 kHz, type 2, elongate (narrow elliptic) pits (left half of monograph), fuzzy pit margin and lack of relief shadows indicate infilling by finer-grained sediment. Rock outcrop occupies the right half of the sonograph.

of 25 cm on an axis normal to the trackline can be discerned. The measurement of an object parallel to the trackline is subject to some distortion due to the width of the outgoing beam. On a high-resolution 500 kHz system operating at a lateral range of 37.5 m this beam error is approximately ± 10 cm. On a lower resolution 100 or 105 kHz system with a 100 m range, this error may grow to be substantial and though the system can discern objects to 0.5 m diameter which lie parallel to the trackline, these objects will probably be printed larger than they actually are. This applies mainly to features less than 1.7 m long (Jim Glynn, Klein Assoc., Inc. ,Salem, N.H., pers. comm. , 1982).

A result of these factors is the over-representation of features in the 1.5-2 m range. Thus, for all measurements made in the quantitative portion of this report, features less than 2.0 m in length have significant error bars and their primary value is obtained when they are used relative to one other and not on an absolute scale. Bean width error also may stretch some of the larger features but as the feature size increases and the range of error stays the same, the percent error decreases. Consequently, for features less than 5 m in length there may be noticeable error. Again the relative measurements are of more value than the absolute ones.

Another limitation of side-scan sonar is that it misses some of the objects whose strong reflecting portions are not parallel to the trackline. Thus, certain features such as furrows might not show up on the record if the beam was shot down the length of the furrow and not off one of the walls parallel to the tow path (Fig. 2). On the side-scan records, long narrow furrows and small (less than 5 m long) features show a marked trend of being oriented parallel or subparallel to the trackline. This parallel orientation is due to the stretching of small features by the beam width error and the

over-representation of trackline parallel features. The result is an under-representation of features that are not parallel to the trackline. This causes estimates of apparent feature density which are smaller than the true density values. Up to 50% of the smaller features may be missed by this form of side-scan inaccuracy.

Though depth or height of features can be calculated from side-scan records (Flemming, 1976), the degree of accuracy in this calculation is too low to obtain depths on such shallow features as the whale feeding traces. Depths of feeding pits, when mentioned, are from SCUBA diver operations.

Discussion thus far has centered on the digitized side-scan systems from which all quantitative data were gathered. In a digital system, corrections are automatically made for the slant range distortion (relative to the tow-fish height above sea floor) and the trackline distortion (printer paper feed speed vs. ship speed). In a non-digital system, these corrections must be made by hand from the records. For consistency and convenience, all measurements used for quantitative purposes were taken from the 105 kHz digital system. Data from the non-digitized 100 kHz and 500 kHz systems were used for qualitative mapping and comparison with diver observations, and calibrations of larger scale features with those of the 105 kHz digital records.

Measurements and statistical techniques

The bottom features have been quantified from the EG & G 105 kHz digital monographs in the following manner: 16 widely scattered areas of bottom features were selected in which the records were collected in calm seas and are of high quality (Fig. 7, Table 1). In each area a minimum of 50, but.

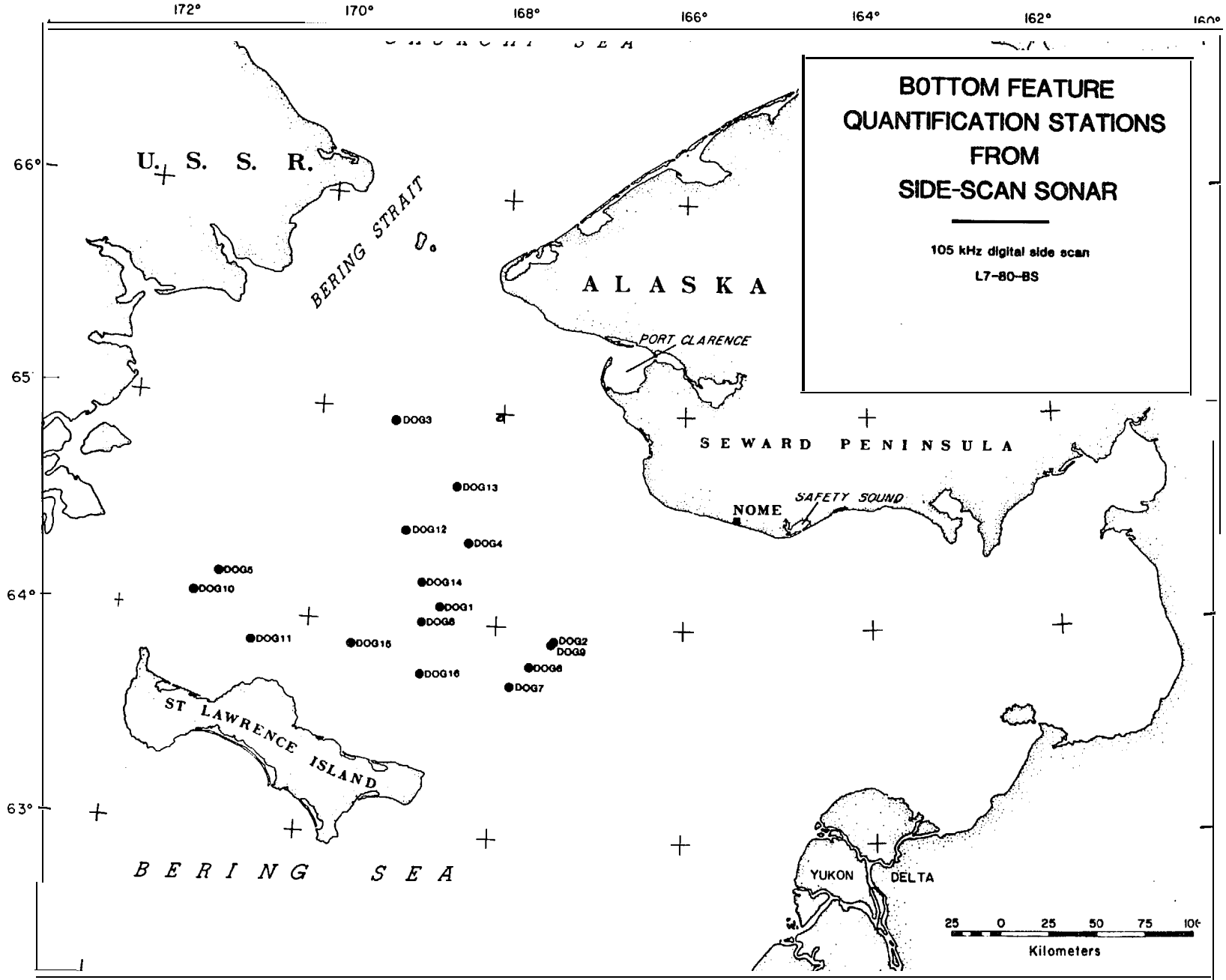

Figure 7 Location of bottom feature quantification stations from 105 kHz digital side-scan sonographs collected by USGS cruise. L7-80-BS

TABLE 1

LOCATION OF 105 kHz DIGITAL SIDE-SCAN QUANTIFICATION STATIONS

STATION	ROLL	DAY	TIME	LINE	BEARING IN DEGREES
DOG 1	42	JD238	00:30:06	55	45
DOG 2	18	223	08:50:00	35	- -
DOG 3	26	229	01:15:00	49	229
DOG 4	34	233	10:35:00	49	228
DOG 5	28	229	14:26:17	47	236
DOG 6	19	223	11:21:00	35	240
DOG 7	19	223	12:35:40	35	233
DOG 8	41	237	22:54:39	55	40
DOG 9	18	223	09:04:52	35	240
DOG 10	29	229	15:50:14	47	229
DOG 11	38	234	21:42:00	51	50
DOG 12	39	235	04:56:55	51	48
DOG 13	40	235	08:01:32	51	47
DOG 14	40	233	18:30:35	49	232
DOG 15	36	234	03:18:52	49	228
DOG 16	43	238	11:38:00	58	233
TATE 1	01-B2-NC	Russian River sector			

All DOG stations are from USGS cruise L7-80-BS.
TATE 1 station is from S1-82-NC Cacchione N. California code 1 geology cruise.

usually 64 or more, features were measured. The measured parameters are length, width, density (of pits per 1875 m^2), and in some cases, orientation. From these numbers, area (area = length x width x 2/3) and length/width ratios were calculated. All parameters were plotted on frequency histograms (Appendix A). Maximum, minimum, mean, standard deviation, and median were calculated for each of the numbers except orientation and density (Table 2). Percent total disturbance was determined by multiplying average pit area (m^2) at a given station by pit density (number of pits per 1875 m^2, a 25 m x 75 m block) then dividing by 1875 and multiplying by 100% (Table 2).

The pits were broken into four size classes by area, 0-5.30 m^2, 5.31 m^2-10.00 m^2, 10.01 m^2-16.00 m^2, and those greater than 16.01 m^2. The reason for using these particular subdivisions in class size was to separate groups of pits which have a greater likelihood of being fresh whale feeding pits from those that show some modification. The assumption was that pits less than 4 m long and 2 m wide are more likely to be freshly made by whales. Given the size of whale gapes (Fig. 8), and what is known about whale feeding, this is valid. Thus, 5.3 m^2 is the area of a 4 m x 2 m feature (area = l x w x 2/3), 10 m^2 is the area of a 6 m x 2.5 m feature, and 16 m^2 is the area of an 8 m x 3 m feature.

This method of statistical analysis doesn't account for pit morphology, only pit area. The pits in the small size class are considered to be fresh whale feeding pits by size and shape criteria alone. The two intermediate size classes are considered to be intermediate stages between fresh and current-enlarged. These intermediate classes probably contain the largest fresh features as well as a whole range of modified features. The largest size class, containing features qreater than 16 m^2 are most surely current-

TABLE 2

RESULTS OF BOTTOM FEATURE QUANTIFICATION FROM 105 kHz DIGITAL SIDE-SCAN SONAR

STATION	DOG 1	DOG 2	DOG 3	DOG 4	DOG 5	DOG 6	DOG 7	DOG 8	DOG 9	DOG 10	DOG 11	DOG 12	DOG 13	DOG 14	DOG 15	DOG 16	TATE 1
TYPE	1	3	2	2	3	2	1	1	3	3	2	2	1	1	3	3	1
n =	64	50	68	64	68	66	64	68	64	64	64	63	67	64	65	121	
LENGTH																	
mean	6.1	3.1	4.7	5.1	2.4	3.9	2.8	5*9	2.7	2.6	1.6	3.1	3.9	3.4	2.3,	1.8	4.6
med.	6.0	3.0	4.3	5*0	2.0	3.0	2.5	4*0	3.0	2.2	1 0 4	2.3	3.0	2.5	2.0	1.8	4.
st.dev.	4.0	0.94	2.3	3.0	1.2	2.1	1.48	4.6	0.8	1.5	0.68	2.0	3.4	2.4	0.95	0.67	1.7
tnax.	20.0	6.0	14.0	15.0	8.0	11.0	7*5	19.0	5.0	9.6	3.8	10.0	20.0	13,.5	6.5	3.4	10.0
min.	2.0	2.0	2.0	2.0	1*0	0.75	1.0	1.0	1.0	0.6	0*75	0.8	1.0	0.8	1.0	0.5	2.0
WIDTH																	
mea n	2.6	2*0	1.7	1.6	1.1	1.1	1.0	2.4	1*5	1.3	0.92	1.0	1.2	1.4	1,.2	1*0	1.8
med.	3.0	2.0	1.8	1.5	1*0	1.0	1.0	1.5	1.5	1.3	1.0	1*0	1.0	1:.0	1.*0	1.0	2.0
st.dev.	1.4	0.6	0.56	0.59	0.31	0.27	0.28	1.9	0.6	0.48	0.27	0.44	0.63	0.97	0.32	0.32	0.49
max.	5*0	4.0	4.0	3.0	2.0	2*0	2*0	10.0	4.0	2.5	2.0	2.5	3.5	4.5	2.1	2.0	3.5
min.	1.0	1.0	1.0	1.0	0.5	0.5	0*5	0.5	0.8	0.4.	0.4	0.4	0.5	0,.5	0.8	0.5	1.0
AREA (Length x width x 2/3)																	
mea n	13.0	4.4	5.4	6.0	1.8	3*0	2*0	14.0	2.9	2 .*5	1.0	2.4	3.7	4.0	1.8	1.3	5.8
med.	13.0	4.0	4.3	4.0	1.5	2.7	1.7	5.3	2.3	2.1	0.78	1.4	2.0	2.0	1*5	1.2	5.3
st.dev.	12.0	2.5	3.4	5*1	1*4	2.1	1.5	220.0	2*0	1.8	0.6	2.6	5.3	4.6	0.8	0.75	3.2
max.	53.0	12.0	19.0	26.0	11.0	9.3	10.0	113.0	13.0	8.3	2.8	12000	35.0	18.0	4.3	4.3	20.0
min.	1.3	1.3	1.3	1.3	0.33	0.38	0.5	0.33	0.66	0.16	0.24	0.27	0.33	0.27	0.67	0.17	1.33
L/W ratio																	
mean	2.3	1.6	3.1	3.2	2.3	3*5	2.8	2.7	1*9	200	1.8	3.2	3.5	2.6	2*0	1.9	2.7
med.	2*0	1.5	2.5	2.8	2.0	3.0	2.5	2.3	2..0	, 2.7	1.5	2.8	2*5	2.3.	2.8	1.7	2.8
st.dev.	0.95	0.49	1.7	1.6	1.1	1.8	1*4	1.6	0.67	0.96	0.91	1*5	3.2	1*4	1.0	0.72	1.1
Class.	E"	WE	NE	NE	E	NE	E	E	WE	WE	NE	NE	E	WE	WE	E	E
Dens.	26	22	52	44	134	35	37	18	19	97	40	,60	39	56	25	34	
%distur	18	5	15	14	13	5	4	14	3	13	2	8	8	12	2	2	

Med. = Median
Min. = Minimum
Max. = Maximum
St.dev. = Standard Deviation
class. = Classification (Hickey, 1973)
E = Elliptical
WE= Wide Elliptical
NE = Narrow Elliptical

Dens.= Density of features per 1875 m^2

% distur = Percent of total bottom disturbance

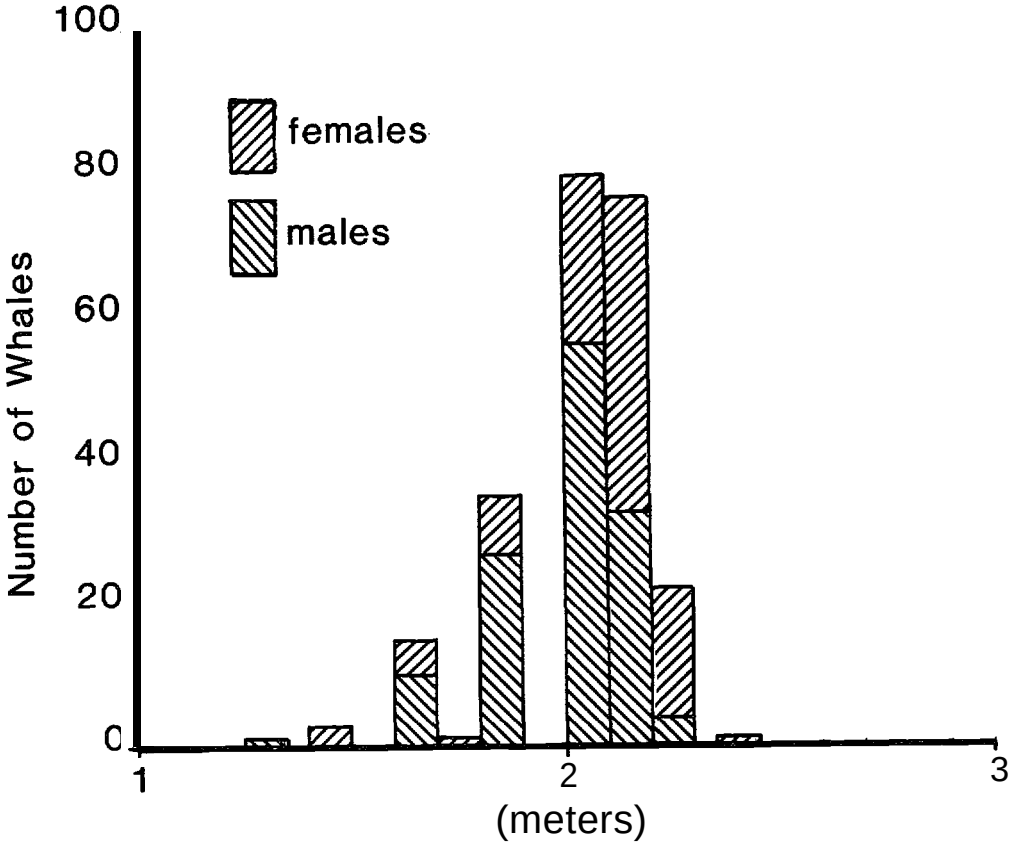

Gray Whale Gape Lengths

Compiled from Rice and Wolman, 1971,
Steve *Leatherwood, oral commun., 1982,*
Dale Rice, oral commun., 1982.

Figure 8 Histogram of Gray whale gape lengths compiled from Rice and Wolman (1971); Dale Rice, NMML, pers. comm. , 1982; Steve Leatherwood, Hubbs-Seaworld Research Assoc., pers. comm., 1982. In cases in which only head length was known, gape length was computed as 75% of head length.

scour-enlarged. This theory is reinforced by the fact that large features on the records often show a regional trend. Typically, as a feature increases in length, its width will also increase.

For each station, the relative percentage of area of the pit size class was calculated (Table 3). The relative percentages for each size were then multiplied by the percent total disturbance at each station to obtain the actual percent disturbance for each of the four size classes.

The drawbacks of quantifying the features from the side scan records need to be discussed. The nature of the pit margins and the line density on the side-scan records cause a fuzziness which makes the accurate measurement of feature size difficult. This fuzziness causes a margin of error of ±.25 m. As noted before, 105 kHz side-scan sonar has substantial accuracy problems in mapping features less than 1.7 m long and noticeable error in the measurement of features up to 5 m in length due to the beam width error. This error, coupled with the under-representation of small features that are not parallel or sub-parallel to the trackline, causes estimates of density and percent disturbance to be anomalously low. Thus, percentages for bottom disturbance, especially for the smaller pit size classes, should be considered minimum values.

OCEANOGRAPHIC SETTING

Water masses

Three water masses have been defined on the northeastern Bering shelf: the Alaskan Coastal Water, the Bering Shelf Water and the Anadyr Water (Coachman et al., 1976) (Fig. 3). The Alaskan Coastal Water is formed largely by river runoff from the area near Bristol Bay and the Yukon River and

TABLE 3

PERCENT OF BOTTOM DISTURBANCE

	CLASS				
	O-5.3 m^2	5.31-10 m^2	10.01-16 m^2	16.01 m^2	TOTAL DISTURBANCE
STATION					(sum of all classes)
DOG 1	0.94 %	0.81 %	2.56 %	12.78 %	18 %
DOG 2	2.4	1.77	0.54	0.0	5
DOG 3	4.92	6.72	2.58	0.76	15
DOG 4	3.98	4.2	2.67	3.05	14
DOG 5	11.86	0.0	1.14	0.0	13
DOG 6	3.4	1.5	0.0	0.0	5
DOG 7	3.52	0*17	0.3	0.0	4
DOG8	0.96	1.16	0.74	11.14	14
DOG 9	2.2	0.57	0.22	0.0	3
DOG 10	10.24	2.75	O*O	0,0	13
DOG 11	2.0	0.0	0.0	O*O	2
DOG 12	4.42	2.44	0.6	0.52	8
DOG 13	3.55	1.11	1.12	2*2	B
DOG 14	4*45	3.35	2.55	2.28	12
DOG 15	2	0.0	0.0	0.0	2
DOG 16	2	0.0	0.0	0.0	2

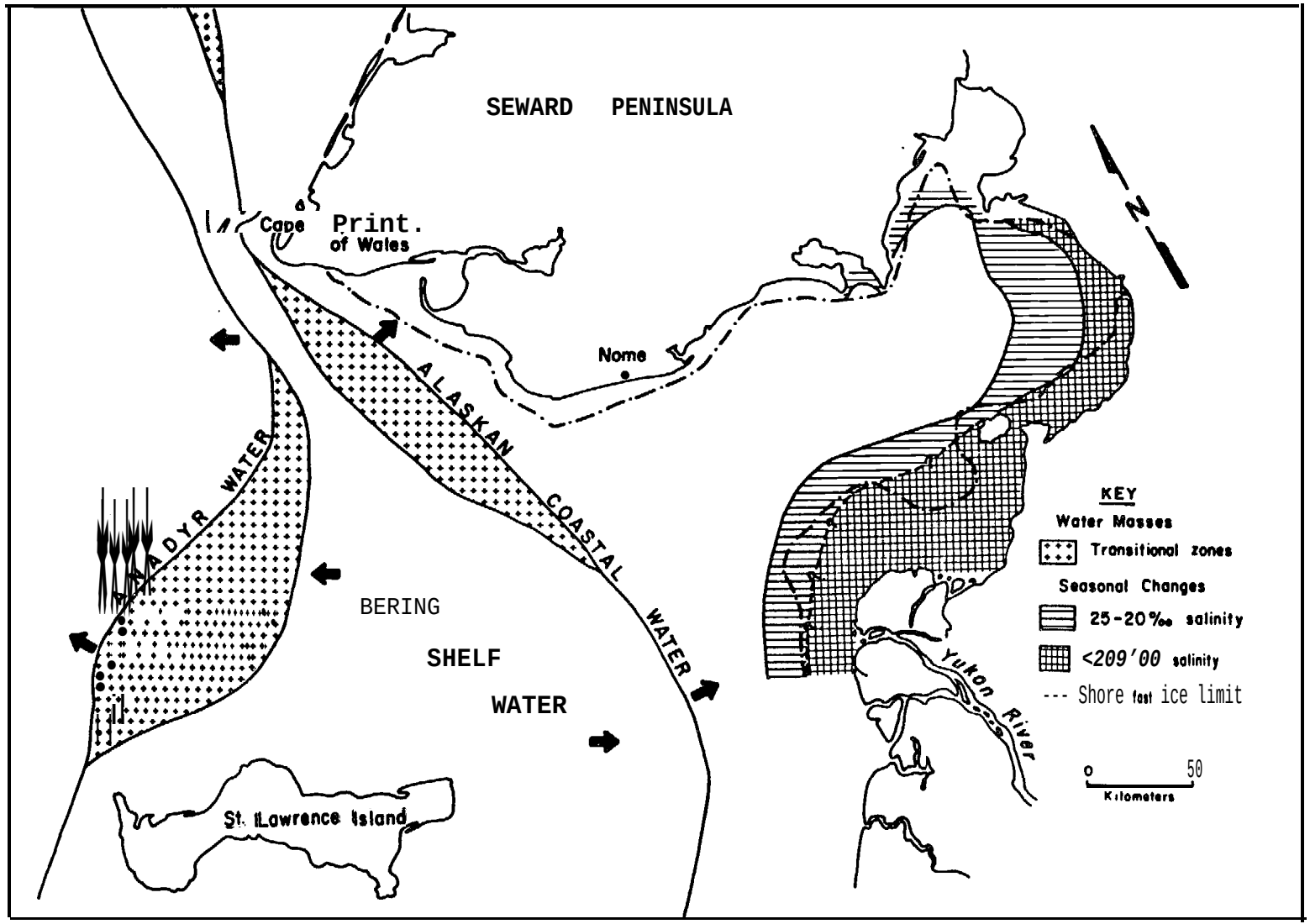

Figure 9 Water masses in the northeastern Bering Sea. The Alaskan Coastal Water (14-31.5 0/00, 8° C) occupies the eastern portion of the map area, the Bering Shelf Water (sometimes called Modified Shelf Water, 31.5-33 o/oo, 0-4° C) covers the central area, and the Anadyr Water (33 o/oo, 1-3° C) occurs on the western portion of the map area. From Nelson et al., 1981.

moves along that coast: it fills Norton Sound and hugs the coast in a narrow band from Nome through the Bering Strait along the northern edge of Chirikov Basin. The Bering Shelf Water originates in the northeastern Bering Sea during winter ice formation and abuts the Alaskan Coastal Water in its net northward flow; it covers most of the central Chirikov Basin area. The Anadyr Water flows through the Anadyr Strait towards the Chukchi Sea.

The Alaskan Coastal Water is the warmest and the least saline of the three water masses (Coachman et al., 1976). It shows marked seasonal variations in salinity, particularly in Norton Sound where fluctuations in discharge from the Yukon River influence salinity. Temperature isgreater than 8° C and salinity ranges from 20 to 30 °/oo. The Bering Shelf water forms quite a sharp boundary with the Alaskan Coastal Water because is much colder, and more saline, ranging from 0° - 4° C and from 31.5 to 33 °/oo.

Currents

The net northward flow of the entire water column has a direct effect on the Alaskan Coastal Water where westward-extending promontories deflect the flow (Fleming and Heggarty, 1966) (Figs. 9, 10). The less dense coastal water is piled up against the shore as a thickened section, and strong currents are produced to move the water. These currents reach a maximum of 180 cm/sec at a depth of 55 m in the most restricted region, the Bering Strait (Fleming and Heggarty, 1966): in the Chirikov Basin, velocities are as low as 5-15 cm/sec (Fleming and Heggarty, 1966; Husby and Hufford, 1971; and McManus et al., 1977). The current regime of central Chirikov Basin is not nearly as strong as at its margins near Bering, Anadyr, and Shpanberg straits: spot meter measurements in the Chirikov Basin are over 20 cm/sec. (Fig. 5). In the

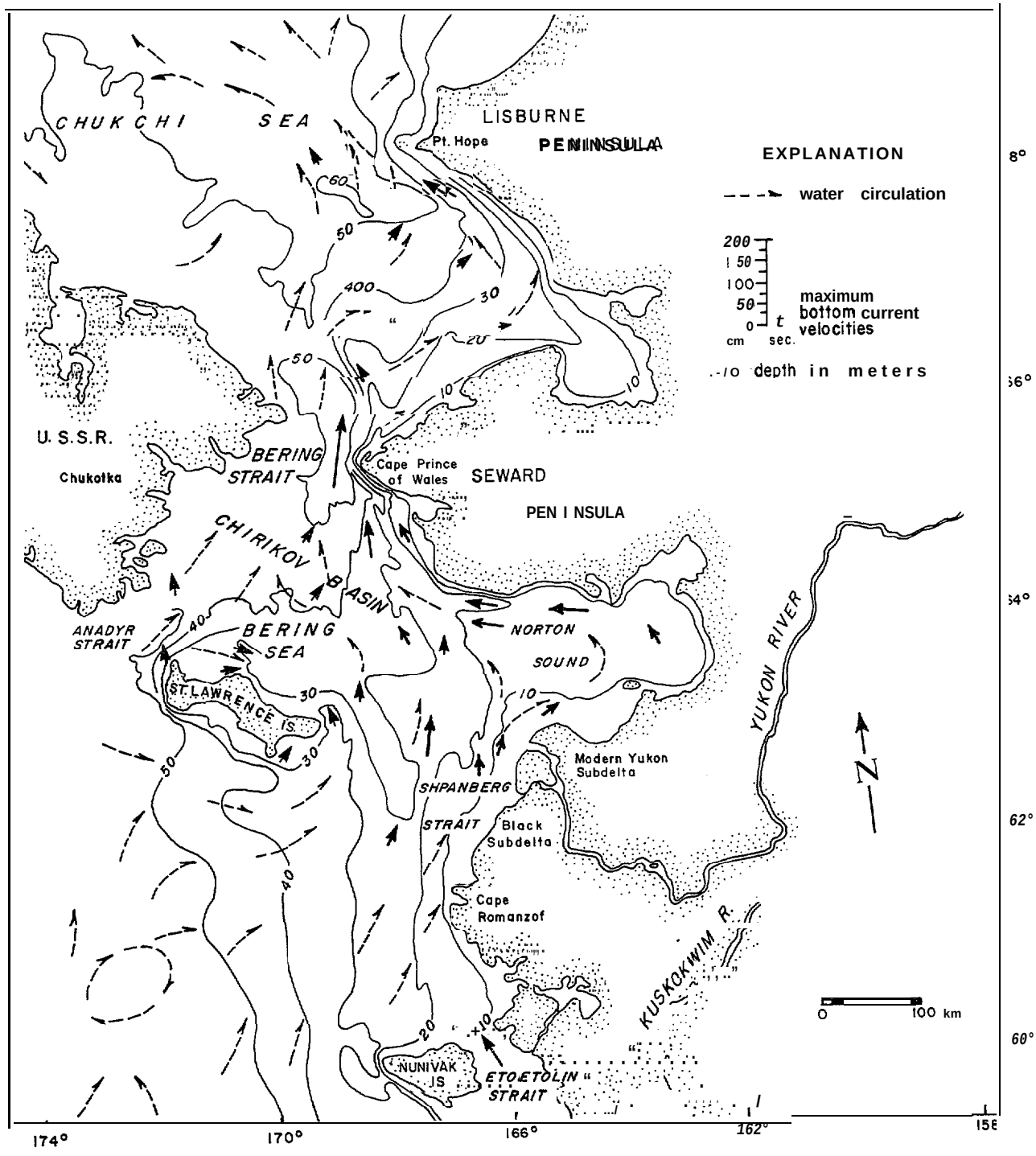

Figure 10 Offshore water circulation and maximum bottom current velocities from available measurements in the northeastern Bering and southerr Chukchi Sea. From Nelson et al., 1981.

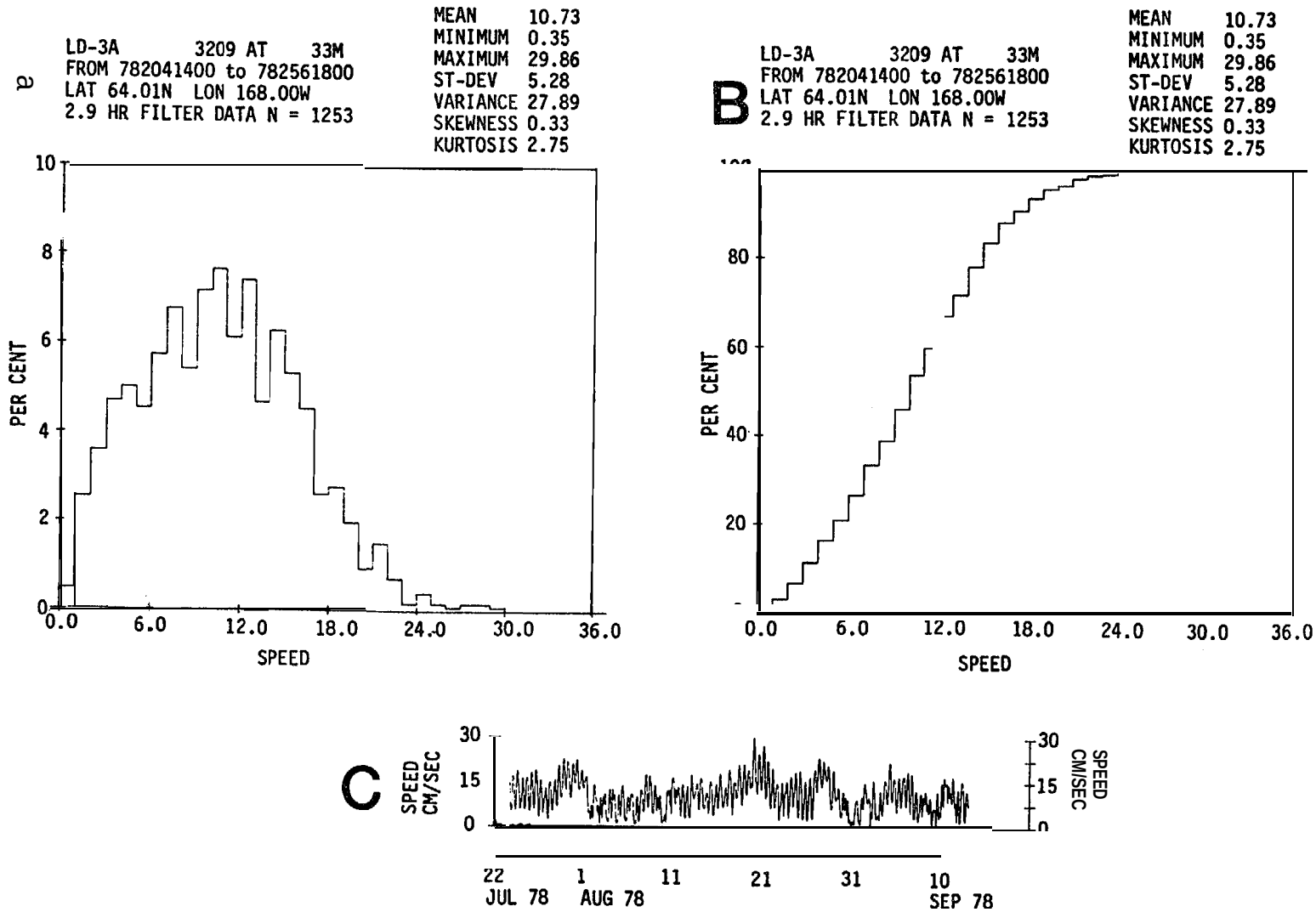

Figure 11 (A) Histogram of bottom current speeds from long term current meter, LD-3A. July-Sept., 1978. (B) Cumulative frequency graph of bottom current speeds for long term current meter LD-3A. (C) Daily bottom current speeds from long term current meter, LD-3A. Location of current meter shown in Figure 5.

northern half of the area and at its margins, current directions are generally northward; in the southern half, current directions are quite variable.

Long-term current meter moorings provide the best information on current parameters. Though moorings have not been placed at the center of Chirikov Basin, data are available from a mooring on the eastern margin of the basin from July-Sept. , 1978 (Fig. 5). Mean current velocity of 10.7 cm/see, speeds exceeding 18 cm/sec about 10% of the time, and maximum velocities of 30 cm/sec were measured (Fig. 11) (J. Schumacher and others, PMEL-NOAA, Seattle, pers. comm., 1982). The current velocity necessary to mobilize a 3 phi (.125 nun) sand on a flat bottom is approximately 30 cm/sec (Miller et al. 1977). On a rough bottom, threshold velocity of erosion becomes significantly less in this and other areas (Cacchione and Drake, 1982). With a known minimum bottom roughness of 10 cm and a grain size of .125 mm in whale feeding areas (Nerini et al., 1980), the velocities to erode sediment can be estimated at 18 cm/sec (Cacchione, U.S. Geological Survey, Menlo Park, pers. comm., 1983). Velocities greater than this were present about 10% of the time during normal weather in the summer of 1978.

Current speeds have not been measured during storms within Chirikov Basin, but in many northeastern Bering Sea areas surrounding it current velocity increases of 100% or more have been measured (Fleming and Heggarty, 1966; Coachman and Tripp, 1970; Coachman et al., 1976; Schumacher and Tripp, 1979; Cacchione and Drake, 1982). Even under moderate storm conditions, wave surge currents become important at the water depths of 20-40 m encountered in northeastern Bering Sea (Cacchione and Drake, 1982).

Storm surges

Moderate storms occur each fall in the northeastern Bering Sea resulting in changes in atmospheric pressure and wind velocity that can cause sea level set up of 1 meter and current speeds to fluctuate by as much as 100% over periods of a day or more (Coachman and Tripp, 1970; Tripp and Schumacher, 1979; Cacchione and Drake, 1982). At the northeastern edge of Chirikov Basin (Fig. 5), a GEOPROBE mooring measured a 100% increase in bottom current velocity (up to 72 cm/sec.) and a 1000% increase in suspended sediment transport during a moderate September storm (Cacchione and Drake, 1982). The GEOPROBE site has maximum spring tidal currents of 30 cm/sec. like those measured in Chirikov Basin (Fig. 9): this suggests that yearly storms can cause significant bottom erosion in Chirikov Basin. Six great storm surge events have occurred this century in the northeastern Bering Sea region and have caused sea-level set up of 4 m. (Fathauer, 1975); this suggests a potential for sea floor scour several orders of magnitude greater than yearly events just described.

Ice cover and seasonality of processes

The entire northeastern Bering Sea is covered by ice almost six months a year. For this reason the gray whale feeds in this region during the summer months only and storm activity which affects the sea floor bottom occurs mainly in the fall months.

Dupre (1982) recognizes three distinct seasons of coastal processes near the Yukon Delta in Norton Sound. The ice-dominated regime lasts from October or November to late Nay. The river-dominated regime, associated with the breakup of ice on the Yukon River, peaks rapidly in early summer and blends

into the storm-dominated regime which grows through late summer and peaks in October or November. In the center of Chirikov basin, where whale features are being modified, the river-dominated regime is greatly reduced in importance and is usually replaced by a period of summer quiescence. Thus, in the basin there exist two seasons in which normal current regimes predominate and the bottom receives minimal disturbance, the ice-dominated regime and the summer quiescence, or, from November to August. The storm-dominated regime from August to November is the time period in which most of the sediment suspension and feature modification probably occurs.

Cacchione and Drake (1979, 1982), Drake et al. (1980), and Schumacher and Tripp (1979) document the importance of late summer/early fall storms to sediment movement. Their work with the GEOPROBE and long-term moorings of current meters found that even a moderate fall storm increased sediment transport by a factor of ten over normal transport rates (Cacchione and Drake, 1982). The inference is that a great deal and perhaps a majority of the sediment erosion, and thus fresh pit modification, is probably storm-related. Thus, bottom features may undergo very little modification during the winter, spring, and early summer and be rapidly modified during the late summer and early fall as the storms increase in strength and frequency.

GEOLOGIC SETTING

Quarternary his tory

The northeastern Bering Sea is a broad, shallow epicontinental shelf region covering approximately 100,000 km^2 of subarctic sea floor between

Seward Peninsula, Alaska and Chukotka Peninsula in the USSR (Fig. 1). The shelf can be divided into four general morphologic areas: 1) the western part, an area of undulating, hummocky relief formed by glacial gravel and transgressive-marine sand substrate (Nelson and Hopkins, 1972); 2) the central part, Chirikov Basin, a relatively flat featureless plain with a fine-grained transgressive sand substrate (McManus et al., 1977; Nelson, 19820; 30 the northeastern part, a complex system of sand ridges and shoals bordering the coastline with fine- to medium-grained transgressive sand substrate (Nelson et al., 1978); and 4) the eastern part, Norton Sound, a broad, flat marine reentrant covered by Holocene silt and very fine sand derived from the Yukon River (Nelson and Creager, 1977; McManus et al., 1977; Nelson, 1982).

During Pleistocene interglacial periods and the present Holocene high sea level stand, sediment eroded from Alaska and Siberia has been carried northward from the Bering Shelf through the Bering Strait into the Arctic Ocean (Nelson and Craeger, 1977). Under lowered sea level conditions, the Yukon and other rivers extended their courses across the continental shelf to the southern Bering Continental Margin where sediment was transported through major submarine canyons to be deposited on the abyssal plain (Nelson et al., 1974). As a result, the Quaternary sediment on the continental shelf is absent in some regions of strong bottom currents and rarely exceeds 100 m; the thickness of the Holocene sediment is only a few meters or less (Nelson, 1982).

During lowered sea level periods of the Pleistocene, the entire present-day northeastern Bering Sea region was emergent. Glacial moraines formed off Siberia, and St. Lawrence Island, and along the coast of what is now the Seward Peninsula (Nelson, 1982). The entire area was covered by tundra and

deposits of freshwater peat and silt. As sea level began to rise, the freshwater silt and peat were covered by transgressive sand (Fig. 12). The moraines were winnowed, removing fine-grained sediment and leaving gravel lag deposits. As the sea transgressed, the basal, medium-coarse beach sand was overlain by an inner shelf fine-grained transgressive sand (Fig. 12). Between 5000 and 2500 years B.P., the Yukon Delta began to form and deposit coarse silt and very fine sand in Norton Sound (Nelson and Creager, 1977; Dupre, 1982).

Surface sediment distribution

The distribution of relict and modern surface sediment is patchy and dependent upon positions of bedrock and glacial debris outcrops on the sea floor, locations of river sediment inflow, and water current velocity and patterns. The gravel found in a 30 km wide belt along most of the coast from east of Nome to the Bering Strait and a 10 km belt along the north coast of St. Lawrence Island is relict and derived from glacial drift, outwash, alluvium, and bedrock in these areas (Fig. 12). Offshore from the bedrock gravel lag of Seward Peninsula, medium-grained sand fringes the northeastern edge of Chirikov Basin.

The southern margins of St. Lawrence Island and Central Chirikov Basin and southeastward into Spanberg Strait are covered by the fine-grained inner shelf transgressive sand; this sand is of particular interest because it is the Ampeliscid amphipod substrate of the gray whale feeding grounds. This sand body is quite thin and rarely is greater than one meter thick (Nelson, 1982). It is finer grained (.125 mm) than the underlying basal transgressive

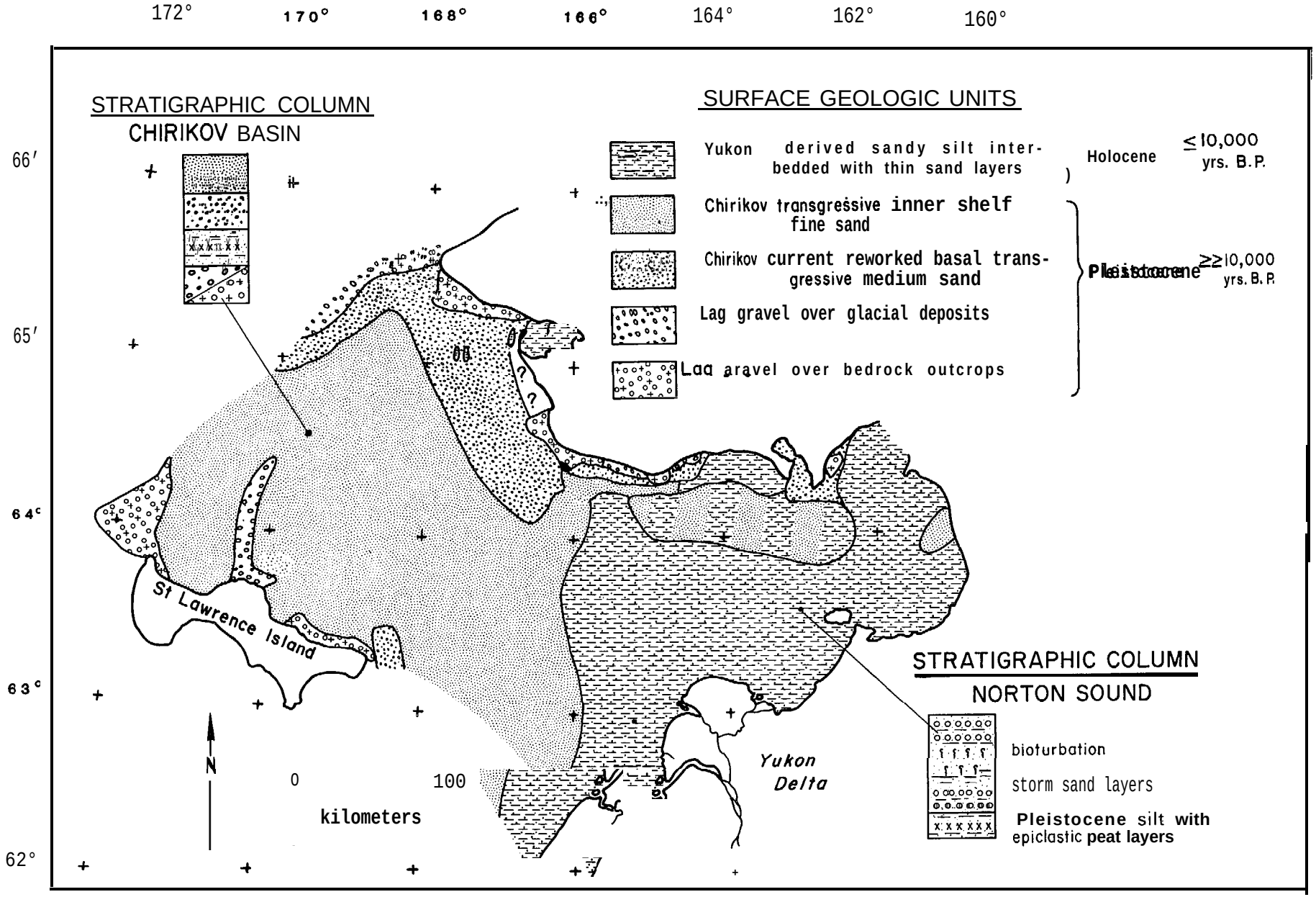

Figure 12 Preliminary map of the northeastern Bering shelf surficial geology (modified from Nelson, 1982)

sand that borders it and is exposed on the margins of Chirikov Basin (Fig. 13).

There are also subtle variations within the inner shelf sand sheet itself. For example, within the the Shpanberg Strait area, which has strong currents, the sand body has a slightly higher percentage of sand-sized particles and is better sorted (Figs. 14, 15). This combination of stronger currents and slightly cleaner or less muddy sand in the straits area results in a sand dollar benthic community compared to the amphipod-dominated community found in most other substrate areas of the inner shelf sand (Nelson et al., 1981).

Norton Sound to the east of the inner shelf sand sheet is covered by a modern very fine sand and coarse silt (.032-.062 mm) derived from the Yukon River (Figs. 12, 15) (McManus et al., 1977). Current and water mass movements prevent deposition of the modern Yukon sediment over the relict transgressive sediment of the Chirikov Basin area (Nelson, 1982).

Surficial geologic processes and bottom depressions

A number of surficial geologic processes produce different types of depressions on the sea floor that can be observed on side-scan records. Description of these physical features is important so that they can be distinguished from biologically produced bottom surface features. This separation is usually possible because most of the physical features require a very specific set of geologic conditions and only occur in certain areas (Fig. 16). Fortunately, even though some of the physical features closely resemble those of biological origin, they generally occur in different locations.

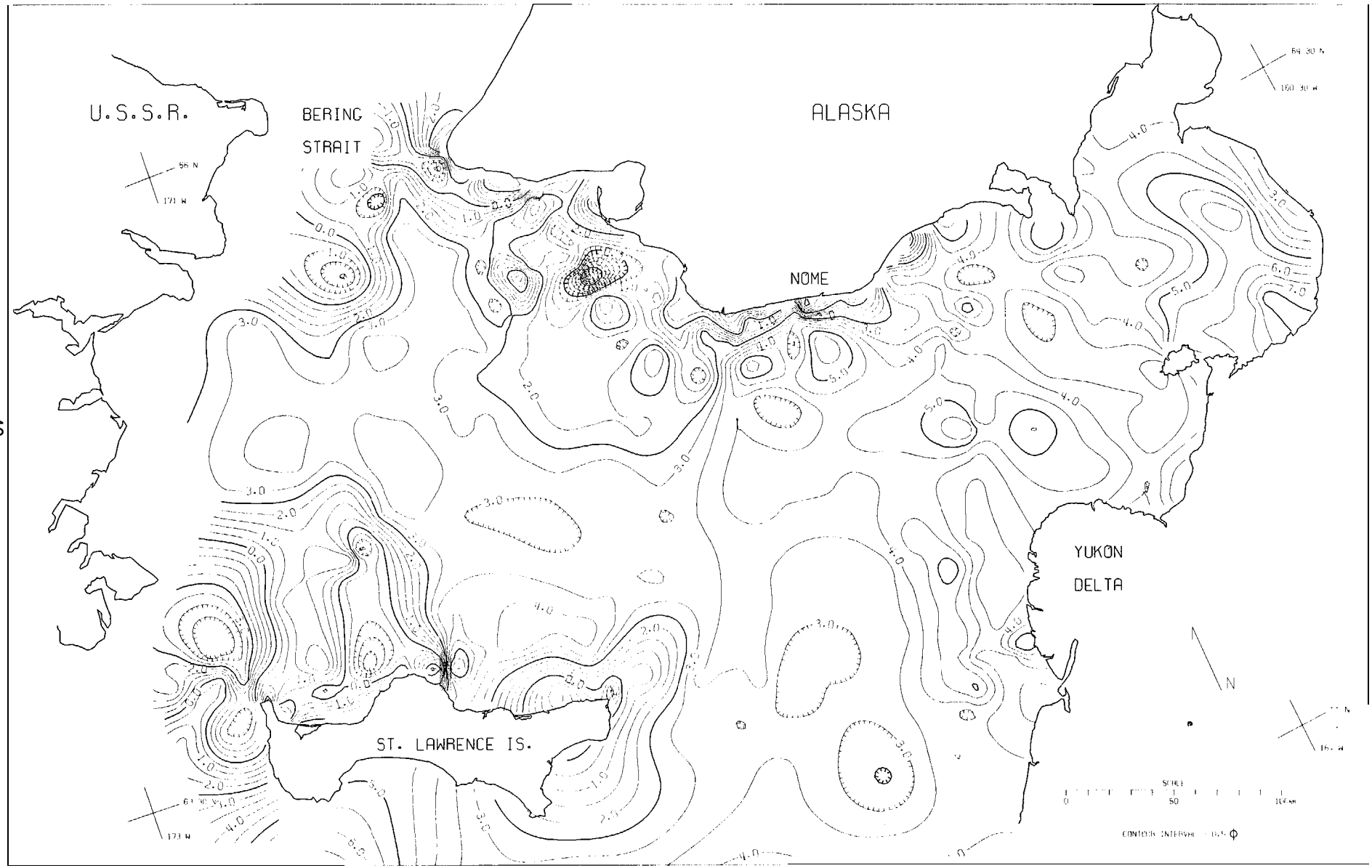

Figure 13 Mean grain size (Folk and Ward) for surface sediment in Norton Basin, northeastern Bering Sea.

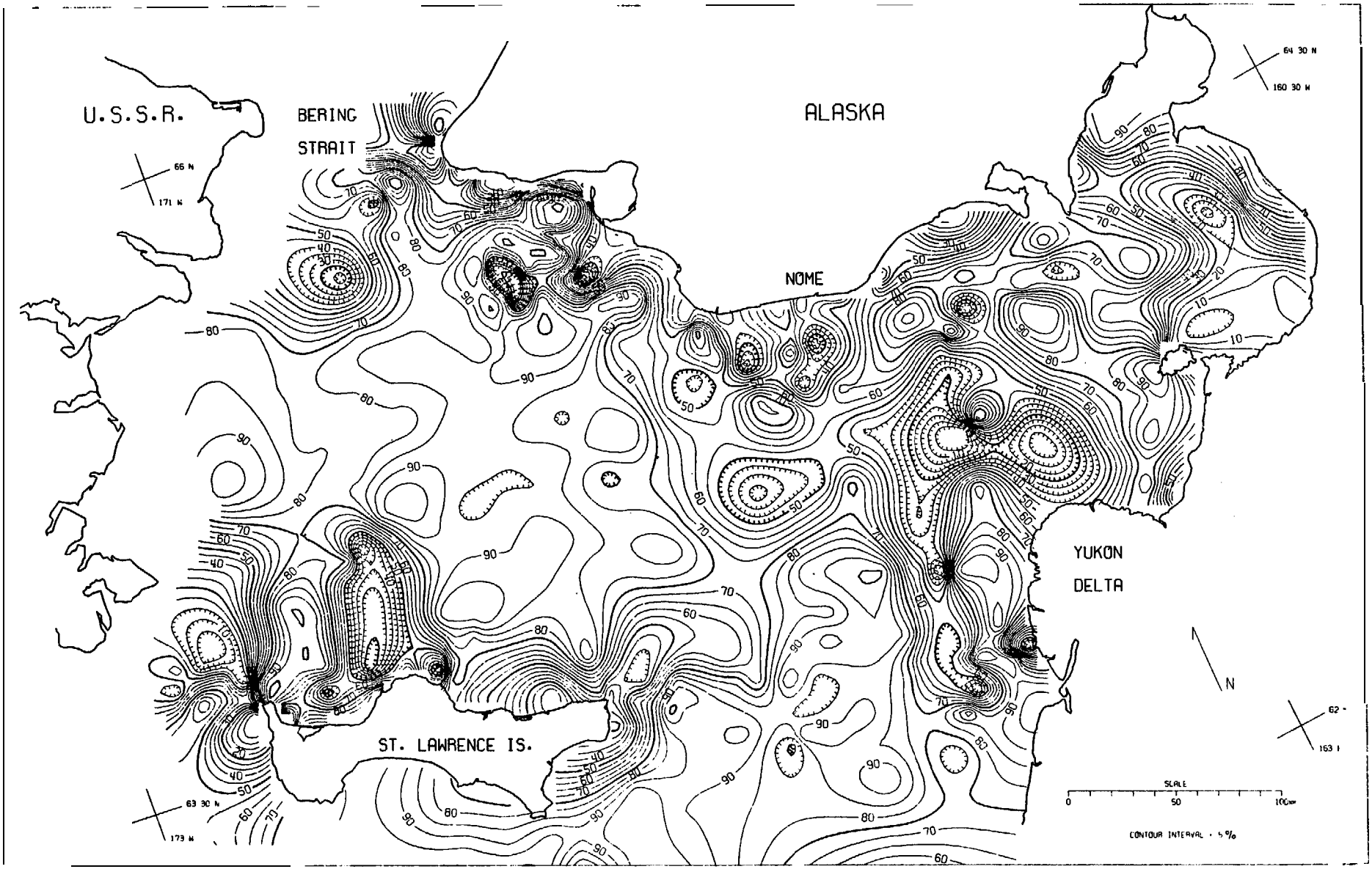

Figure 14 Percent sand in surface sediment of Norton Basin, northeastern Bering Sea.

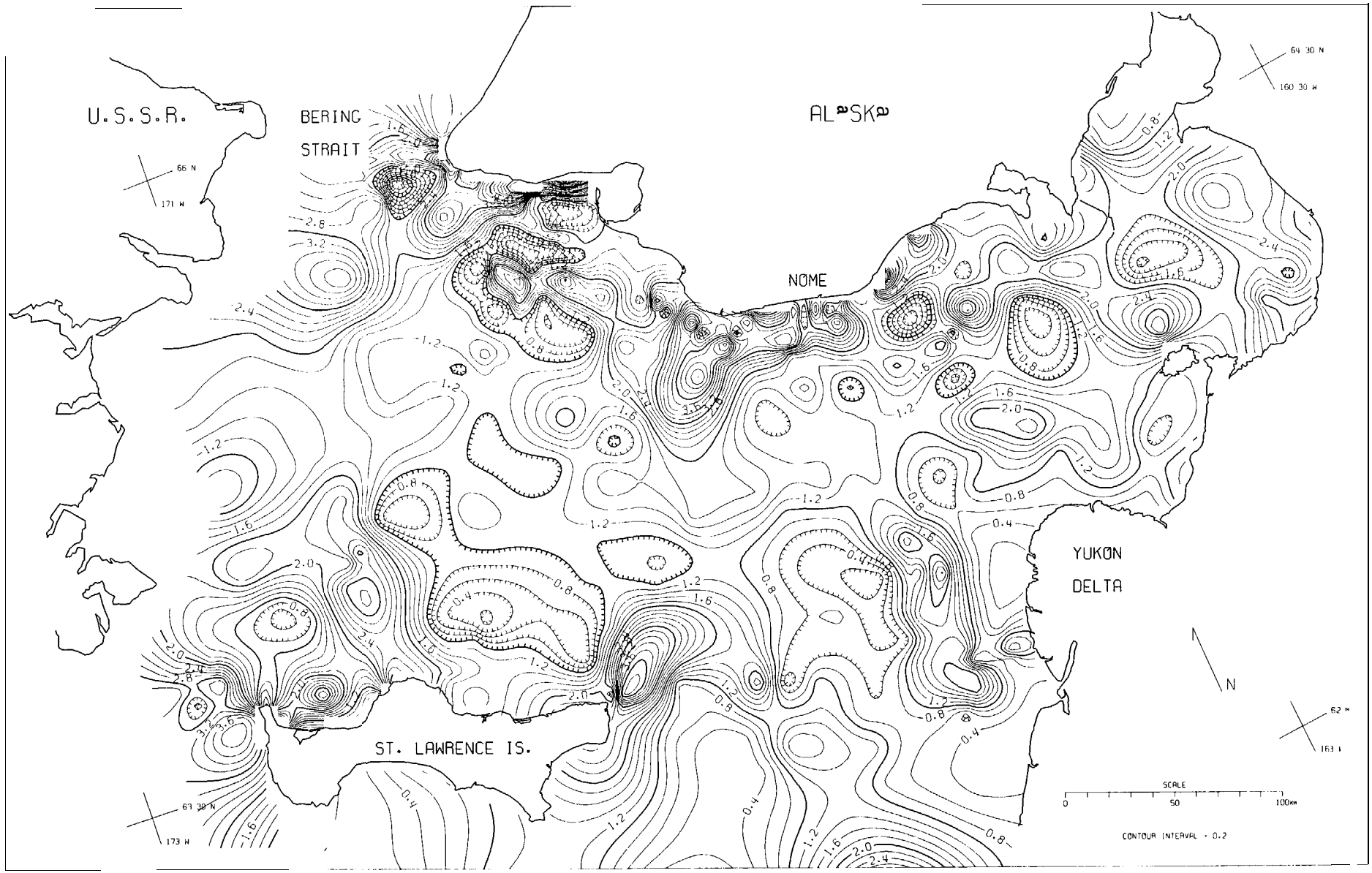

Figure 5 Sorting values (Folk and Ward) for surface sediment in Norton Basin, northeastern Bering Sea.

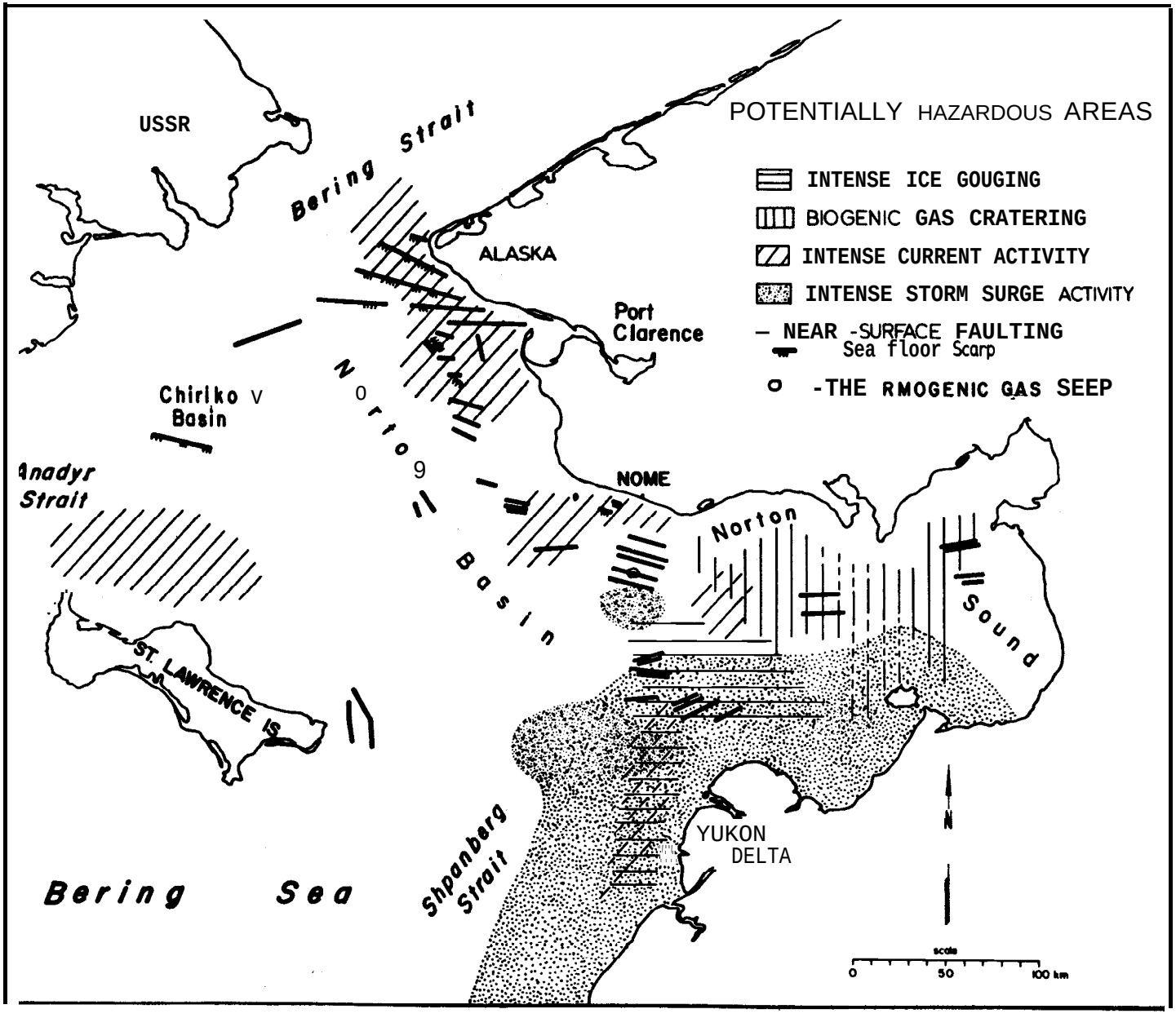

Figure 16 Potentially hazardous areas of the northeastern Bering Sea. Current scour depressions occur in the area of intense current activity off the Yukon Delta. From Thor and Nelson (1981).

Ice scour on the northeastern Bering Sea continental shelf has been identified on side-scan sonar and is classified into two types. The first is a single furrow (Fig. 17A) and the second is a series of multiple subparallel furrows (Thor and Nelson, 1981). The single scours are formed when single ice keels plow through the surficial sediment while multiple gouges are produced when multi-keeled floes rake the bottom. Ice scour occurs in water depths of 40 m or less, but it is most dense in water 10 to 20 m deep. In general, ice scour follows ice movement, parallel to isobaths and coastline configuration. Ice scour is concentrated in ice shear zones where the edge of shorefast ice meets offshore moving ice pans creating pressure ridges. This occurs most notably along the Yukon Delta margin (Fig. 16). Ice scour is rare in Chirikov Basin because of the increased depth of the water and the lack of extensive ice shear zones.

The second type of bottom depression that has been recognized in the northeastern Bering Sea is the current-induced scour depression (Fig. 17B). These irregular-shaped forms typically are 20-150 m in diameter and have a generally shallow (less than 1 m) depth of scour (Larsen et al., 1979). The depressions are found in areas where the grain size is very fine sand to coarse silt and where bottom current velocities are relatively high (greater than 20 cm/s mean speed) under non-storm conditions. These features typically occur where strong currents shear against margins of bathymetric constrictions or relief covered by very fine sand. Local topographic disruptions, such as ice scour help set off flow separation and greatly enhance this current-scour process. These scour depressions occur mainly along the Yukon Delta front and in northern Norton Sound (Fig. 16).

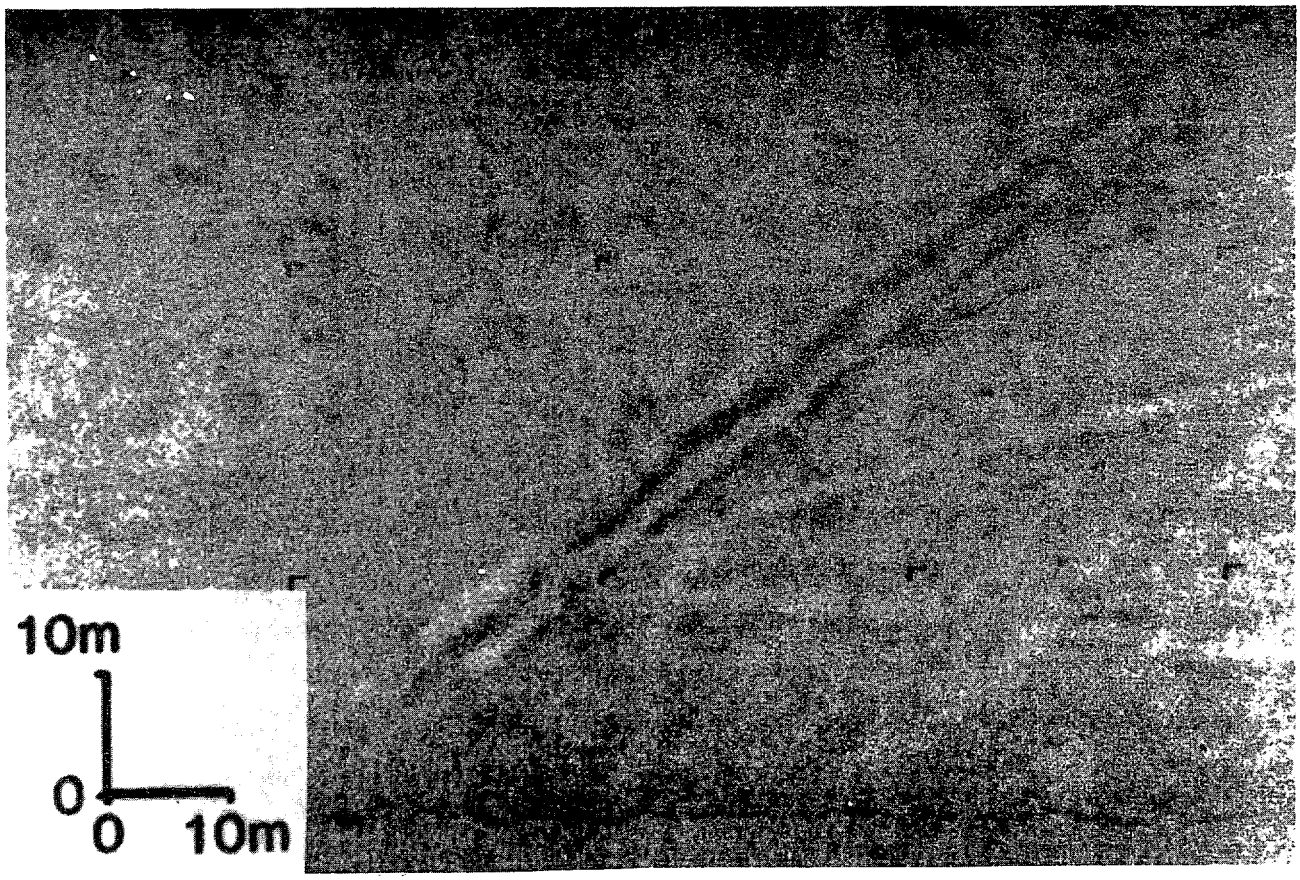

Figure 17A

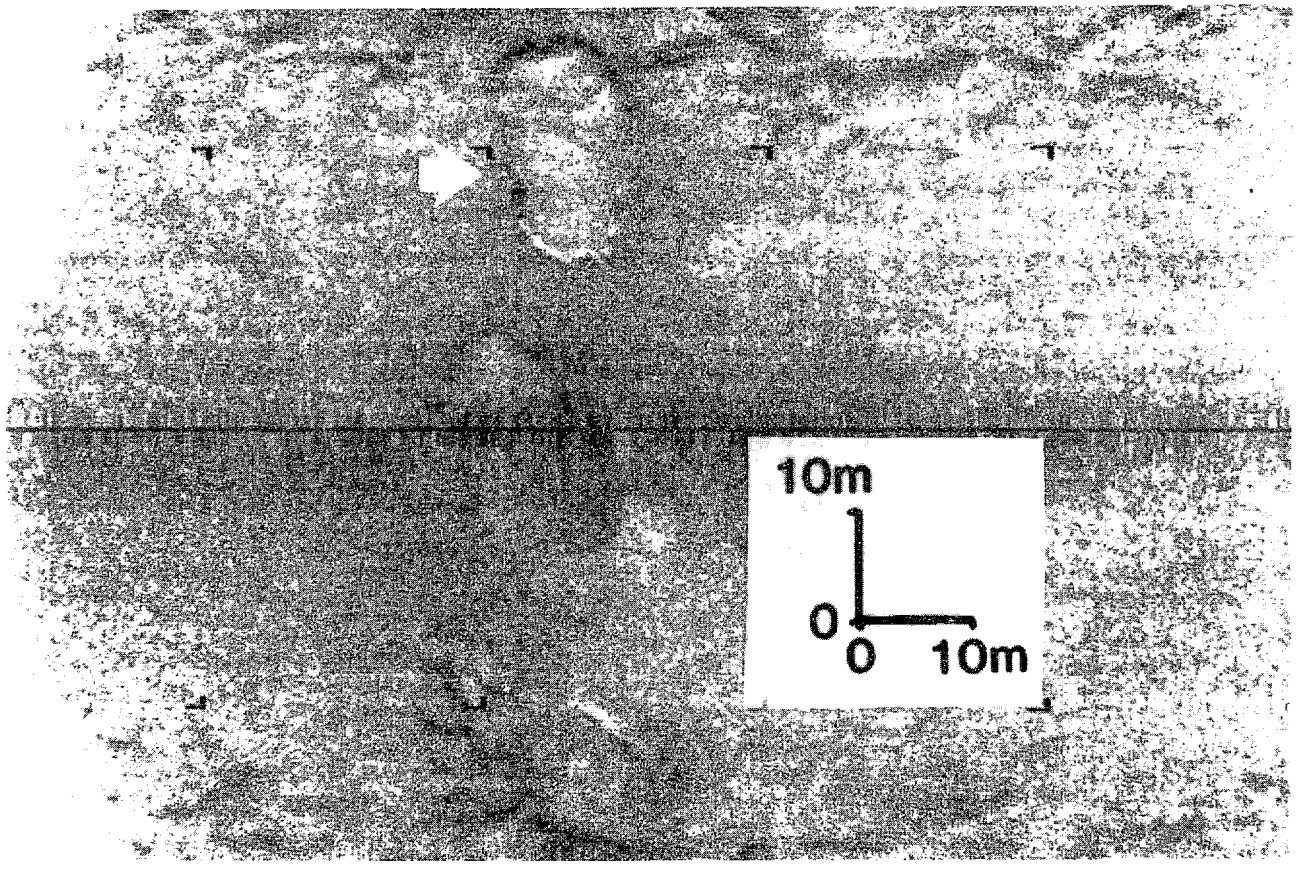

Figure 17B

Circular gas craters also form in regions of gas-charged sediment in Norton Sound (Fig. 17c) (Nelson et al., 1980). Biogenic gas formed by the decomposition of organic debris is trapped in the peaty mud in a saturated state by the overlying cover of Holocene mud. Periodically, during storms, the gas escapes through the thin Holocene mud blanket and forms craters. The craters are found predominately in Norton Sound and are circular, 1-10 m in diameter and are less than 1 m deep. Sea floor gas craters are typically associated with near-surface peaty mud, gas-charged sediment, and acoustic anomalies shown on seismic profiles; the latter occur because of gas saturation in the near-surface sediment. No craters of this type are found in the central Chirikov Basin, apparently because the sediment cover in this region is composed of fine sand that allows gas escape and prevents any near-surface gas saturation (Nelson et al., 1980). The lack of acoustic anomalies in Chirikov Basin to the west of Norton Sound indicates that sediment gas saturation does not exist in this area and that gas craters should not be present (Holmes and Thor, 1982).

BIOLOGICAL SETTING

The Bering Continental Shelf is an area of rich macrobenthic communities of low diversity but high density (Neiman, 1961; Filatova and Barsanova, 1964; Kuznetsov, 1964; Rowland, 1972; and Stoker, 1973). The major species show a preference for certain sediment types and grain sizes (Nelson et al., 1981; Stoker, 1978). In areas where the homogeneous sediment types are widespread, they form vast stable environments in which large numbers of individuals of these species can flourish.

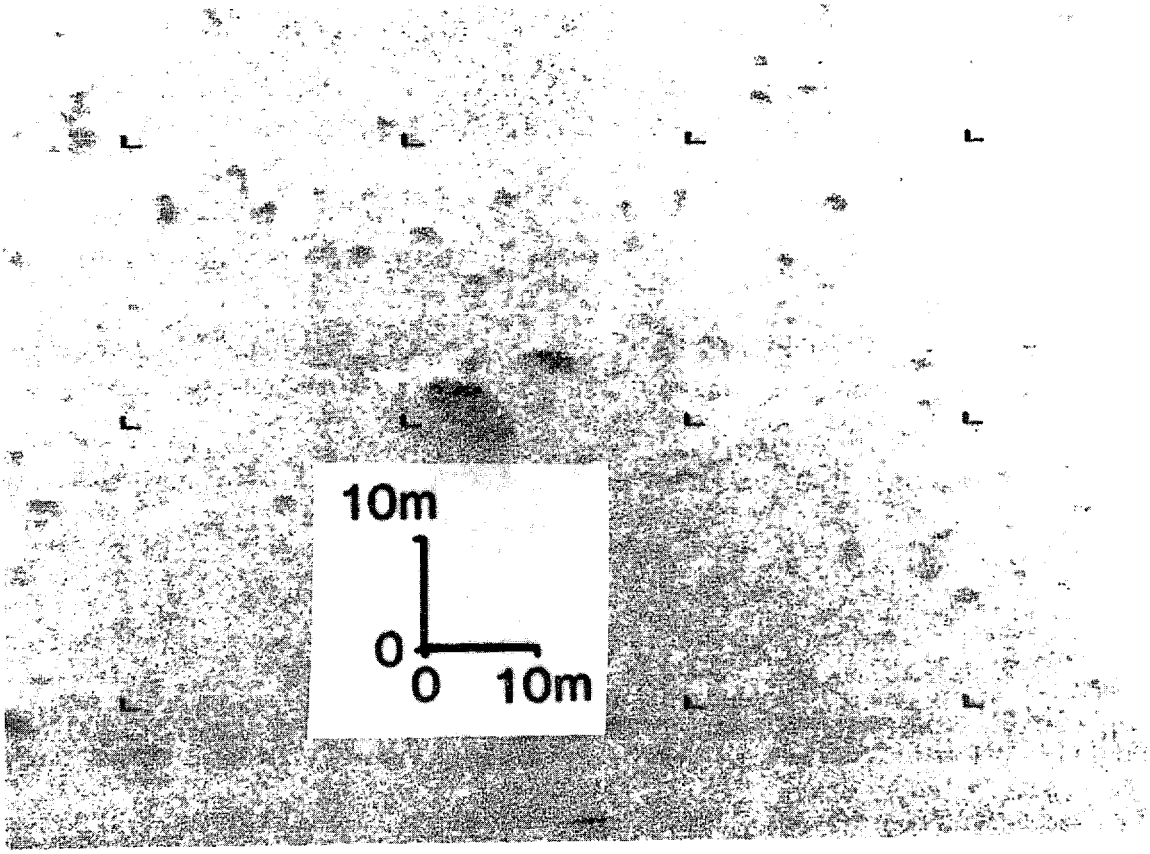

Figure 17C

Figure 17 105 kHz sonograph of (A) ice scour from Norton Sound, (B) current scour depressions from the Yukon Delta front, (C) circular gas expulsion craters from Norton Sound. Arrows show location of features in B and C.

In response to the rich benthic food resources, large populations of walrus, bearded seals, and gray whales inhabit the northeastern Bering Sea at least seasonally and, by their feeding, are likely to be responsible for considerable reworking of the shallow shelf sediment over much of this area.

The gravel lag layers are dominated by epifaunal species such as crabs and sea urchins which cause little disruption of physical sedimentary structures (Fig. 12) (Nelson et al., 1981). The medium and well-sorted sand bodies on the edges of the central Chirikov Basin show reworking by sand dollar and tellinid clam communities. The muddy, very fine sand and silt of Norton Sound are characterized by a deposit feeding community. The central Chirikov Basin is covered by an inner shelf fine-grained sand that shows intense bioturbation by ampeliscid amphipods. This intense bioturbation from the sediment surface to a depth of 10 cm is easily discernible in sediment radiographs from the central Chirikov Basin (Fig. 18) (Nelson et al., 1981).

The areas with a dominance of Ampeliscid amphipods show a definite association with the Chirikov fine sand sheet (Figs. 4, 12, 19) and with the Bering Shelf Water (Figs. 4,9,19) but presence of these amphipods is not exclusively limited to these environments. Water depth preferences range from 20 to 40 m and the amphipods are most common in the fine sand on the flat low-relief shelf area of Chirikov Basin. The optimum substrate habitat for the ampeliscid amphipods is a moderately sorted, slightly silty, very fine sand with 80-90% sand sized particles (Figs. 13, 14, 15); they are not found in the transgressive fine sand where it is well sorted and reworked by strong currents, an area occupied by the sand dollar community (Figs. 4,12) (Nelson et al., 1981). Ampeliscid amphipods are not common in Norton Sound due to

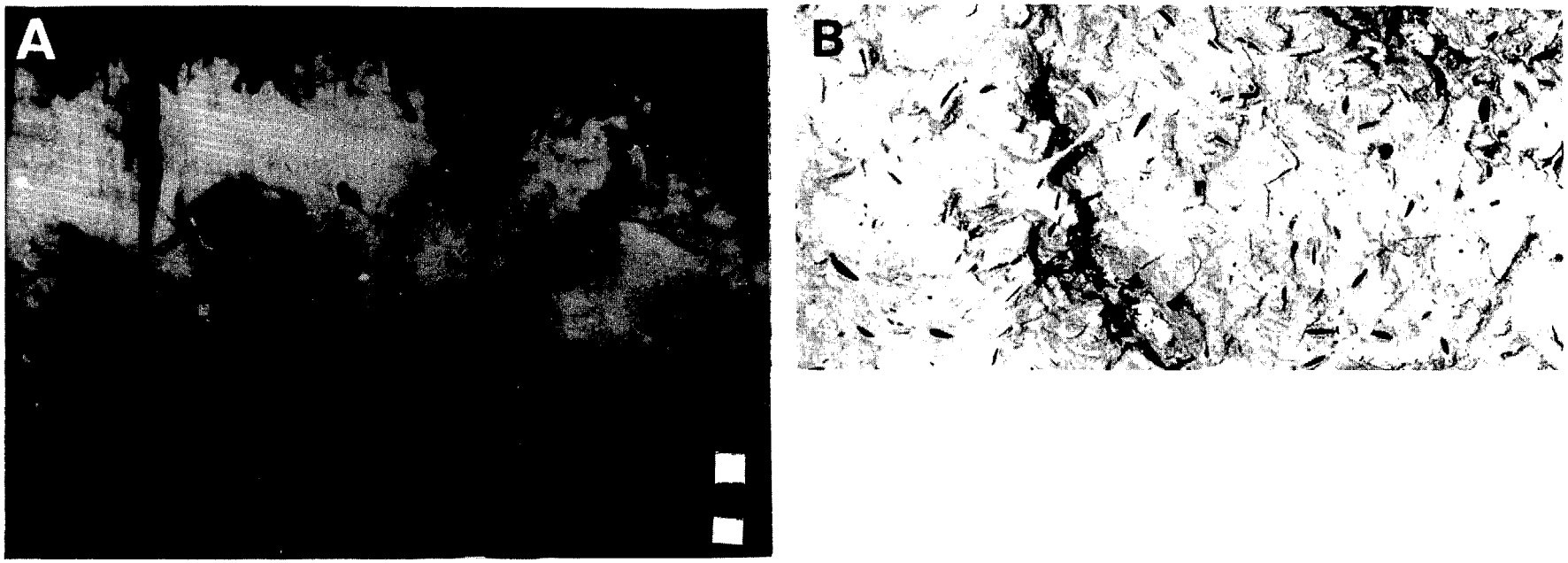

Figure 18 (A) Radiograph of a box core, showing the v-shaped burrows of the **amphipod, Ampelisca macrocephala.** The core was taken from the fine transgressive sand body in the center of **Chirikov** Basin at a water depth of 27 m. **(B)** Plan view photo of the box core top taken immediately after collection. Slit-like, mucus-lined burrows are typical of the amphipod **Ampelisca macrocephala.**

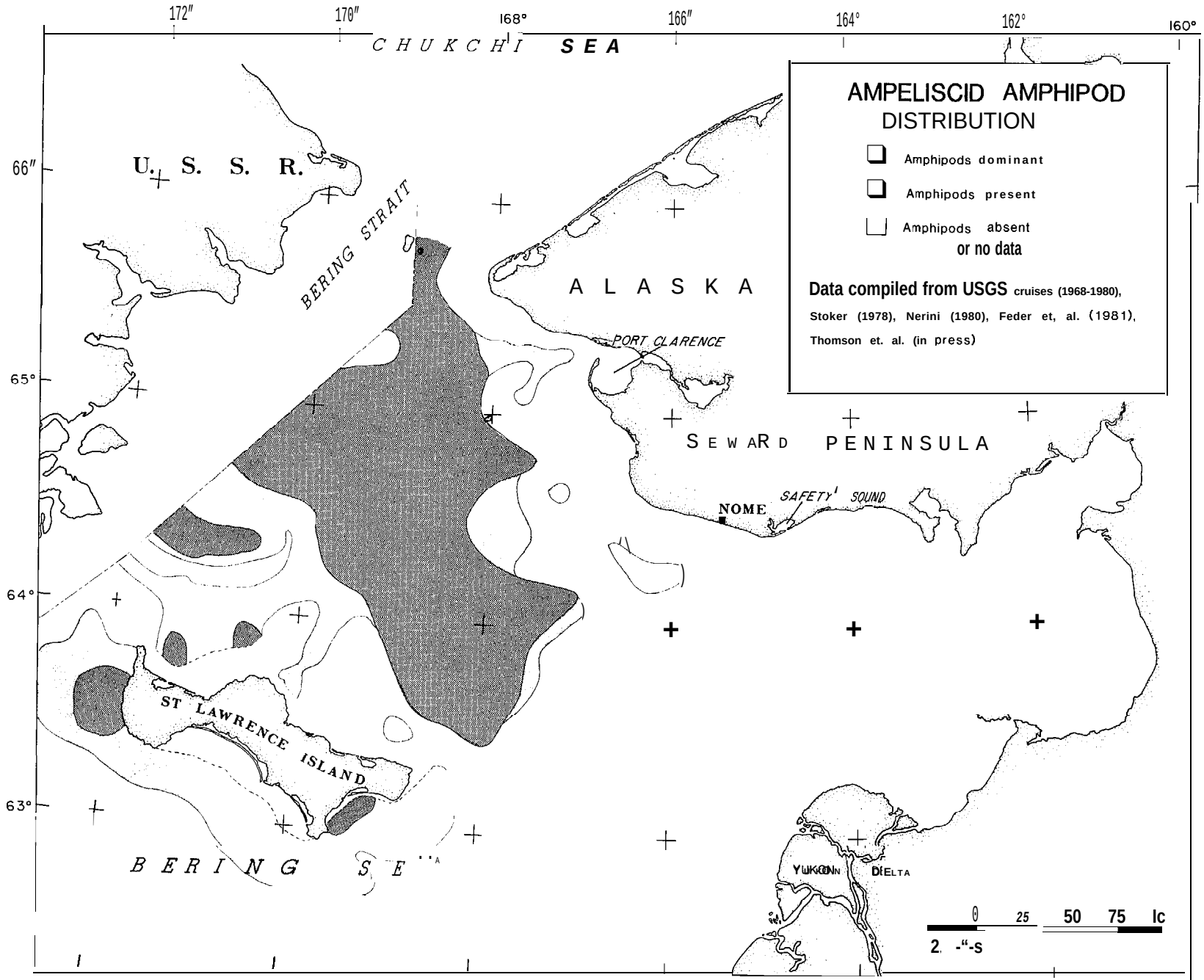

Figure 19 Distribution of Ampeli scid amphipods in the northeastern Bering Sea. Compiled from USGS cruises 1960-1980, Stoker (1978), Nerini (1980), Feder and Jewett (1981), Thomson (1983).

the decreased salinity (Ken Coyle, Institute of Marine Studies, Fairbanks, pers.comm., 1982) and grain size (Nelson et al., 1981).

The main prey species of the gray whale in Chirikov Basin is the Ampeliscid amphipod, Ampelisca macrocephala (Rice and Wolman, 1971). Ampeliscid amphipods are detritus feeders that build narrow V-shaped, mucus-lined tubes. When the population of amphipods becomes large, the densely packed tubes coalesce and create extensive mats that fix the surface of the sediment. Productivity and resultant biomass are very high in these areas. Stoker (1978, 1981) calculated an average total biomass of 533 g/m^2 (his group IA, dominated by ampeliscid amphipods) in central Chirikov Basin. Nerini (in press) calculated a total biomass of 483 g/m^2, with 34% of this biomass contributed by the amphipod community for the same area. The American section of Chirikov Basin contains nearly 30,800 km^2 of area with Ampeliscid amphipods present (Fig. 4). The southern nearshore area of St. Lawrence Island contains an additional 9,000 km^2 (Fig. 19).

GRAY WHALE FEEDING ECOLOGY

The gray whales feed mostly during the summer. The stomachs of migrating whales are generally empty (Rice and Wolman, 1971) as are those of the whales in the breeding lagoons (Scammon, 1874). Rice and Wolman (1971) reported that the southbound whales were 11 to 29% heavier than the northbound whales. The majority of evidence suggests that the whales feed only occasionally during migration, calving, and mating; they take most of their nourishment for the year during the summer on Alaskan shelves. Nerini (1981) cites numerous reports of whales actively feeding during migration; it is clear that they do

feed sporadically and sometimes voraciously in migration to and from the southern waters, but the relative proportion of total yearly food intake this accounts for is unknown, although probably minor (Oliver, Slattery, Silberstein, and O'Connor, 1983; Swartz and Jones, 1982; Hudnall, 1981; Wellington and Anderson, 1978; Sund, 1975; and Howell and Huey, 1930).

The Bering Sea and Arctic Ocean undoubtedly are the main feeding areas of the gray whales. After their migration from the breeding and calving lagoons of Baja California, and once they are north of the Aleutian Islands, the whales move into various feeding grounds in these waters (Pike, 1962). The largest group feeds in the central Chirikov Basin and nearshore areas of St. Lawrence Island; it is the focus of this study (Fig. 20) (Braham, in press; Moor and Ljungblad, in press; Braham et al., 1977; Votrogov and Bogoslovskaya, 1980; S. Leatherwood, pers. comm., 1982; Consiglieri et al., 1930) .

Ljungblad, in press), 85% were associated with sediment plumes, which is a sure indication of benthic feeding. Gray whales are not common in Norton Sound and this area seems to receive minimal feeding pressure (Nerini et al., 1980).

Another group of gray whales stays near the Alaskan peninsula and extends into Bristol Bay, where they are frequently spotted feeding in the surf or in very shallow water in Bristol Bay (Consiglieri et al., 1980; Braham et al., 1982; S, Leatherwood, pers. comm., 1982). Their main prey species in these areas are unknown.

Soviet whalers have been taking gray whales from the nearshore western side of Chirikov Basin and in the Gulf of Anadyr at least as far south as Cape Navarin (Zimushko and Lenskaya, 1977; Zimushko and Ivanshin, 1980, Zenkovich,

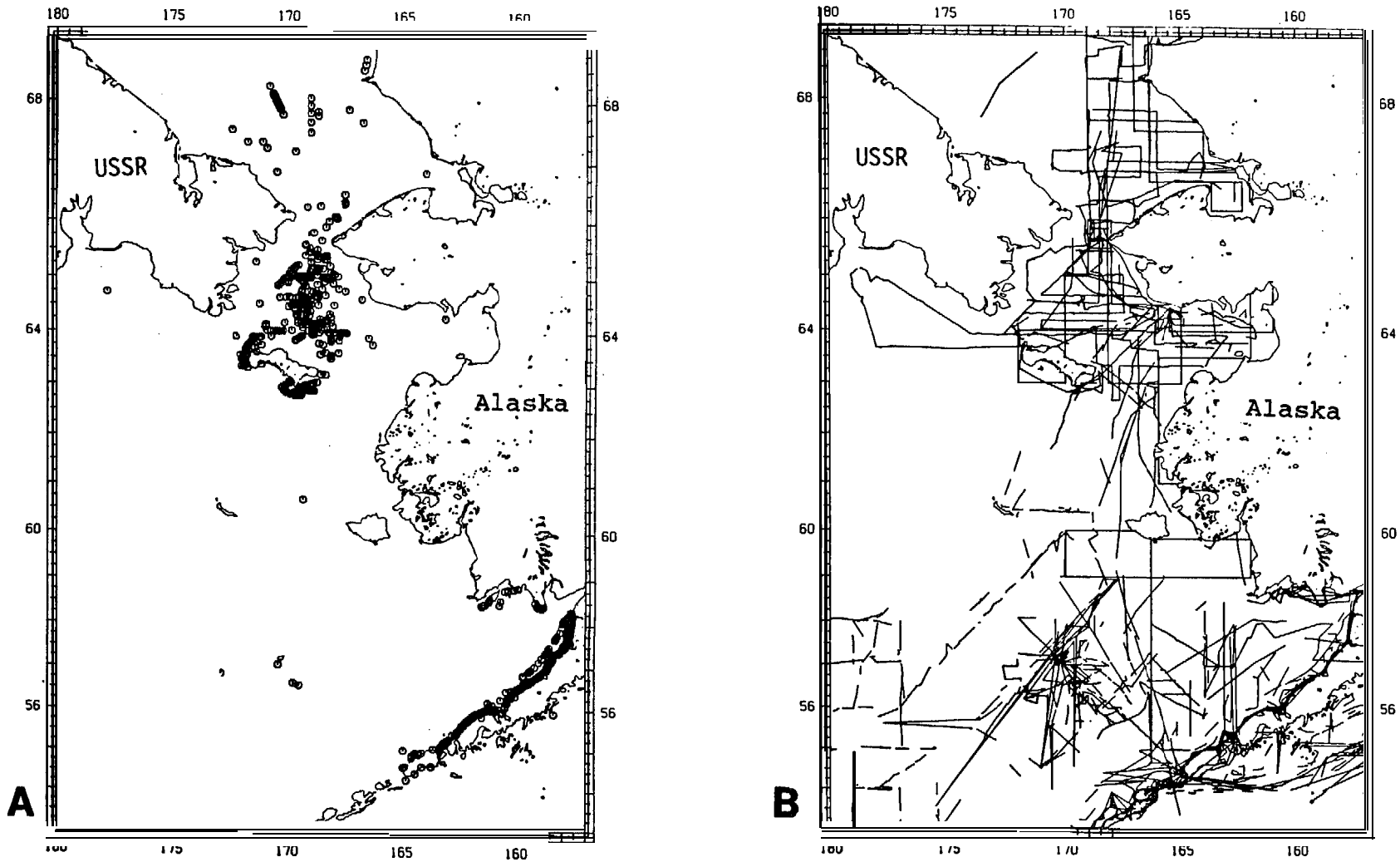

Figure 20 (A) Distribution of gray whale sightings in the northeastern Bering Sea from June-August 1978 (from Consiglieri, Braham, and Jones, 1980). (B) Ship and aerial tracklines completed for whale observations during June-August 1978 (from Consiglieri, Braham, and Jones, 1980).

1934, 1937, 1955). Zenkovich (1937) reported that feeding whales were apparently segregated by age. He noted the presence of a feeding ground near Cape Navarin in the Gulf of Anadyr used only by two-year-old male gray whales.

Another large group of feeding whales is found in the Chukchi Sea, along both the Alaskan and Siberian Coasts as well as in the central part of the Chukchi Sea and along the northern ice edge (Bogoslovskaya et al., 1981; Coyle, 1981; B. Nelson, Alaskan Dept. of Fish and Game, Nome, pers. comm., 1982). Gray whales have been spotted in the Beaufort Sea as far east as the MacKenzie River Delta, but this was probably an isolated occurrence (Rugh and Fraker, 1981).

A few, small isolated groups of gray whales do not go north to feed but instead shear off from the main population and spend the summer feeding at certain points along the migration route. One such group feeds in the outer Strait of Juan de Fuca and along the west coast of Vancouver Island, British Columbia (Hudnall, 1981; J. Oliver, Moss Landing Marine Station, pers. comm., 1982). A well-developed ampeliscid amphipod mat community exists in Pachena Bay, Vancouver Island and is being exploited by a small group of gray whales (J. Oliver, pers. comm., 1982). Even though the Chirikov Basin has historically been regarded as the main feeding area (Rice and Wolman, 1971), other areas certainly receive substantial feeding pressure. This pressure should increase as the gray whale population continues to rebound.

The feeding habits of the gray whale are diverse. As an omnivore, this whale feeds primarily by benthic suction, but also by engulfing and surface skimming (Nerini, 1981). This provides a high diversity of potential prey and a good survival potential for the whales. It also makes inaccurate the

assessment of feeding resources by benthic means alone. Nevertheless, this inaccuracy is very small, as the vast majority of gray whale feeding is benthic in nature (Nerini, 1981; Rice and Wolman, 1971).

The grays are the only whales that regularly consume benthic infauna (Nemoto, 1970). Stomach contents of gray whales taken in the feeding grounds generally contain infaunal amphipods (Rice and Wolman, 1971; Pike, 1962; Zenkovich, 1934). Frequently the stomachs also contain quantities of sand, gravel, and cobbles (Zenkovich, 1937).

Other than the main prey species, the Ampeliscid amphipod, Ampelisca macrocephala (Coyle, 1981; Rice and Wolman, 1971; Pike, 1962; Zenkovich, 1934), other Ampeliscid amphipods such as Ampelisca estrichii, Ampelisca birula, Byblis sp., and Haploops sp. are also heavily utilized by the whales. Closer to Siberia, the main prey species is the amphipod, pontoporeia femorata (Bogoslovskaya et al., 1981; Zimushko and Ivashin, 1980; Zimushko and Lenskaya, 1970). In addition to A. macrocephala and P. femorata, a number of other amphipods, polycheate worms, incidental infauna, and nektonic forms such as mysids and bait fish are consumed (Nerini, 1981).

The manner in which the whales extract the amphipods from their sandy habitats has long been a subject of speculation. Scammon (1874) reported whales surfacing "besmeared with the dark ooze from the depths below" and indeed it is a common and almost invariable sight for benthic feeding grays to be associated with large sediment plumes in the water column. Plankton nets towed through these mud plumes have documented the presence of displaced infauna in the water column (Oliver et al., in press).
Sea birds are frequently observed diving and apparently feeding in

the mud plumes (Harrison, 1979). All these observations suggest that the whales are disturbing the sea floor.

From diving and behavior observations by Nerini (1982), J. Oliver (oral and writ. comm., 1982), S.J. Swartz (UCSC, oral comm., 1982), F.H. Fay (IMS, Fairbanks, oral comm., 1982), and Hudnall (1981) it is speculated that the grays roll to one side, mouth parallel to the bottom and use a suction formed by the retraction of the large muscular tongue in the mouth cavity to rip Up patches of amphipod-rich sediment. The sediment is then expelled through the baleen on the opposite side of the mouth and the amphipods are retained on the hairy inner side of the baleen plates to be swallowed at a later time. This hypothesis is supported by the observed feeding behavior of the captive gray whale, Gigi (Ray and Schevill, 1974).

Though never seen directly in the wild, the suction feeding method is supported by whale behavior observed in shallow water by Steve Swartz (UCSC, pers. comm., 1982), John Oliver (Moss Landing, pers. comm., 1982), and Hudnall (1981). In all cases, the whales rolled on their sides, mouth parallel to the bottom, but further observation was impaired by the ensuing sediment plume.
before drawing the amphipod-rich sediment into their mouths.

Previous theories that grays actually came into contact with the sea floor and "bulldozed huge furrows" and "engulfed power-shovel helpings of crabs" (Walker, 1971) or "stirred up the bottom sediments with their snouts" (Rice and Wolman, 1971) seem unlikely as abrasion by bottom sediment would probably be much too severe for the relatively tender cetacean skin. It is untenable that gray whales plough the sea floor for the hundreds of kilometers

necessary to filter sufficient amphipods to account for yearly and total gains of body weight.

Uneven wear on the inner side of the baleen plates of 31 whales studied by Kasuya and Rice (1970) shows that 27 of the whales fed predominately with the right side of their heads. Kasuya and Rice (1970) also showed a greater frequency of healed or open wounds and lesser numbers of parasitic barnacles on the right side of the rostrum. This suggests the idea of "right-handed" or "-mouthed" whales and implies that the whales do occasionally come into contact with the abrasive sea floor.

Benthic feeding produces a variety of pits and depressions in the sea floor. The feeding traces left by the whales are the main focus of this paper. Elongate furrows up to 10 m in length were discovered in areas of heavy whale feeding in the Bering Sea by Nerini and others (1980) and M. Larsen (USGS, Menlo Park, pers. comm., 1980). SCUBA divers measured pits ranging in length from 0.6 m to 3 m and attributed them to feeding gray whales (Nerini and Oliver, in press). S. Swartz (UCSC, pers. comm., 1982) has observed whales making pits, as long as their gape and up to a meter wide, in the highly mobile sands of the breeding lagoons in Baja California, Mexico. Core samples near these pits produced very little macroscopic fauna, so these pits are not technically feeding pits but might be attributed to "mock feeding", test feeding, or some other unexplained behavior. John Oliver (Moss Landing, pers. comm.) has observed oval pits up to 1.5 m long in ampeliscid amphipod-bearing sediment associated with an actively feeding juvenile gray whale in Pachena Bay, Vancouver Island. The oval pits often occur in groups as a multiple suction feeding event (Nerini, 1981, J. Oliver, pers. comm., 1983).

In order to determine the shape and size of features likely to be made by a whale foraging on the benthos, a histogram of gray whale gape (mouth) lengths based mainly on data from Rice and Wolman (1971) has been compiled (Fig. 8). Gape lengths were calculated by multiplying the head length by 0.75 (Dale Rice, NMML, Seattle, pers. comm., 1982). The average gape length for male gray whales was 2.0 m (n = 131) and for females, 2.1 m (n = 105). The average gray whale head, when viewed from above, is triangular and the line from the snout to the posterior end of the gape is straight. Thus, the majority of the mouth is parallel to the bottom and a large percentage of the gape may be utilized during feeding. Since the actual percentage of mouth area used is unknown, these measurements can only provide parameters for the maximum size of feature which a non-moving whale can produce.

If a whale were swimming or drifting in the current while sucking up the sediment, then the size of the resulting feature could be considerably larger. The length of feature made by a moving whale would be controlled by the duration of the suction event together with the speed of the whale and the effect of current movement on the whale. By coordinating its propulsion and suction, a whale could create an elongate pit of substantial length.

Observations of feeding whales show both stationary and mobile feeding modes. Bud Fay (Institute of Marine Sciences, Fairbanks, pers. comm., 1982) reported that whales feeding in the surf off the southern side of St. Lawrence Island remained stationary and head down with their flukes in the air. Norris et al. (1982) gave evidence that gray whales near the entrances to lagoons in Baja California made use of currents to sweep food into their mouths. Both of these observations apparently apply to whales feeding in the water column and not on the benthos.

Records of dive times and positions of diving and surfacing of bottom-feeding whales near St. Lawrence Island show that whales feed in rather small areas. They often surface near or behind where they dive implying minimal movement on the bottom (B. Wursig, Moss Landing Marine Lab, pers. comm., 1982). A juvenile gray whale at Pachena Bay, observed by SCUBA divers, was moving along the bottom while feeding. The resulting pits were up to 1.5 m in length, longer than the gape of the small whale (J. Oliver, pers. comm., 1983). Although the size of the pit left by a non-moving whale generally may be expected to be approximately the size and shape of the gape, there is considerable potential for smaller (suction out of only a portion of the mouth) or larger (suction while moving) pits.

The average depth of the pits is still an unresolved question but they are clearly less than 50 cm in depth because they are *not* observed in horizontal line bathymetry of the monographs. SCUBA divers on the NMML cruises in 1980 (Nerini et al., 1980) found pits as deep as deep as 40 cm, although these may have been older features enlarged by current scour. Divers on the L.G.L. cruises in 1982 (Thomson, in press) found pits and furrows near St. Lawrence Island averaging 10 cm in depth. The ampeliscid tube matting which is the focus of the whales' feeding efforts is seldom deeper than 10 cm (Nelson et al., 1981). Thus, for the purpose of harvesting amphipods, excavations deeper than 15 cm appear unnecessary.

The gray whale is not the only marine mammal which feeds by excavating benthic infauna. The Pacific Walrus (Odobenus rosmarus) consumes a diet consisting almost exclusively of clams but not excluding certain epifauna such as crabs (Fay, 1982; Frost and Lowry, 1981). The walrus forage for their infaunal prey by hydraulically creating pits and furrows to excavate the

clams. The walrus apparently excavate pits (up to 30 cm in diameter) when foraging in water of good visibility or when hunting for large, isolated deep-burrowing clams such as Mya sp. They create very long, narrow furrows when foraging in water of poor visibility or when searching for smaller, more numerous, near-surface clams such as Spisula sp. or Macoma sp. (Oliver, Slattery, O'Connor and Lowry, 1983). These furrows rarely exceed 40 cm in width but may be several tens of meters long and are distinguishable on the side-scan record due to their extensive length (Figs. 21, 22). Generally, the whale and walrus consume different prey species. This eliminates feeding competition between the two but does not always imply distinctly different feeding grounds.

epifauna but is also known to eat clams. The feeding excavations of the Bearded Seal are likely to be much smaller than those of the walrus simply because of the relative size of the two animals. Competition between the walrus and bearded seal, combined with a rapidly increasing walrus population, has caused the bearded seals to rely more on epifaunal prey and less on clams (Lowry et al., 1980).

Another possible creator of sea floor pits is the sculpin. Divers in the Bering Sea have reported that sculpins are frequently found in round, shallow depressions which are proportional to the size of the sculpin (Thomson, in press). There is some question as to whether the sculpins made the pits or are simply occupying natural depressions or mammal feeding pits. Even though sculpins may grow as large as .75 m, size would still be a limiting factor.

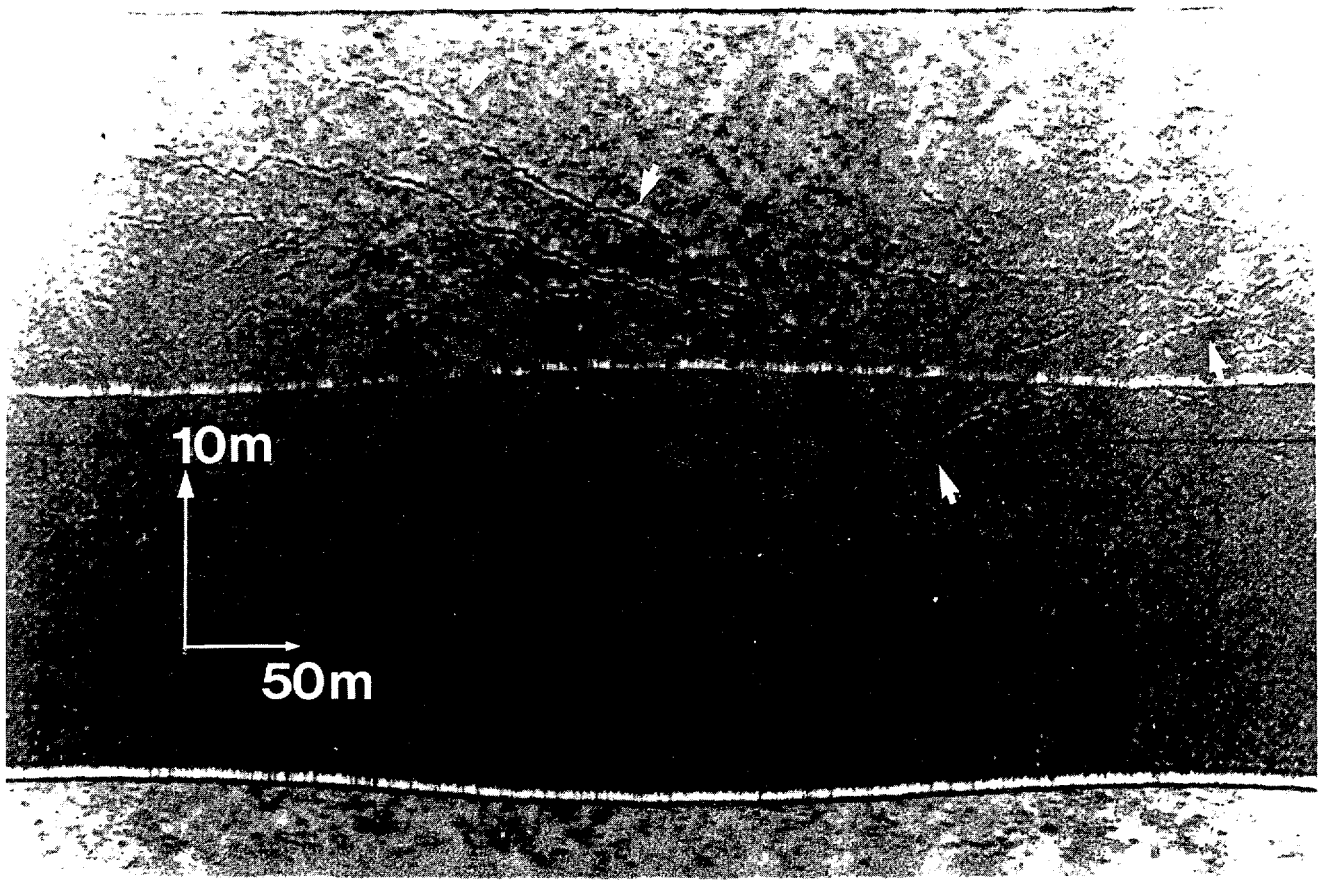

Figure 21 Sonograph of several long, narrow walrus feeding furrows, 100 kHz, eastern Chirikov Basin (see arrows) .

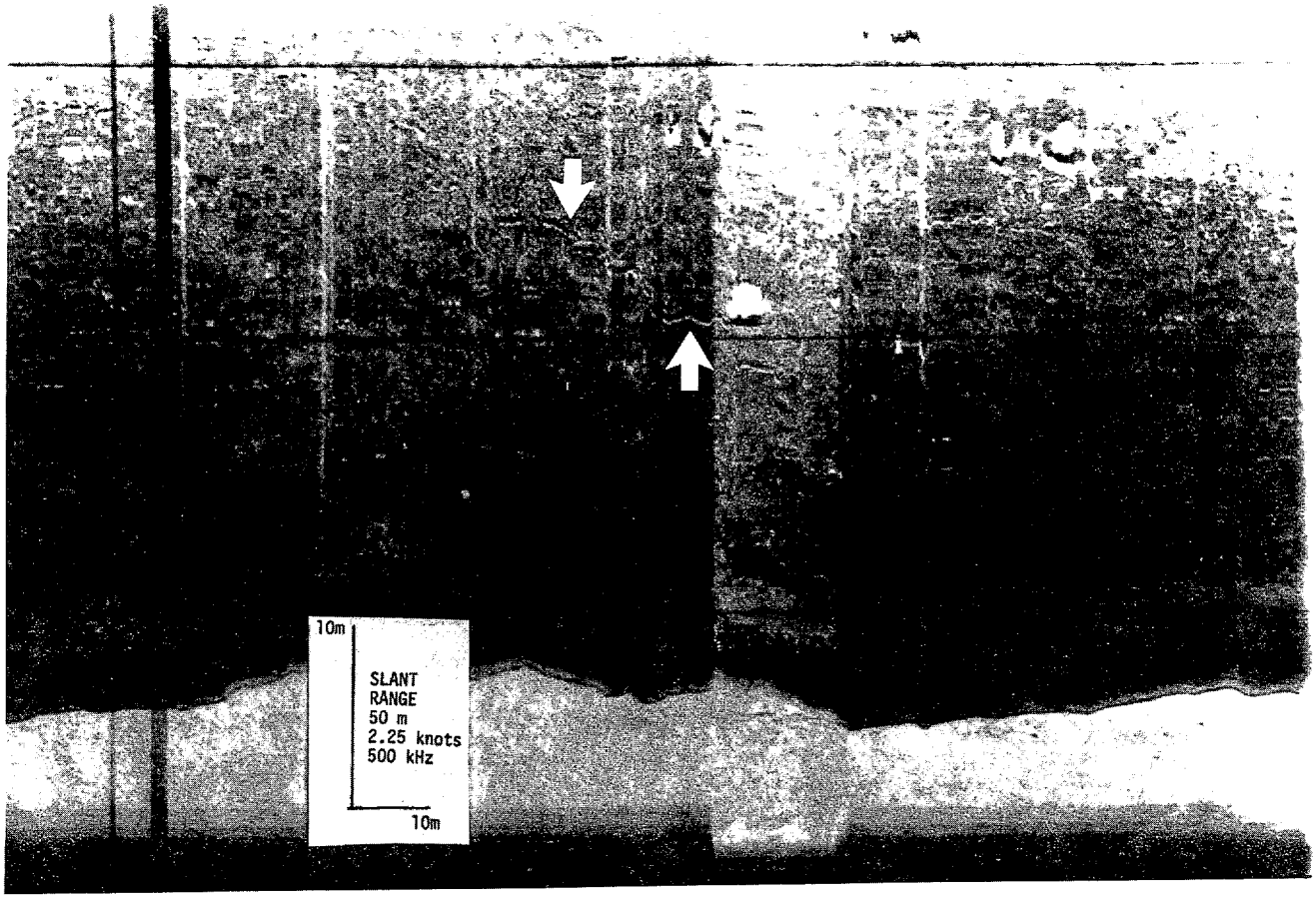

Figure 22 Sonograph of a single walrus feeding furrow, note the large rocks on the record, 500 kHz, northern Chirikov Basin (see arrows for furrow).

WHALE FEEDING PIT TYPES

Compilation of substrate types (Figs. 12-15), high concentrations of Ampeliscid amphipods (Figs. 4, 19), and the summer distribution of gray whales (Figs. 20) all show that the main feeding grounds of the gray whale occur in central Chirikov Basin and around the margins of St. Lawrence Island. Previous studies of physical surficial features on the sea floor (Fig. 16) reveal a general lack of these structures in areas of whale feeding. Consequently, the highly disturbed sea floor in the central Chirikov Basin and nearshore regions of St. Lawrence Island can be attributed to the feeding behavior of the gray whales and subsequent current scour activity triggered by the whales. Diver observations and calibration with high resolution side-scan monographs show that a wide variety of feeding traces exists, but some basic patterns can be described and categorized.

Whale-created pits vary greatly in size but in general they are fairly shallow. Depending on age, the pits may have distinct or gently sloping edges. They may be partially infilled and appear only as a fine textured patch with no edges at all, or they may be greatly enlarged with very distinct edges.

We divide the features into three categories. Type 1 features are any combination of recognizable fresh feeding traces and current-scour-enlarged pits. A fresh feeding trace is defined as a series of oval pits ranging from 1 m to 3 m long and 0.5 m to 1.5 m wide, arranged in an organized pattern implying a multiple suction feeding event (Figs. 23, 24). These groupings of pits are discernible on 105 (Fig. 24) and 500 kHz monographs (Thomson, in

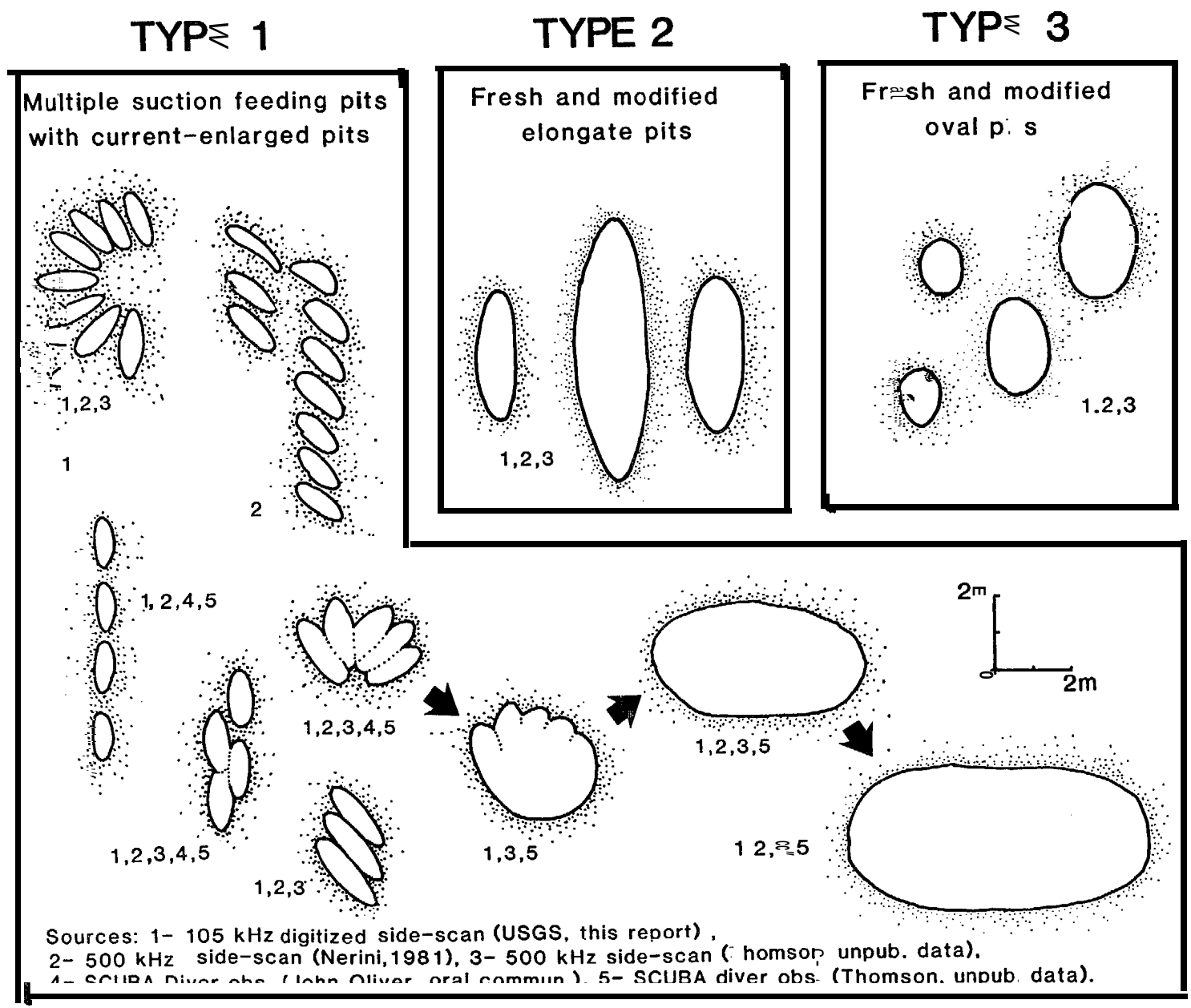

Figure 23 Sketches of three types of bottom pits, attributed to Gray Whale feeding and subsequent current scour, based on observations from side scan sonar and by SCUBA divers in Chirikov basin and the nearshore areas of St. Lawrence Island. All drawings are to the scale shown for Type 1.

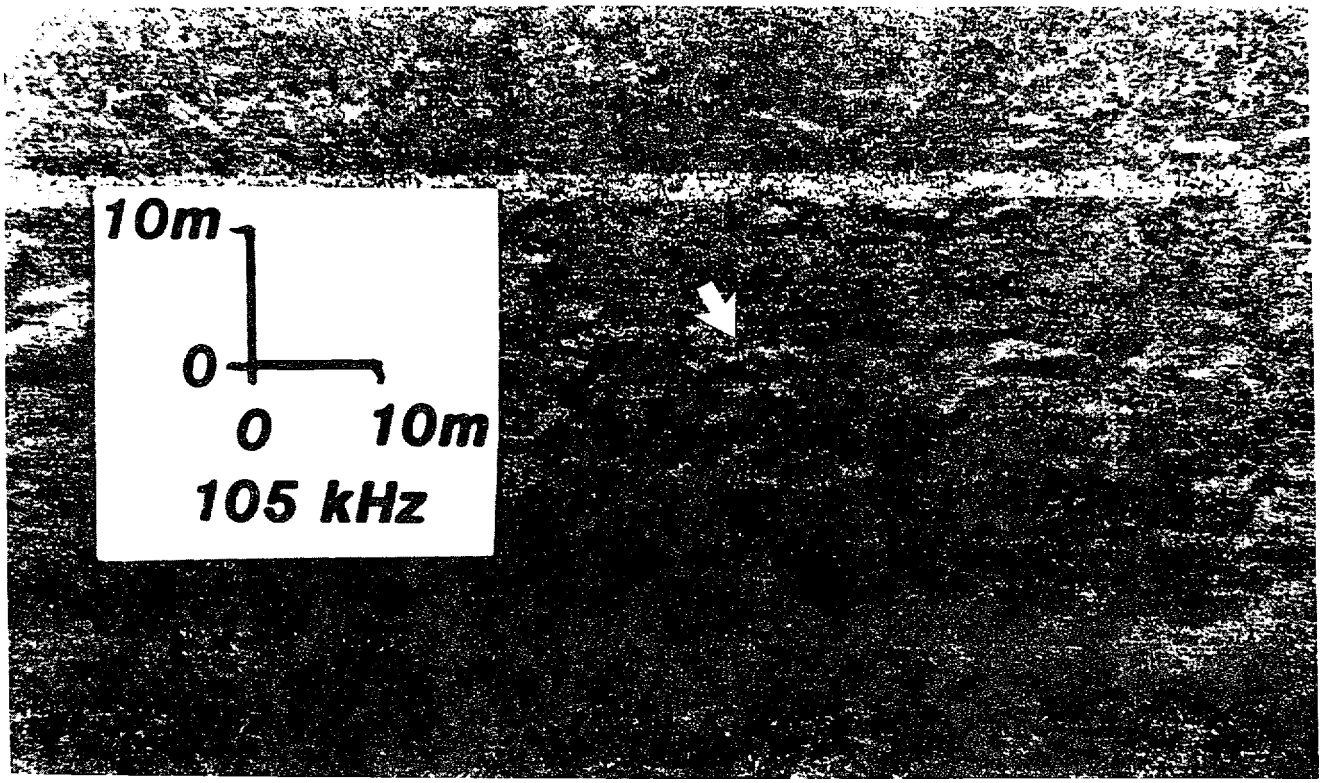

gu

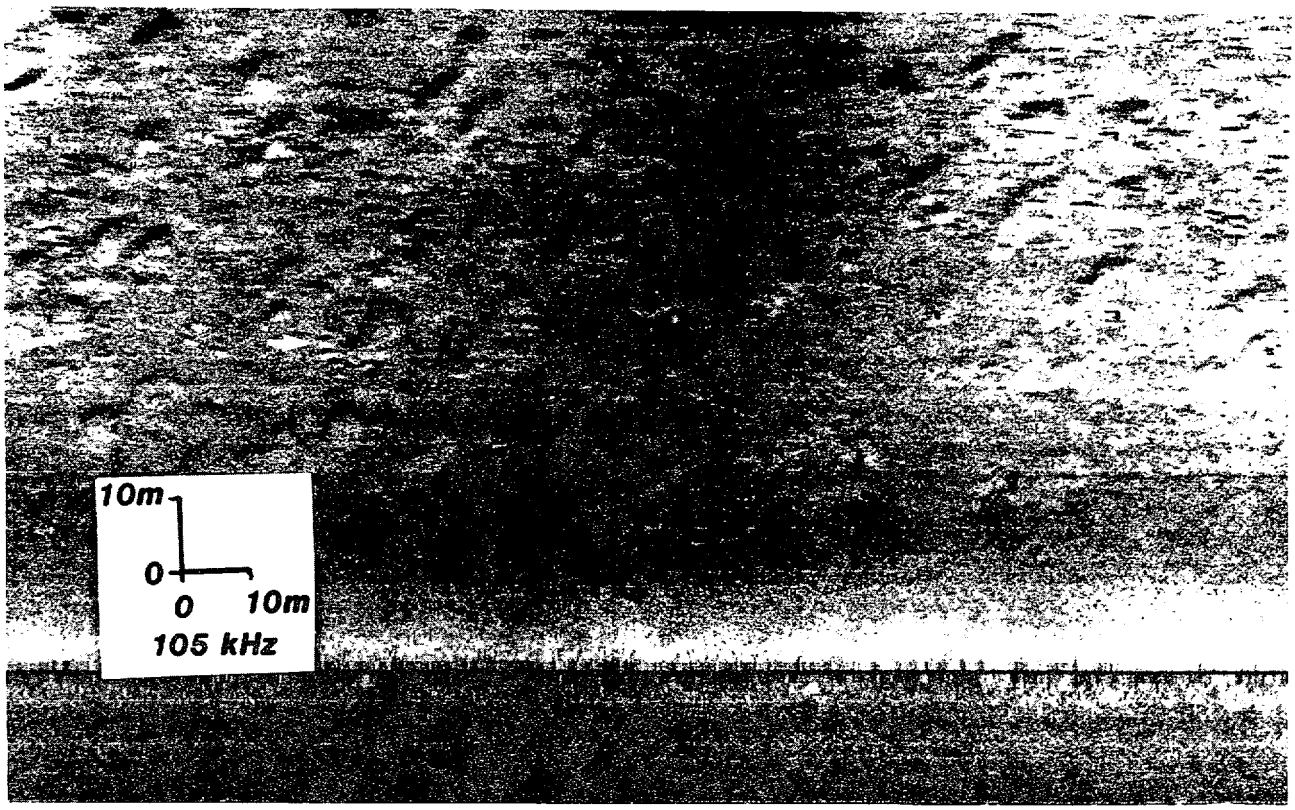

gu

nl

press; Nerini et al., 1980), and have been observed by divers (John Oliver, pers. Comm ., 1983).

The arrangement of pits in a grouping is highly variable, but organized arrangements are seen frequently and these facilitate the recognition of a "fresh feeding area" or "multiple suction feeding event" (Fig. 23). The most common configurations are radiating pits resulting from a whale feeding while slowly turning, large U-shaped groups of pits caused by a whale turning on a larger radius, strings of several pits caused by whale feeding while moving in a straight line, and parallel adjacent pits caused by a whale feeding while moving laterally or drifting (Fig. 23).

Whale fluke marks and depressions made by the body bumping the bottom can be found associated with the multiple suction feeding events. Five hundred kHz side-scan records from the west side of St. Lawrence Island show frequent elongate depressions associated with multiple suction feeding events implying that certain feeding conditions might favor increased contact with the bottom. In general, recognizable fluke or body depressions are rare.

The current-scour-enlarged pits are large (up to 5 m x 20 m) and frequently have a distinct lineation that is parallel to predominant currents (see orientation histograms, Appendix A and Fig. 5). These pits apparently originate as fresh feeding traces. The whale feeding event removes the ampeliscid tube mats that bind the sediment and the exposed fine sand is then subject to erosion by current scour. Frequently, the scour-enlarged pits are seen with remnants of the fresh feeding pits still partially visible (Figs. 23, 25). Type 1 features can consist of fresh feeding traces and current-scour-enlarged pits together implying active feeding and active scour (Figs. 6D, 6E, 25-27); fresh feeding traces alone, suggesting active feeding but

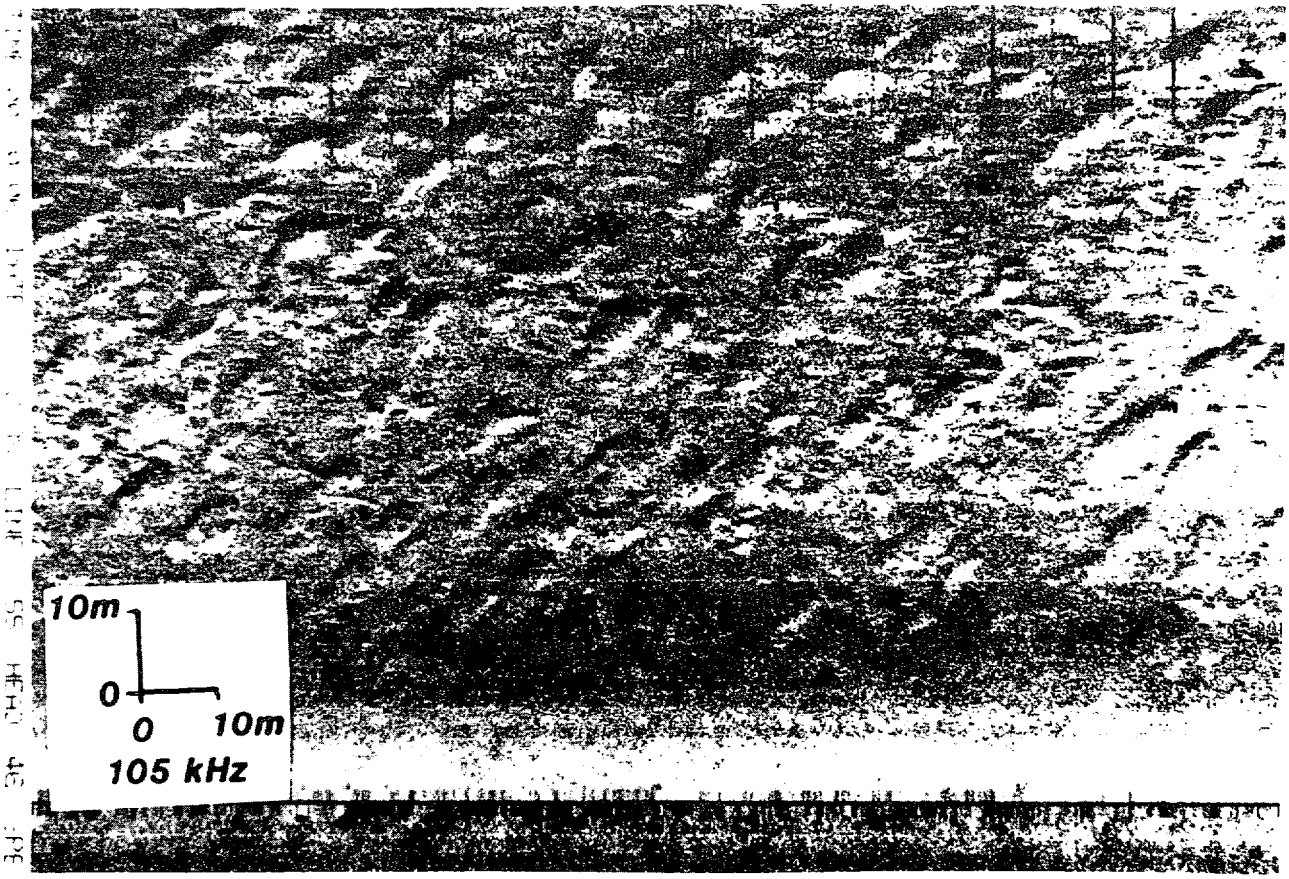

Figure 26 Sonograph of station Dog 1, 105 kHz, Type 1, current-scour enlarged and oriented pits. Sonograph location is shown in Figure 7.

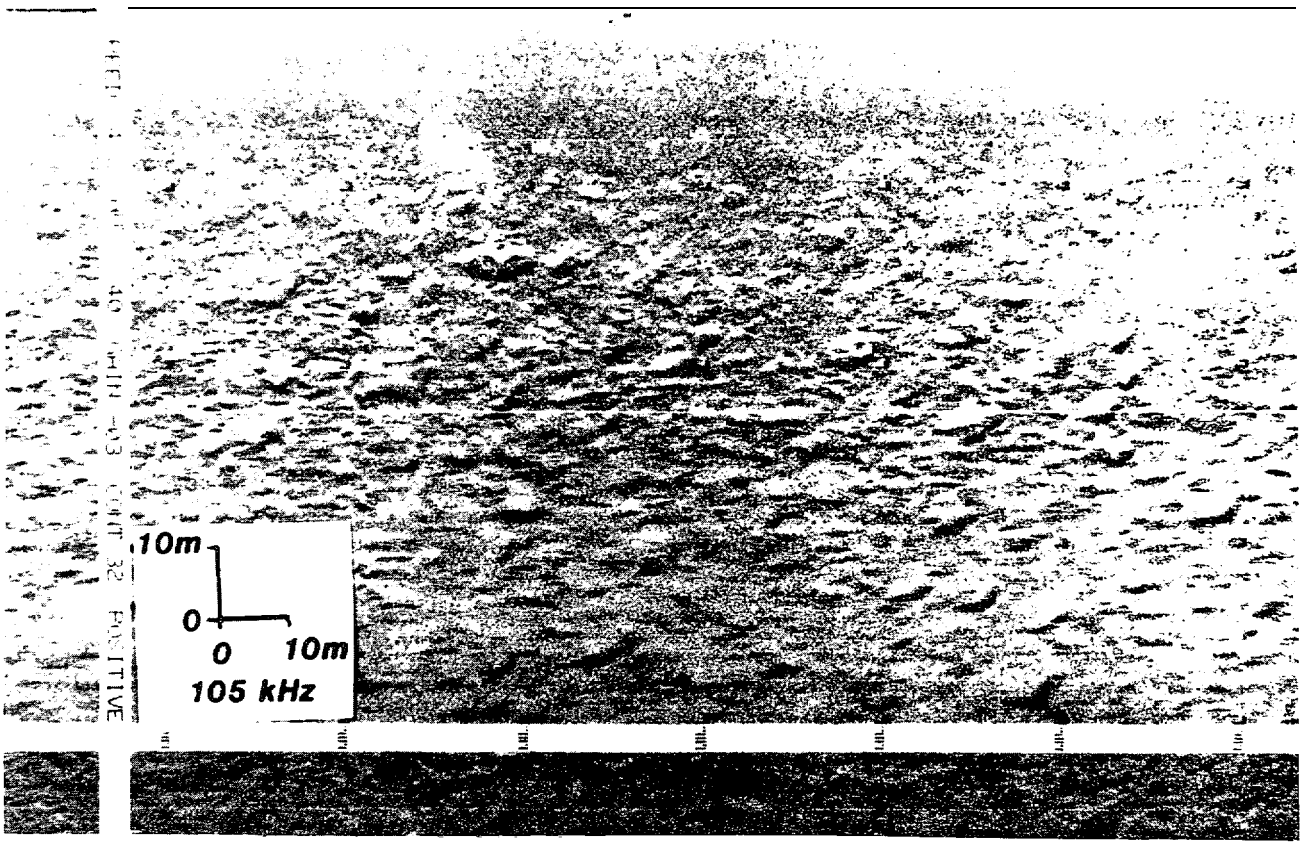

Figure 27 Sonograph of station Dog 14, 105 kHz, Type 1, current-scour enlarged pits. Sonograph location is shown in Figure 7.

insufficient current to initiate scour (Fig, 43); or current-scour-enlarged pits alone, indicating scour in an area where feeding has occurred but is not presently active (Fig. 6G).

Type 2 features are elongate pits measuring up to 20 m but averaging between 3 m and 5 m in length and 1 m to 2 m in width. They are discernible on 105 (Figs. 28-32) and 500 kHz monographs (Figs. 6F, 6H) (Thomson, in press) . SCUBA divers have not inspected these features yet. Their probable origin is either the feeding trace of a moving whale or a slightly modified set of fresh feeding pits. Occasional multiple suction feeding features are found in Type 2 areas (Fig. 31).

Type 3 features are oval pits averaging from 1.5 m to 3.1 m in length and 0.9 m to 2 m in width. They are discernible on 105 (Figs. 6A, 6B, 33-39) and 500 kHz monographs (Thomson, in press) and have been observed by divers (Nerini et al., 1980; Thomson, in press). Generally, they occur in a fairly random scattering across the sea floor, but in some cases, they can be found in ordered groups, either as elongate strings of oval pits (Fig. 33) or in clover-shaped clusters of pits. With some notable exceptions (Figs. 6A, 34, 36), Type 3 features are of low density.

Types 1, 2, and 3 are distinguished by their average length vs. width ratios. Type 3 features have l/w less than 2.3, Type 1, l/w = 2.3-3.0, and Type 2, l/w greater than 3.0. Adopting Hickey's (1973) terminology to describe the shapes of dicotyledonous leaves by their length-width ratios, the Type 3 features are wide elliptic, the Type 1 features are elliptic, and the Type 2 features are narrow elliptic to very narrow elliptic.

Figures 6 and 40 show the distribution of Types 1, 2, and 3 in Chirikov Basin and the area immediately south of St. Lawrence Island. Type 1 features

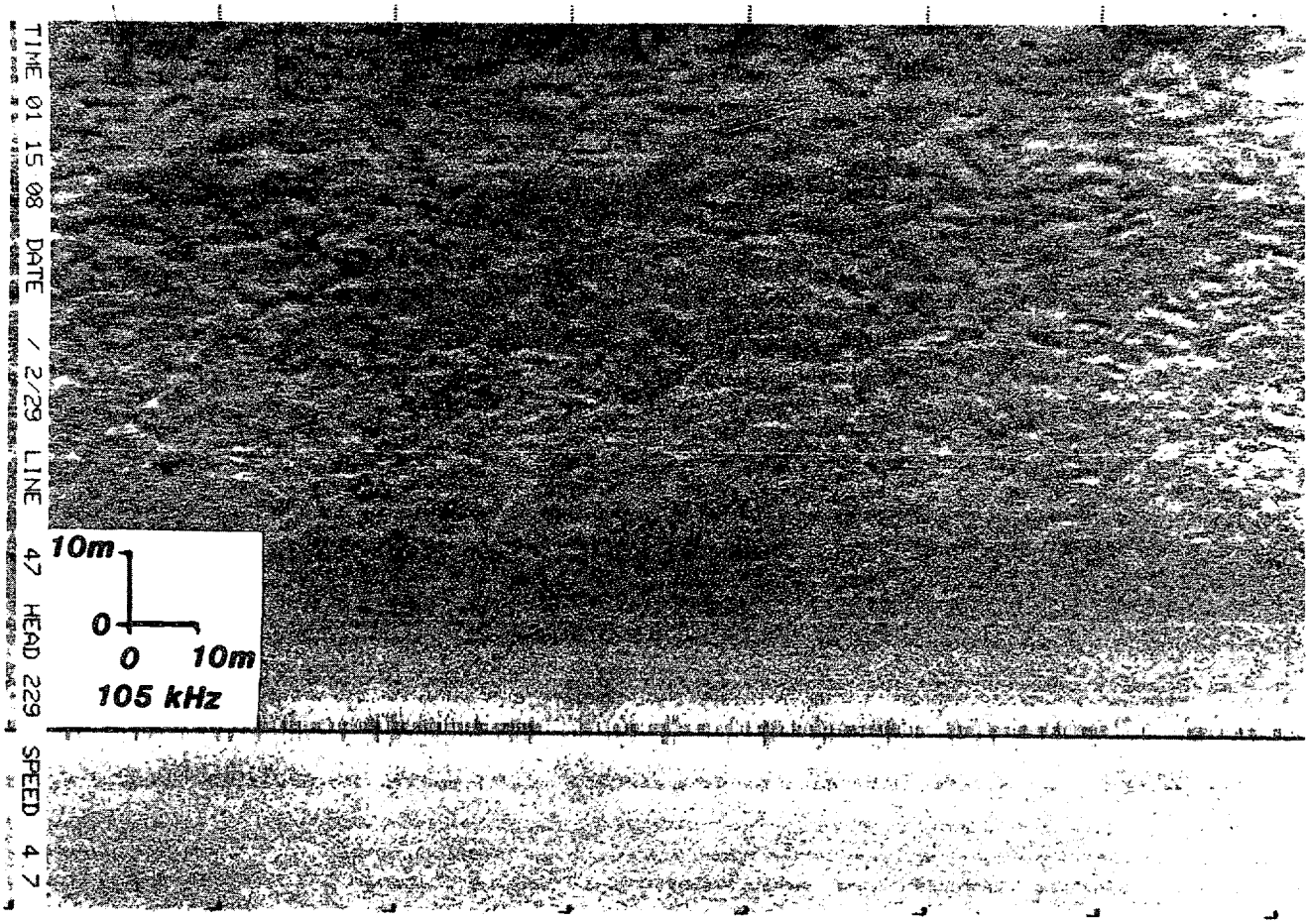

Figure 28 Sonograph of station Dog 3, 105 kHz, Type 2, elongate pits pervasive throughout the record. Sonograph location is shown in Figure 7.

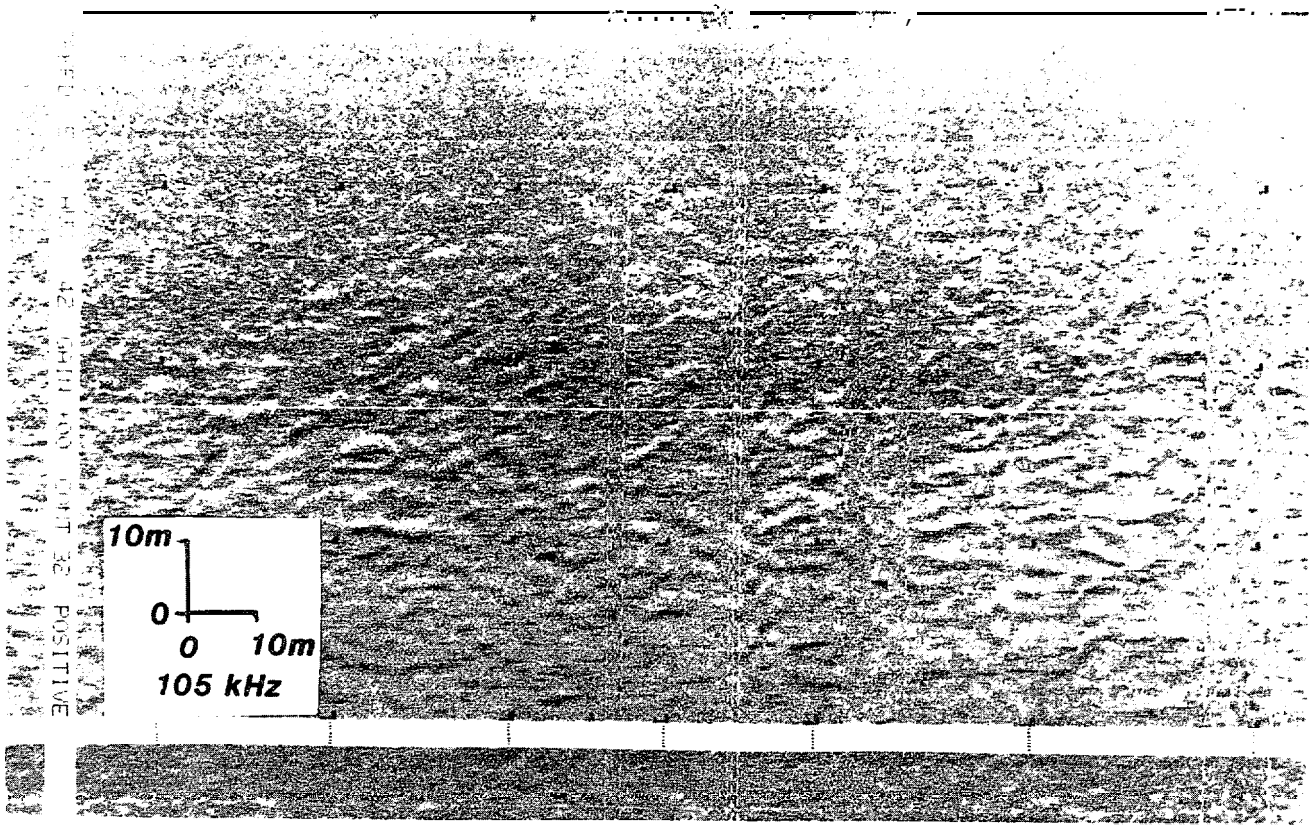

Figure 29 Sonograph of station Dog 4, 105 kHz, Type 2, elongate pits pervasive throughout the record. Sonograph location is shown in Figure 7.

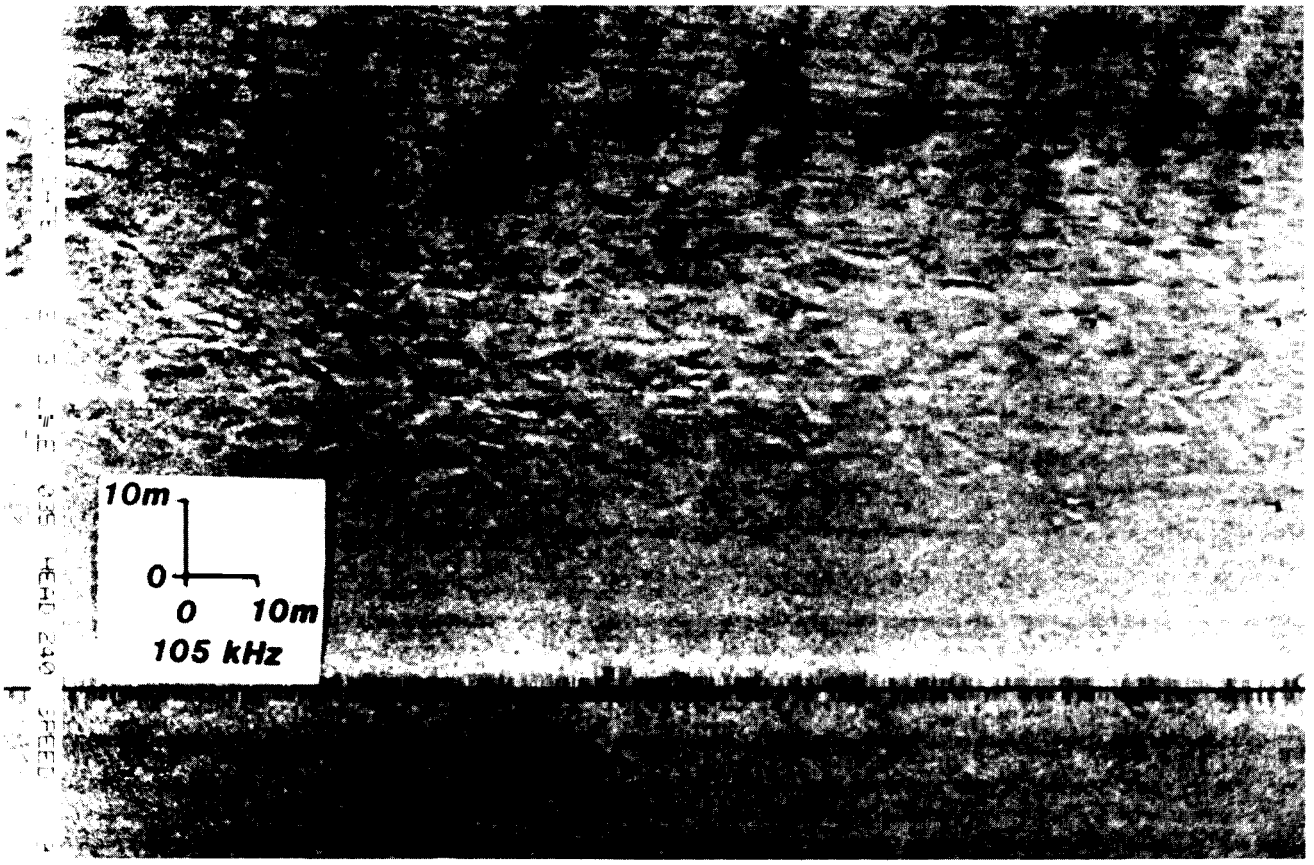

Figure 30 Sonograph of station Dog 6, 105 kHz, Type 2, elongate pits pervasive throughout the record. Sonograph location is shown in Figure 7.

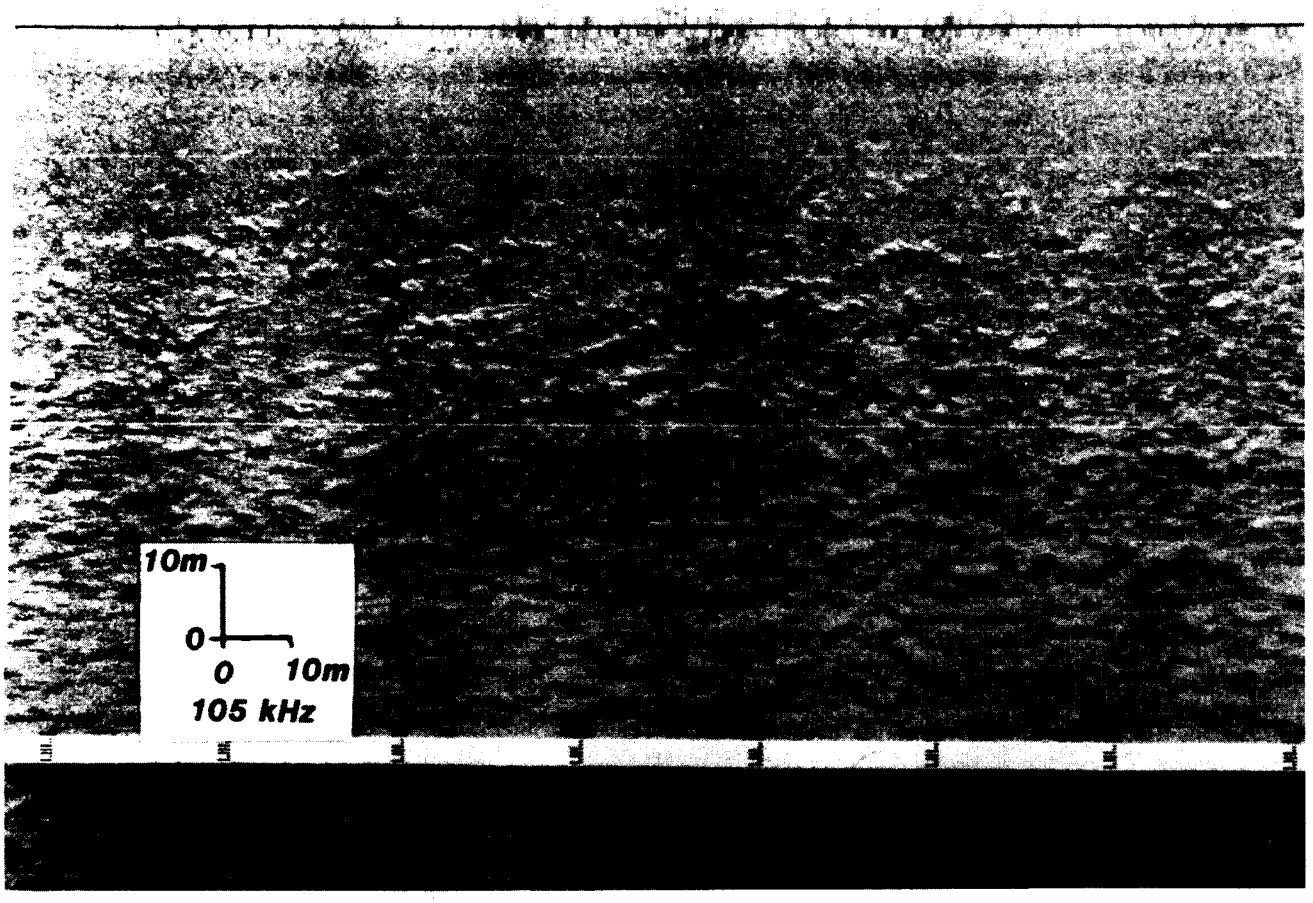

Figure 31 Sonograph of station Dog 12, 105 kHz, Type 2, dense fresh and partially modified pits. Sonograph location is shown in Figure 7.

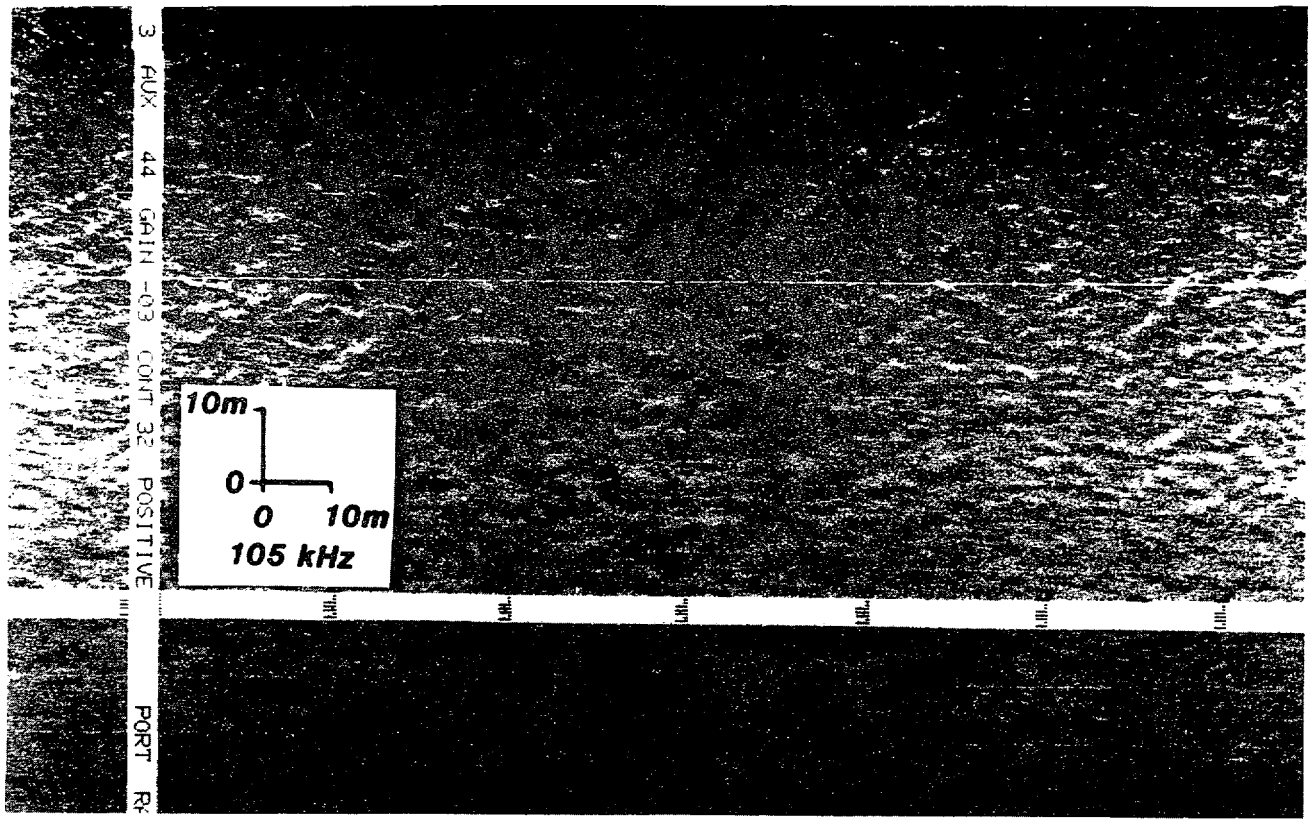

Figure 32 Sonograph of station Dog 13, 105 kHz, Type 2, common elongate pits. Sonograph location is shown in Figure 7.

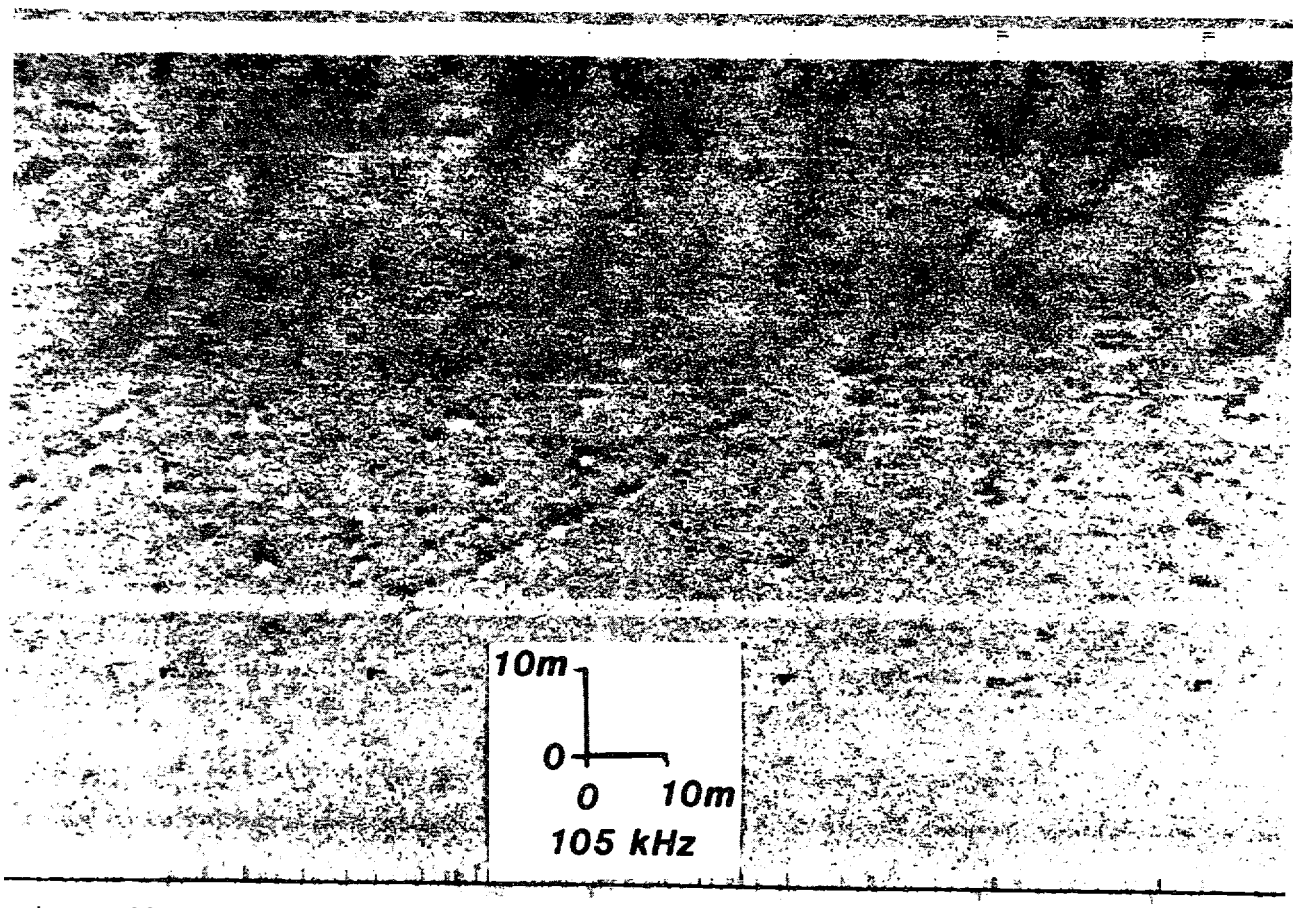

Figure 33 Sonograph of station Dog 2, 105 kHz, Type 3, scattered oval pits. Note elongate chain of pits in center of sonograph. Sonograph location is shown in Figure 7.

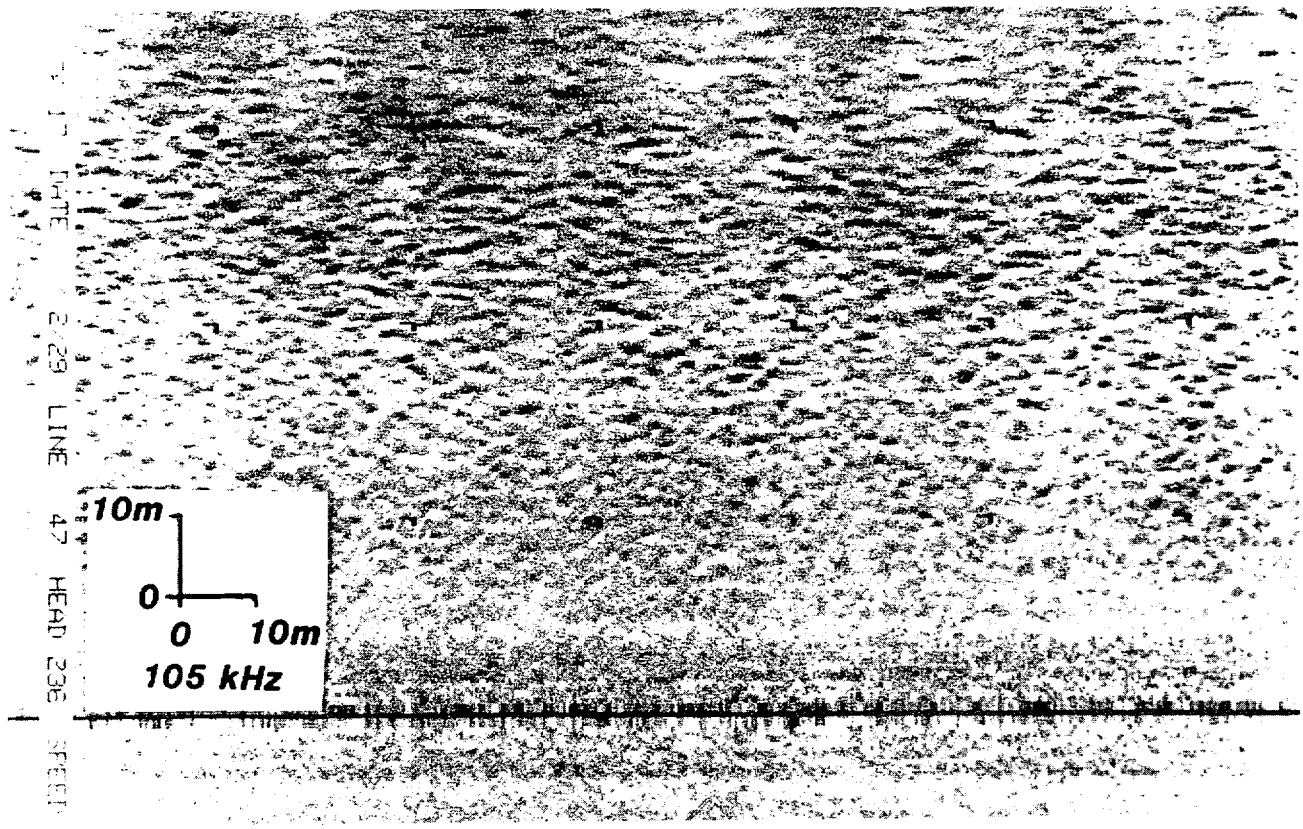

Figure 34 Sonograph of station Dog 5, 105 kHz, Type 3, dense oval pits. Note side-scan distortion which stretches pits that are near the margin of the record. Sonograph location is shown in Figure 7.

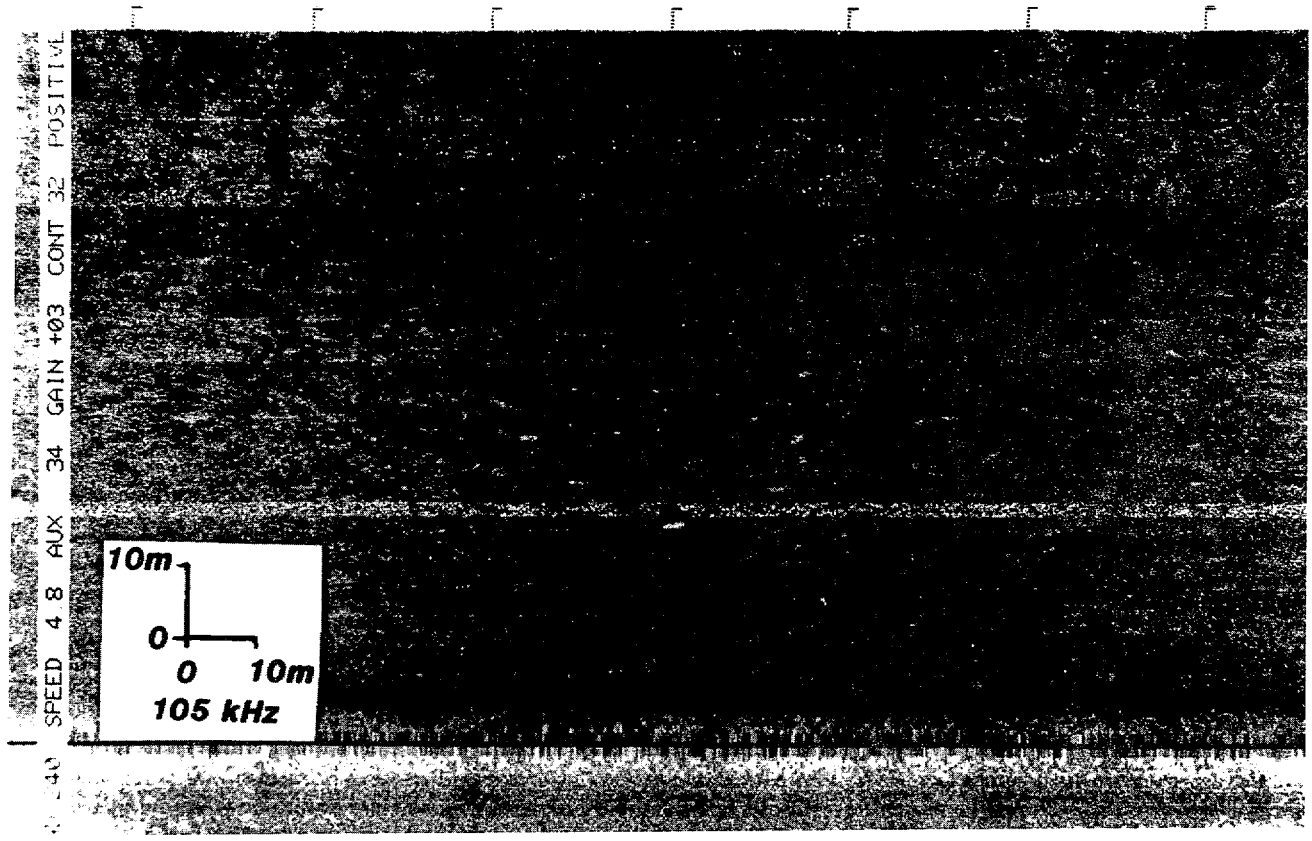

Figure 35 Sonograph of station Dog 9, 105 kHz, Type 3, scattered oval pits. Sonograph location is shown in Figure 7.

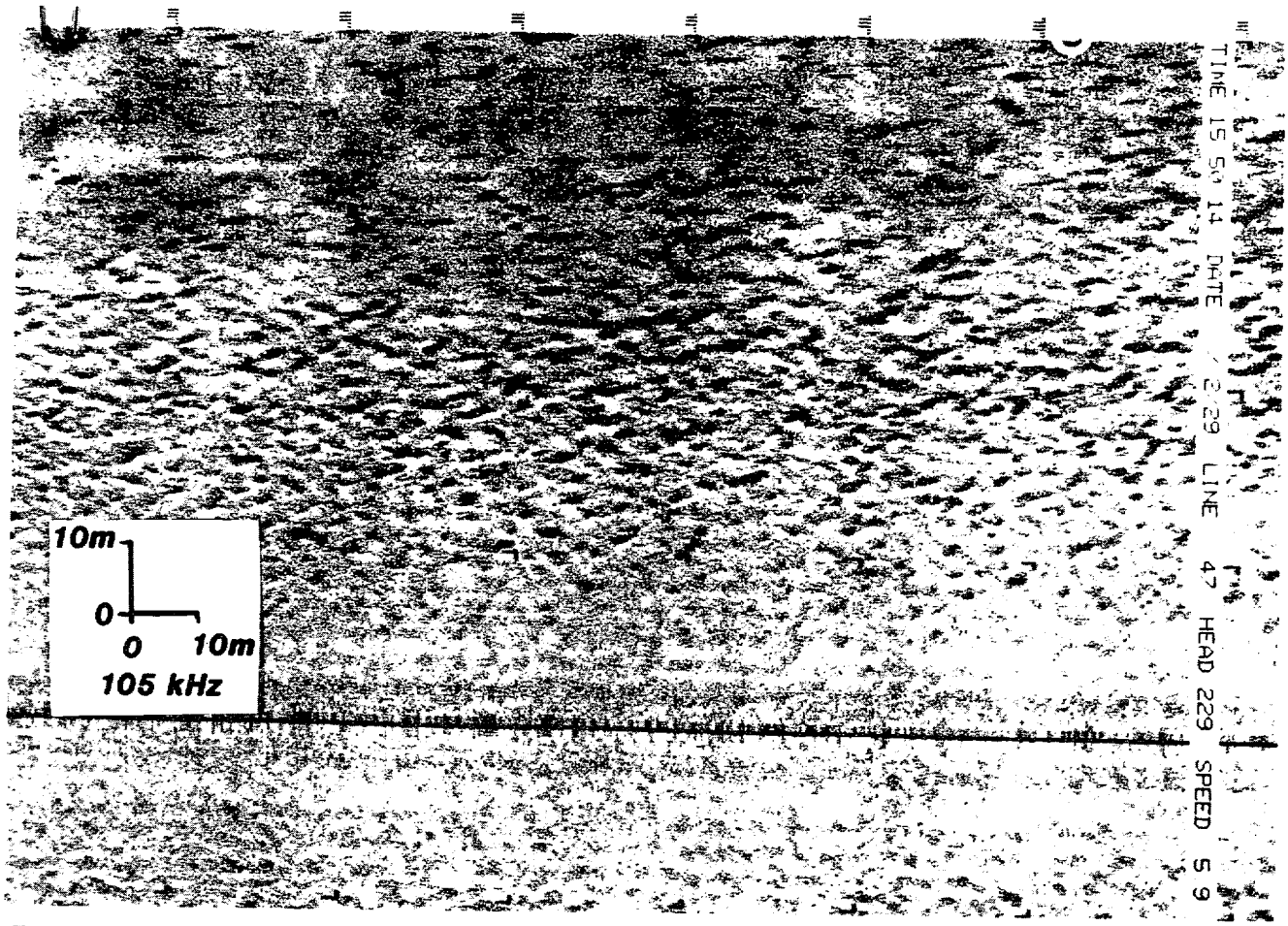

Figure 36 Sonograph of station Dog 10, 105 kHz, Type 3, dense oval pits. Sonograph location is shown in Figure 7.

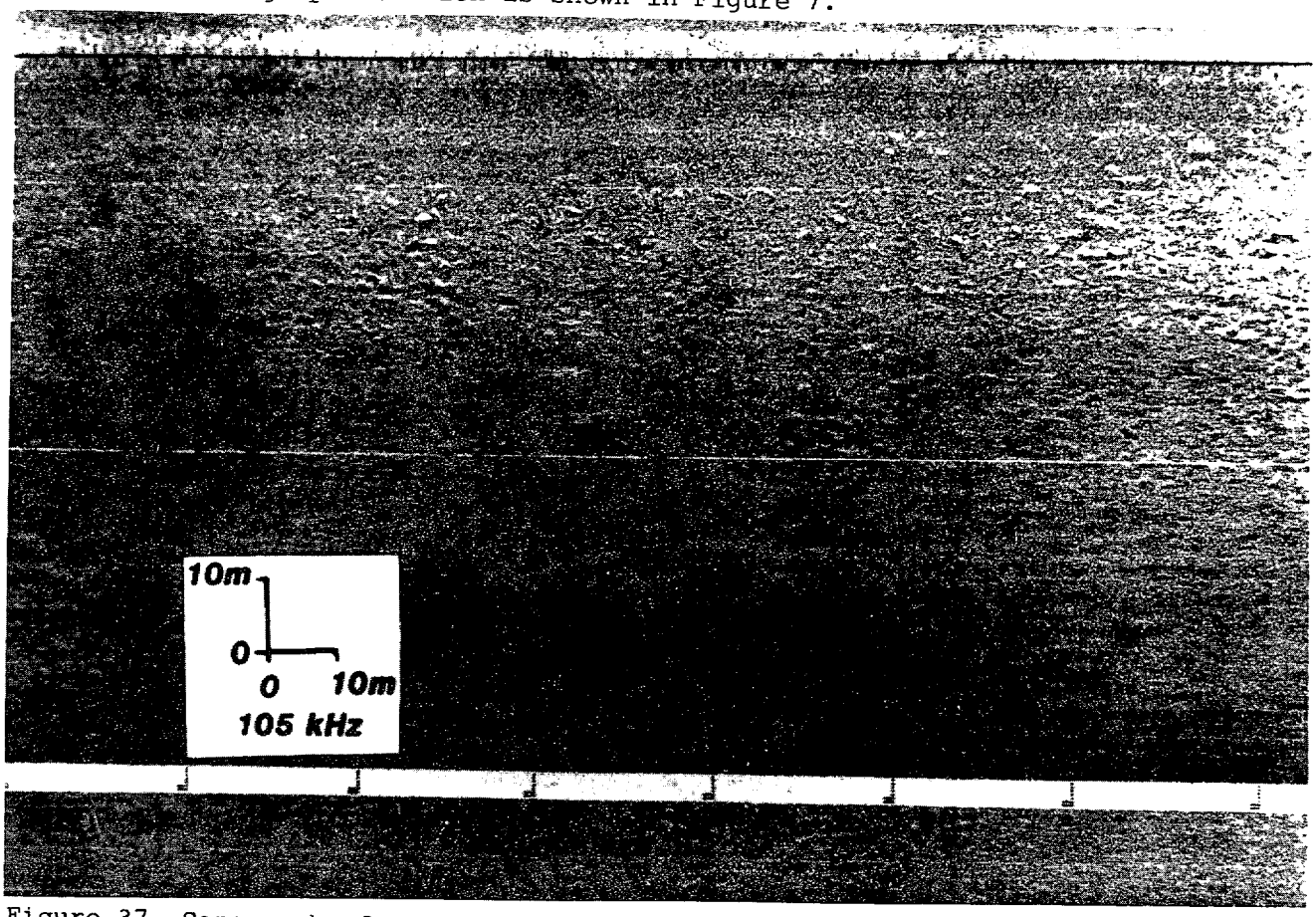

Figure 37 Sonograph of station Dog 11, 105 kHz, Type 3, sparse oval pits. Sonograph location is shown in Figure 7.

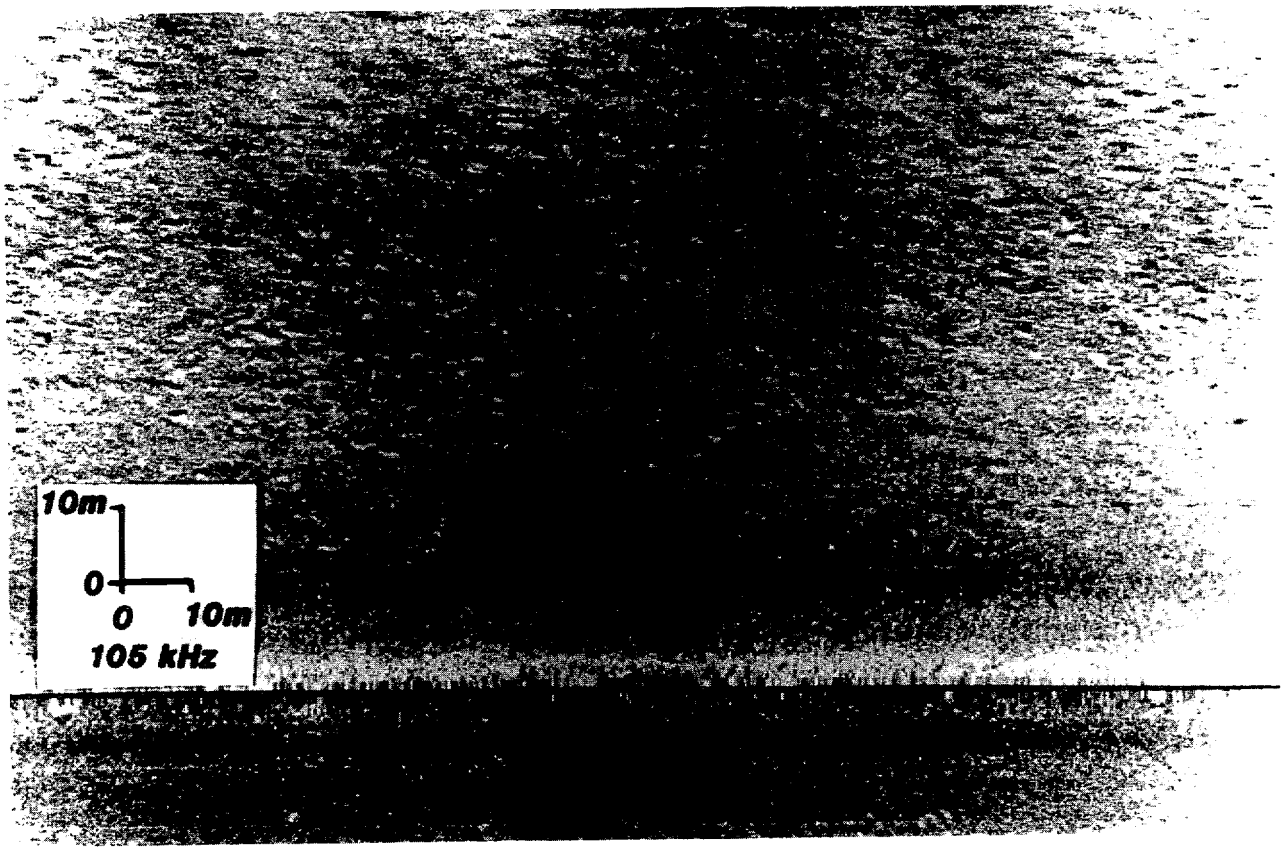

Figure 38 Sonograph of station Dog 15, 105 kHz, Type 3, sparse oval pits. Sonograph location is shown in Figure 7.

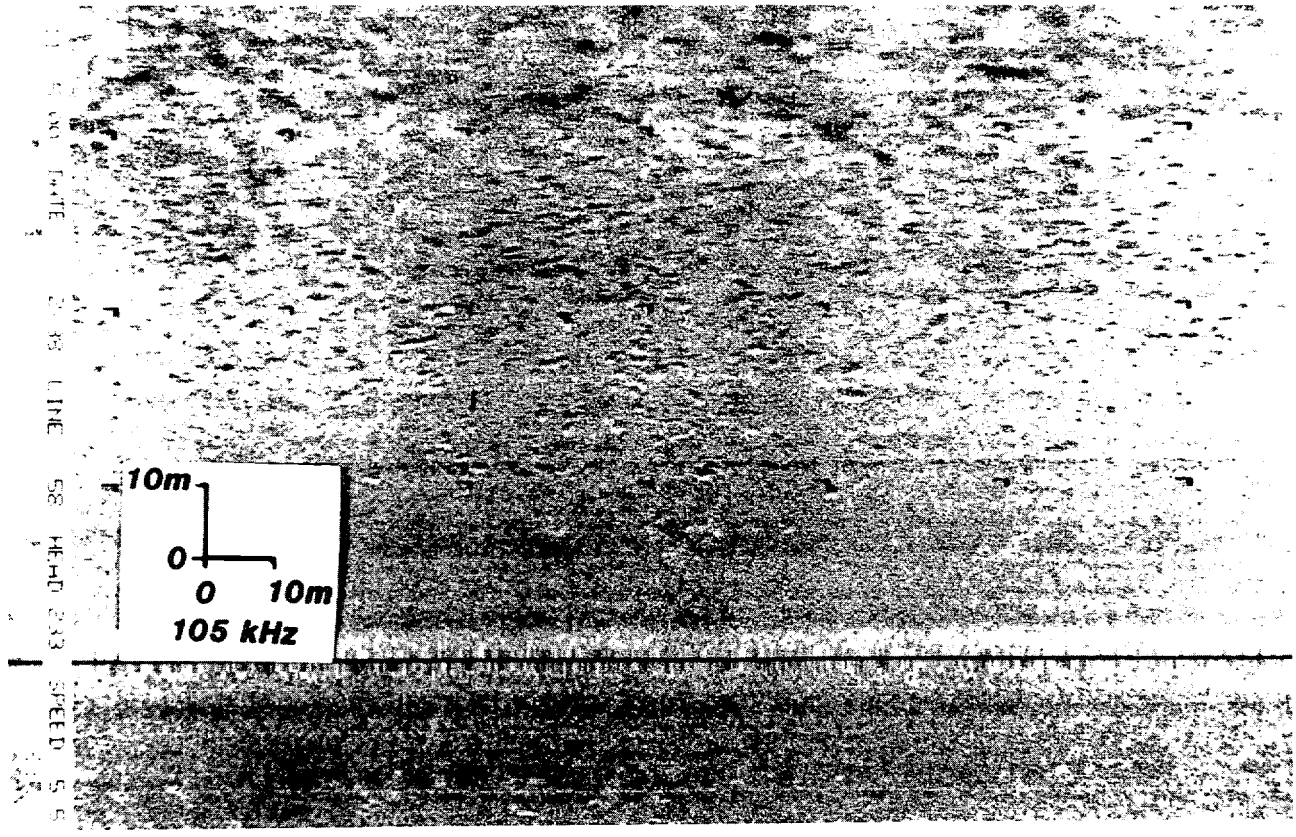

Figure 39 Sonograph of station Dog 16, 105 kHz, Type 3, sparse oval pits. Sonograph location is shown in Figure 7.

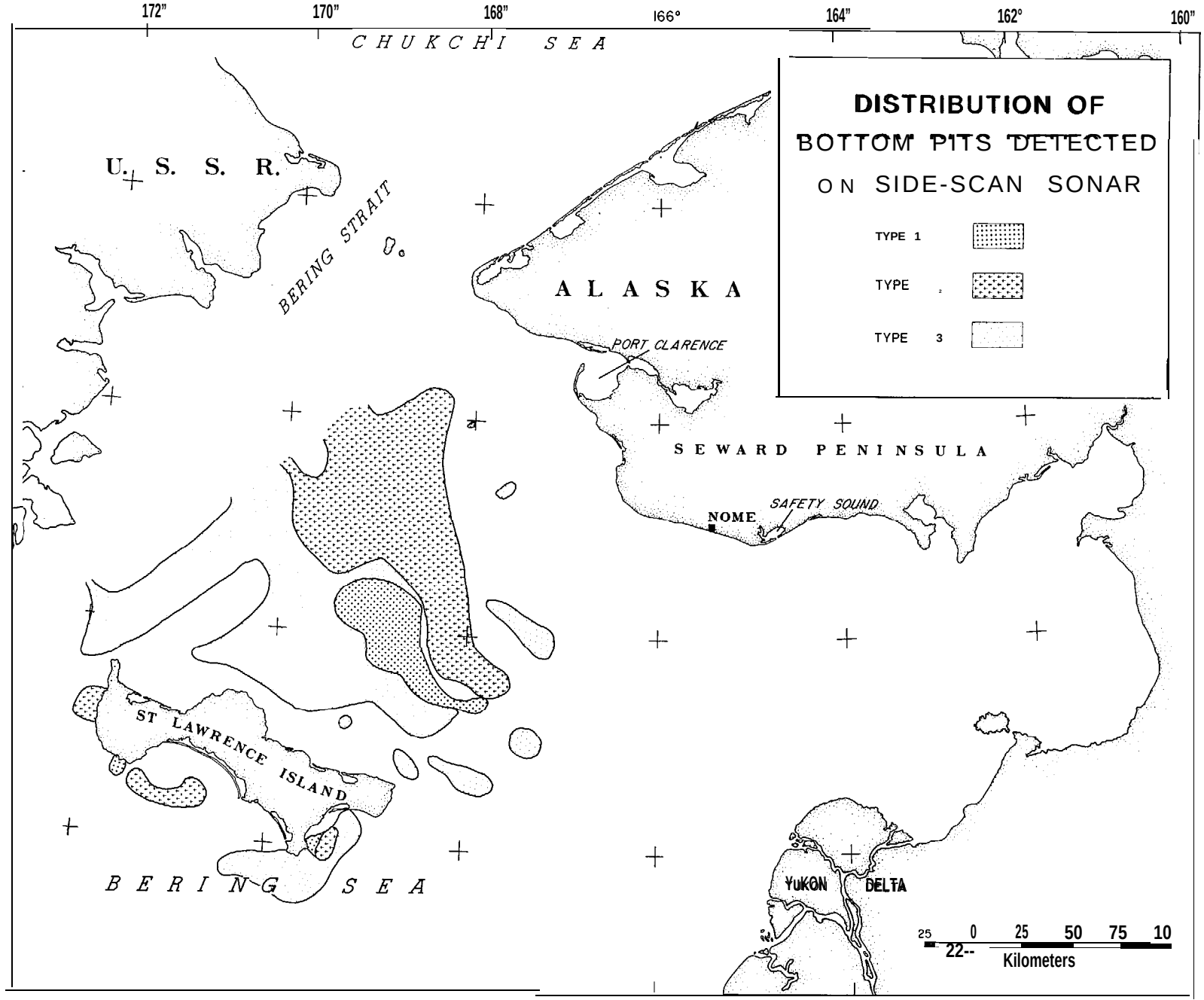

Figure 40 Distribution of three types of bottom pits, mapped by side-scan sonar and attributed to Gray Whale feeding on the seafloor of Chirikov basin, northeastern Bering Sea.

occur in the southeast portion of the center of the basin and in two isolated locations on the south side of St. Lawrence Island. Type 2 features are located in a large zone in the center of the basin and in three localities on the south side of the island. Type 3 features are found to the south of Type 1 and 2 zones in the center and south parts of the basin and to the south of these zones at the southeast cape of the island. Type 3 features occur as a halo around the other two types of features. In all, there exist 20,000 km^2 of sea floor in Chirikov Basin and 2,000 km^2 around St. Lawrence Island that bear evidence of gray whale feeding activity (Fig. 40).

The quantification of pit dimensions and area for stations Dog 1-Dog 16 (Fig. 7) and station Tate 1 are presented in Tables 2 & 3, Figures 41 and 42, and Appendix A. The range of total bottom disturbance in Type 1 areas is 4-18%, 5-15% in Type 2 areas, and 2-13% in Type 3 areas. Type 1 areas have high percentages of total disturbance, but a majority of this comes from the largest size class of pits. In general, the Type 2 areas are the most thoroughly reworked and uniformly disturbed areas of sea floor. The pitting occurs on an undulating bottom that bears evidence of much previous disturbance. The pit size distribution shows a fairly even representation of all four size classes (Table 3). Type 3 areas commonly contain pits of only the smallest size class and the density of pits is usually quite low. Exceptions to this are stations Dog 5 and Dog 10, which are close together and have high pit densities.

The smallest fresh feeding size class (0-5.3 m^2) is assumed to represent fresh feeding traces and this bottom disturbance ranges from 0.94-4.45% in Type 1 areas, 3.4-4.92% in Type 2 areas, and 2.0-11.86% in Type 3 areas. The average percent bottom disturbance by the fresh feeding pit size class (0-5.3

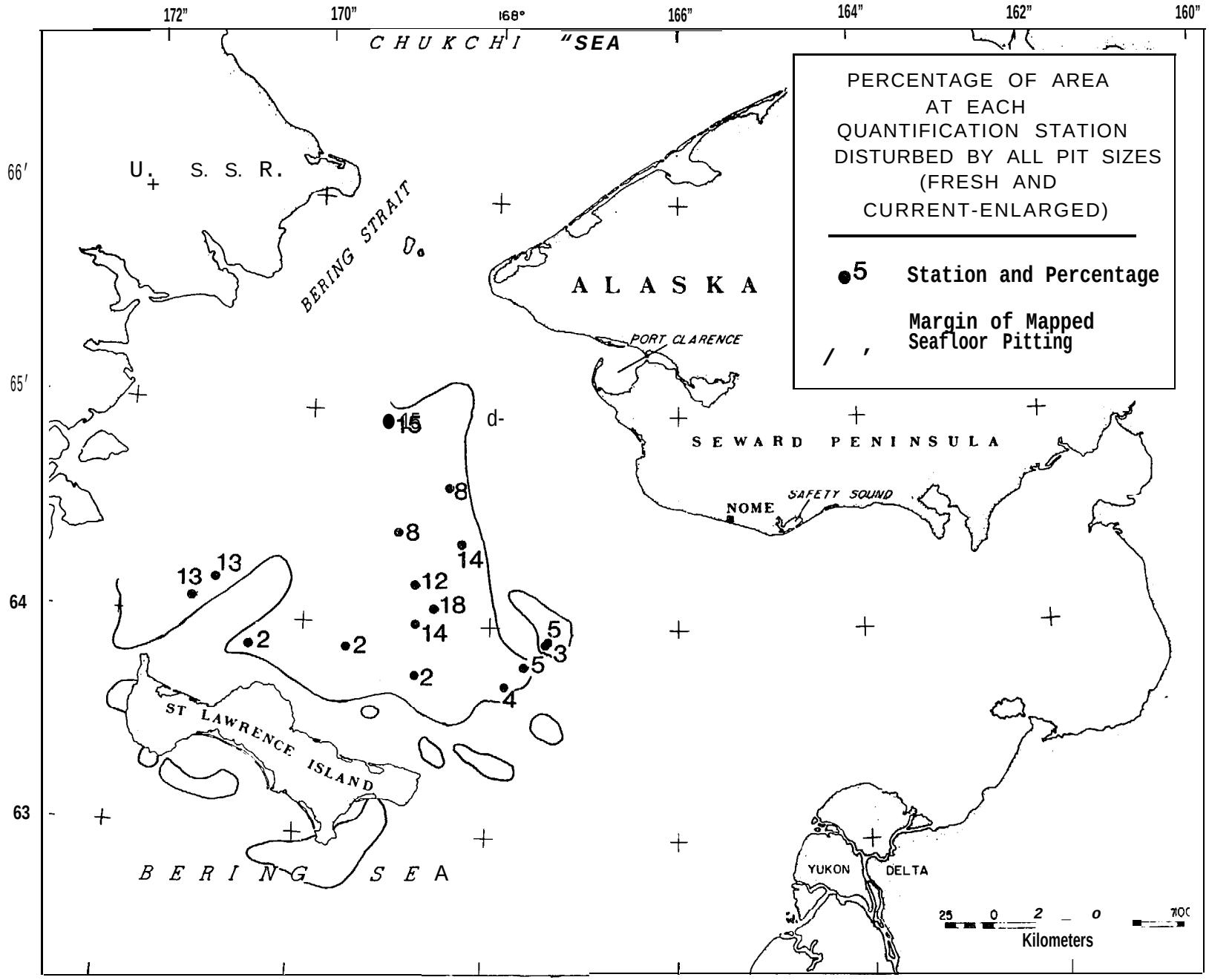

Figure 41 Total percentage of area at each side-scan quantification station disturbed by all fresh and current-enlarged feeding pits.

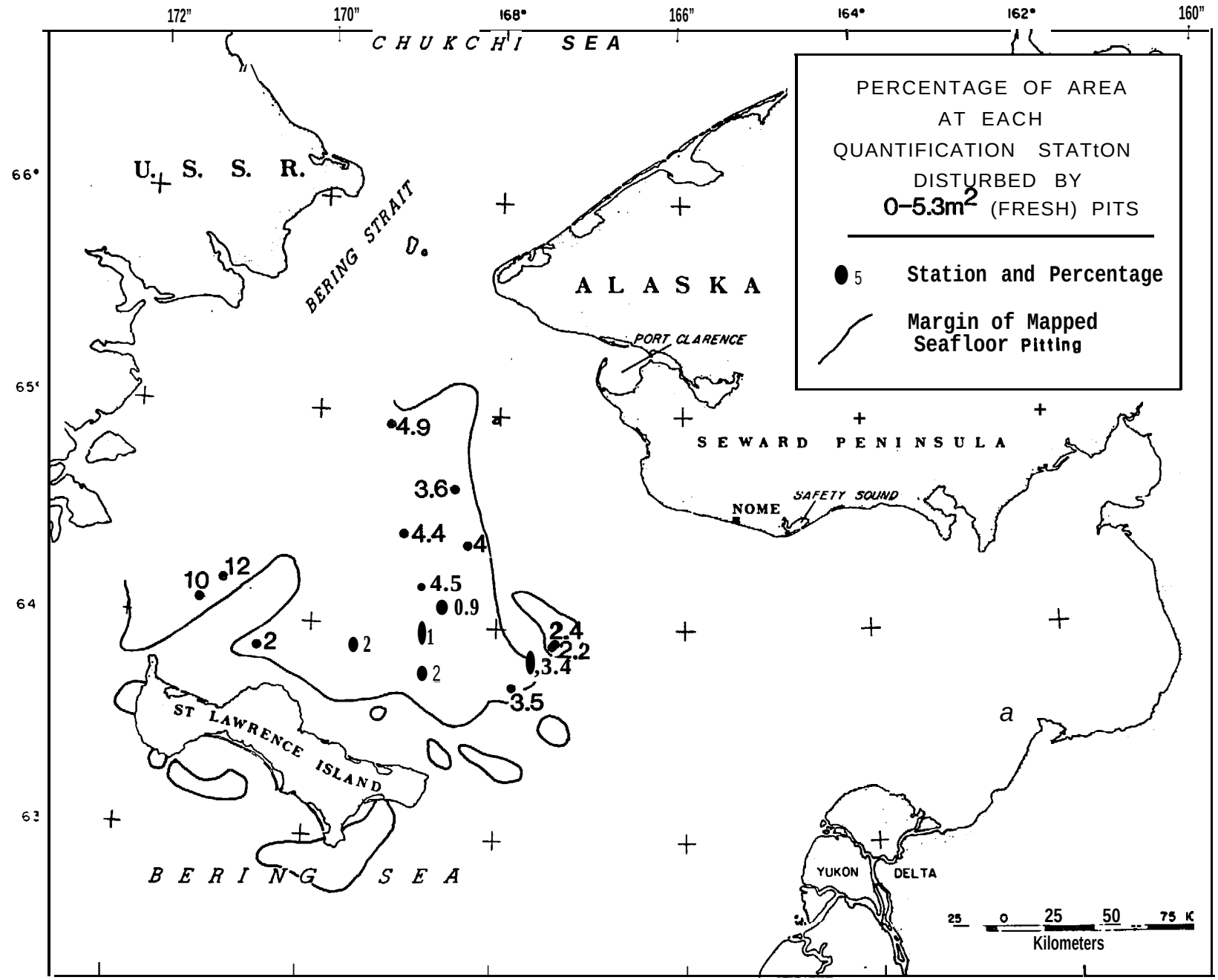

Figure 42 Percentage of area at each side-scan sonar quantification station disturbed only by fresh feeding pits in the smallest size class (0-5.3 m^2).

m^2) is 3.4% for the entire study area. It is important to remember that these percentages are taken from monographs which underrepresent small features that are not parallel or sub-parallel to the trackline; consequently, these figures are low by an unknown amount that could be as large as 100% and the percentages given must be recognized as minima.

ORIGIN, MODIFICATION, AND DISTRIBUTION OF SEA FLOOR PITS

Type 1 features

Type 1 features are a combination of fresh whale feeding pits and current-scour-enlarged pits. The postulated mechanism of formation of the enlarged pits is as follows: whale feeding activity removes the amphipod mat which fixes the surface of the sediment. In areas or periods of strong bottom currents, the fine sand exposed under the mat is then subject to removal by current scour. The remaining mat around the margins of the pits is undercut and slumps into the pit. This continues until the pits are quite large. At a certain point, colonizing amphipods are able to re-establish a mat community in the center of the pit and restabilize the area.

The amount of time this process takes is not known. Divers from the L.G.L. 1982 cruises discovered amphipod tube mats slumping in on the pit margins as well as apparently new colonization of the amphipod tube mat in the center of the larger pits. The divers also found that certain pits accumulated debris such as seaweed and appeared to have some infilling rather than enlarging. It is likely that the pits enlarge most readily during the storm season when bottom currents are greatly augmented by the effect of wave swell and sediment movement. Thus, the pits may be inactive or be gradually

infilling during the long period of relative quiescence from November to September and receive most of their modification between September and November. This explains why the pits do not appear to be in the active process of modification during the summer months when they are inspected by divers.

The Type 1 area, then, is composed of a complex group of bottom features in different stages of modification. Certain Type 1 areas contain only fresh feeding pits (Fig. 43). This indicates that current velocities are not sufficient to enlarge these pits. Other Type 1 areas contain only current-enlarged pits suggesting that the whales have not actively fed in this area for some time. A less likely possibility is that they are feeding on the margins of the enlarged pits.

Frequently, Type 1 areas show distinct populations of fresh and enlarged pits supporting the theory that pit formation and enlargement are seasonal and not continuous activities. If either pit formation or modification were continuous throughout the year, one would expect to see a continuum of pit sizes ranging from fresh to greatly enlarged. Since both the times of feeding and of strong currents are seasonal, separate classes of pit sizes are expected in the Bering Sea setting. For example, two separate populations of pits can be seen in station Dog 1 (see Appendix A, Fig. 26). This separation is manifested in the pit length histogram, and in the length vs. width plot. Bimodality of the pit length histogram indicates two populations of pits whereas one population of gradually enlarging pits would be represented by a single curve skewed to the right. This situation also occurs in station Dog 8. In station Dog 14, the pit length histogram is a single curve skewed to the right but the area histogram is bimodal. The length vs. width plot also

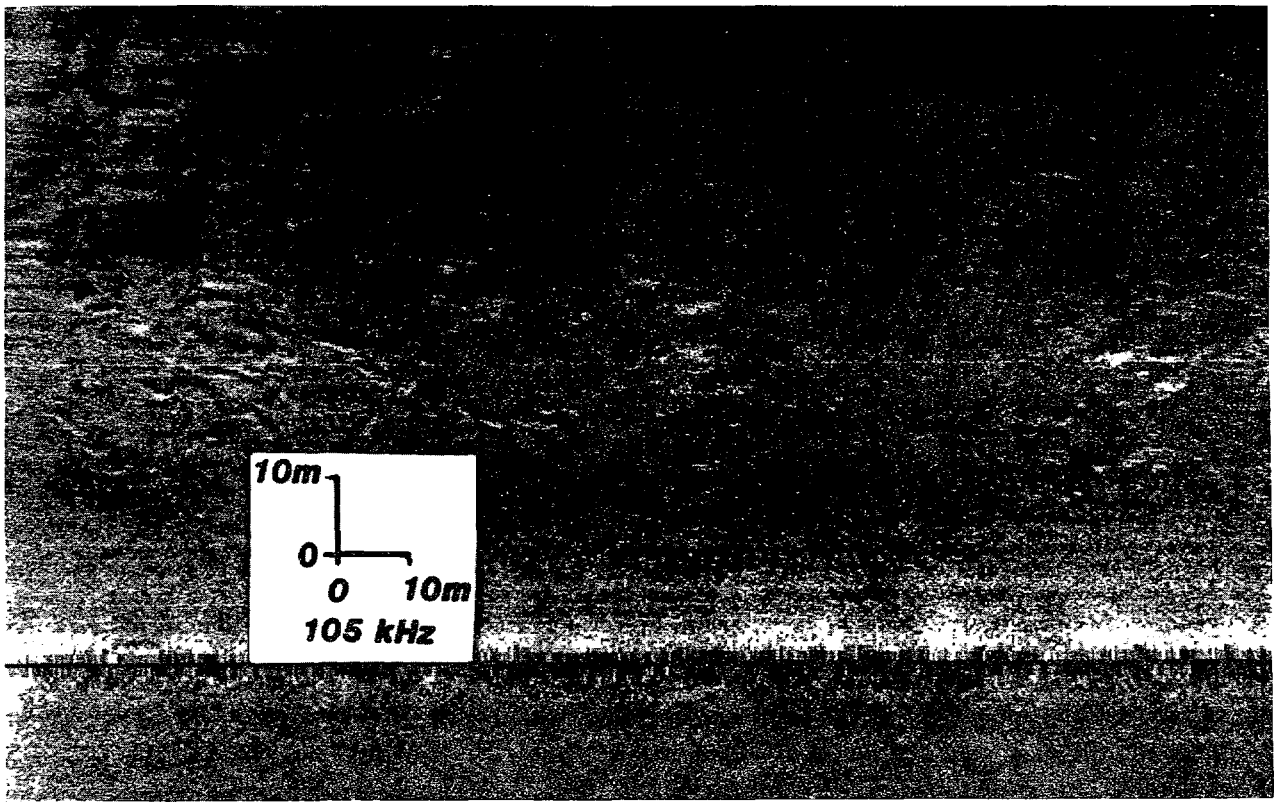

gu

events. Sonograph location is shown in Figure 7.

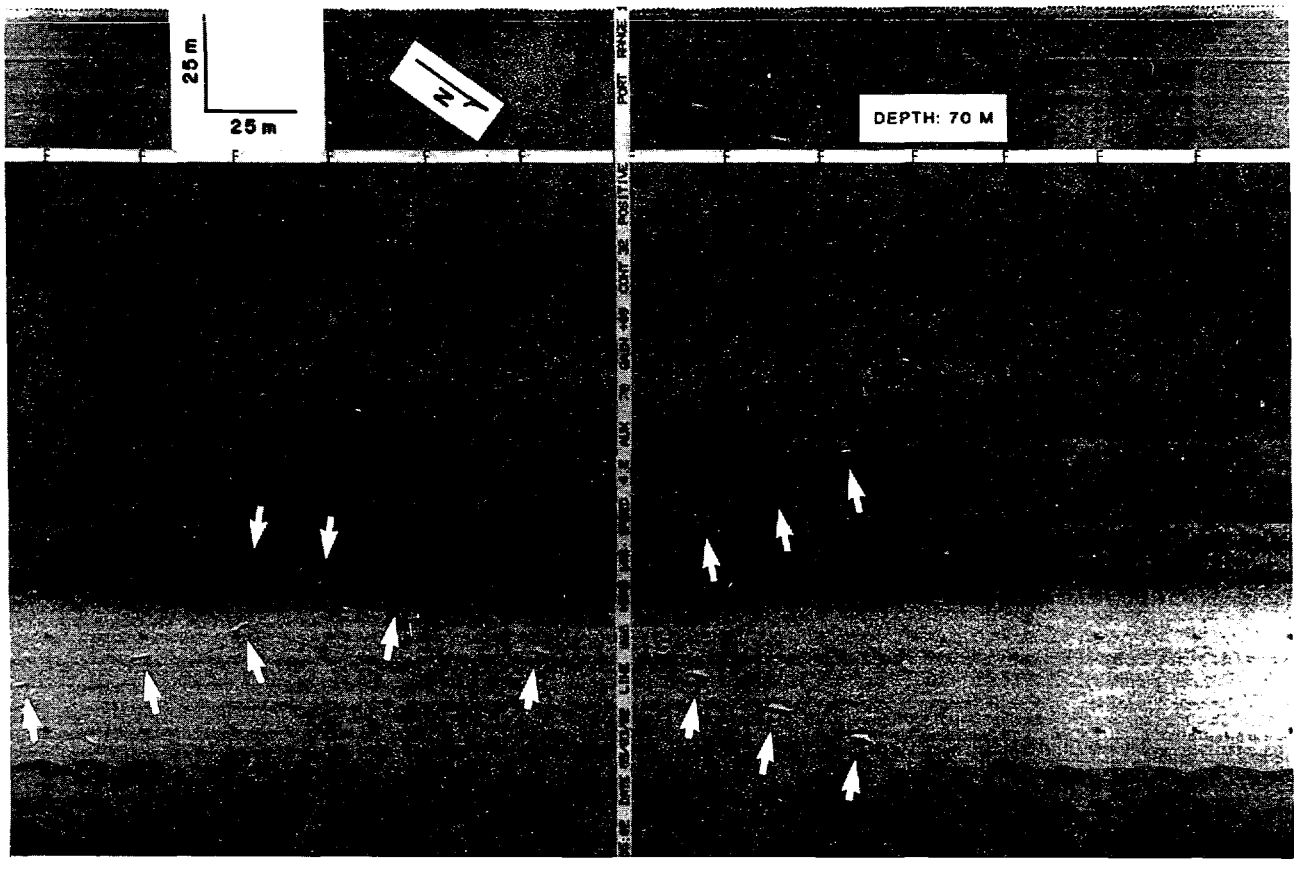

gu

shows separation between two populations. Thus, it is necessary to examine all measured parameters to establish the modification history of pits at a given site.

Type 2 features

Type 2 features are elongate pits whose average l/w ratio is greater than 3. These features occur mainly in the center of the basin in the area of most dense amphipod concentration and appear to result from the reworking of an already heavily worked area. Frequently, the margins of the Type 2 features are much less distinct than those of the Type 1 or Type 3 features. This and the even distribution of Type 2 pits through all size classes implies that the Type 2 features are undergoing continual rather than seasonal modification. The location of the Type 2 features in the central and northern portions of the basin where more consistent, stronger, northward-trending currents occur supports this possibility (Fig. 5). Also, the general bottom configuration in the Type 2 area is gently undulating, probably a result of heavy feeding pressure in the area leading to reworking of pitted areas. The area is underlain by old modified feeding pits which profoundly alter the bottom topography and attest to the intense feeding pressure in the area.

The predominance of elongate pits suggests an alternate current modification regime or an alternate feeding mode. The case for a different current regime has already been established. The same information may be used to explain an alternate feeding mode. Whales could create elongate pits as they are moved along by stronger currents while feeding. Though it is unlikely that whales would independently alter their feeding behavior from one area to the next, it seems feasible that local conditions may affect their

actions. Type 2 features appear to have a random orientation that would not be expected from a current-influenced feeding activity. Therefore, we cannot eliminate the possibility that the whales are making these features by coordinating suction and propulsion.

The possibility that these features are made by self-propelled (not current-propelled) whales is reinforced by data collected off the coast of California during the northward migration of the gray whales. Cacchione **(1983) reports:**

> "The side-scan records taken on the central shelf in water depths of 70 to 120 meters are generally devoid of sea floor relief, as reported earlier, except for occasional elongate, coast-parallel depressions that probably are sea floor gouges caused by migratory gray whales. These features are usually linear gouges (infrequently "S" -shaped) about 2 to 8 meters long and 1 to 2 meters wide. They generally occur in groups of 3 to 8 arranged in a line oriented parallel to the bottom contours. The commonly measured spacing between multiple gouges is about 10 to 30 meters. In all of the records, the maximum density of whale gouges is about 10 to 20 gouges/0.1 km^2 and is located in water depths of 70 to 100 meters . . ..During the L1-81-NC Code-1 cruise, we observed numerous gray whales at the ocean surface migrating along the shelf toward the north."

The presence of elongate features associated with migrating whales who are obviously moving while interacting with the sea floor verifies that this mode of bottom interaction is possible in Type 2 areas (Fig. 44). One hundred and twenty one of the California features were measured, their average length was 4.6 m and their average width was 1 .8 m. These records were taken on 105 kHz digital Seafloor Mapper, the same side-scan system used in the Bering Sea for our measurements. Both length and width histograms (Appendix A, station Tate 1) plot as one population of pits, but the length vs. width plot shows that several features are much larger than the average (up to 10 m x 3 m). The presence of such large features, thought to be recent whale events,

suggests that whales may be able to produce sea-floor pits on a scale much larger than the size of their gapes. In general, the individual pits in a given group are of similar size indicating that the group was made by a single whale. The size range between groups is very large indicating that both whale size and mode of bottom interaction have a high degree of effect on the size of features produced. The "S-shaped" linear gouges mentioned by Cacchione are probably straight features distorted by swell "action on the towfish.

Extrapolating what we learned from the California features, the Type 2 area becomes more understandable. The length of Type 2 features in the Eering Sea averages from 3.1 to 4.7 m and the width ranges from 1 to 1.7 m. These values are like those of the California features and the two probably are made by similar whale behavior. The California features are in widely scattered but readily distinguishable groups implying that between 3 and 8 pits were made per dive. 'Pit density is much higher in the Bering Sea, and it is essentially impossible to distinguish discrete groups of pits. The Bering Sea features, also, are more modified and are superimposed on an undulating topography left by previous feeding seasons. Their margins are much less abrupt than those of the California features.

Length histograms of Type 2 features (Appendix A, stations Dog 3, Dog 12) show bimodality indicating modification of the long axis of the pits. Stations Dog 4 and Dog 13 exhibit length histograms with single populations skewed to the right; this suggests that either continual modification or very long fresh features are represented. It seems unlikely that a long feature could be further elongated without substantial widening, especially when the features are randomly oriented to begin with. Thus, the presence of very long (greater than 10 m) Type 2 pits is an enigma. In Type 2 station Dog 12 (Fig.

31) it appears that several of the longer features are created by closely adjacent multiple suction feeding events. This lends credence both to the theory of coordinated suction and propulsion by the whale and the theory of drifting with the current while feeding. With minimal current activity, the small elevated spots between the pits are easily smoothed out giving the impression of a single large elongate pit. Though present in Dog 12, this situation is not apparent at all Type 2 locations.

Total percent of bottom disturbed for Type 2 areas ranges from 5 to 1 5%. In the smallest size class, this translates to a 3.4 - 4.9% scour. Since the Type 2 features tend to be larger than Type 1 fresh feeding features, the second size class (5.3 m^2 - 10 m^2) may also represent fresh feeding in the Type 2 areas. The total scour for the two smallest size classes, the apparent fresh feeding classes, then ranges from 4.6 to 1 1.6%. This represents fairly heavy feeding pressure as would be expected in the area of highest amphipod density and most frequent whale sightings (Figs. 19, 20).

It is important to note that taking the side-scan towfish through rough water occasionally distorts Type 3 features so they resemble Type 2 features. This happens when slacking of the tow cable causes the towfish to decelerate thus stretching out features on the record. This artifact can be easily identified since the stretching of features occurs on a parallel band across the record. These bands reflect the periodicity of the waves and thus are regular and pervasive throughout the sonograph.

Type 3 features

In general, Type 3 features show much less size variability than the Type 1 and Type 2 features (Table 2). In almost all cases, the majority of Type 3

pits fall into the smallest size class. Apparently, there is very little enlargement and any modification probably occurs by marginal slumping or the silting-in of features. These shape discrepancies raise doubts as to the origin and modification history of these pits. Their oval to round shape does not allow accurate long axes orientations to be taken, so no inferences about regional trends can be drawn. Their relationship to prevailing currents also cannot be defined.

The distribution of the Type 3 pits is perhaps the key to their origin. Type 3 features occur around the margins of the Type 1 and Type 2 features with the largest zone of Type 3 features occurring in the southern central Chirikov Basin. This is a zone of low amphipod concentration (Fig. 19) and different substrate texture (Fig. 13). It is possible that the variable amphipod distribution causes scattered whale feeding behavior. However, in some areas of the southern Chirikov Basin containing high concentrations of feeding whales, the sea floor is very densely pitted with Type 3 features. This situation occurs above the northwest cape of St. Lawrence Island at stations Dog 5 and Dog 10. (Figs. 34, 36). The implication of this is that these areas are *major* feeding areas and the pit morphology is a function of the sediment type rather than whale feeding behavior. Surprisingly, the amphipod population is not extremely dense in this area. Perhaps the whales are exploiting an alternate food source. Percent total disturbance in these areas is high, ranging from 13 to 14%. The small size class accounts for nearly all of that scour and ranges from 10 to 12% of total bottom disturbance.

The coarser grain size in much of Type 3 areas compared to Type 1 and 2 areas may inhibit current scour modification and this may cause a lack of

scour-enlarged pits. If feeding pits from older feeding seasons are not modified, the small size classes may over-represent fresh feeding which the high proportion of small pits to the total disturbance suggests. This too helps to explain high quantities of apparent fresh disturbance in low amphipod prey areas. It is possible that the increasing grain size of the substrate towards the southern margin of the basin (Fig. 13) may allow pit shape to tend towards ovalness. Also, the coarser sediment is less cohesive and therefore more subject to slumping around the pit margins, thus widening the pits.

Another possibility for the creation of round pits is the formation of gas expulsion craters or "sea floor pockmarks" (Nelson et al., 1980). Although all evidence suggests that the round pits of the Type 3 areas are created by feeding whales, the smaller gas expulsion craters would be very difficult to distinguish from the Type 3 features (compare Fig. 17C with Figs. 33, 35, 37). Even though methane-producing epiclastic peats underlie the sediment in Type 3 areas, the surficial fine-coarse sand and gravel in this area does not form an impermeable cap; this is a necessary condition to trap enough gas to allow expulsion and crater formation during storm surges. It is the paucity of gas-charged sediment in Type 3 areas, the lack of acoustic anomalies throughout Chirikov Basin showing no gas charging (Holmes and Thor, (1982), and the absence of any larger (10 m diameter) round pits (not recognizable as current scour pits) in the Chirikov basin that decreases the chance that small pits of Type 3 areas are gas expulsion craters. Although they are in areas that would probably be favorable to walrus feeding, these pits are of a much larger scale than could be produced by a walrus.

Food resource

The distribution and density of the small-size class of pits, when assumed to represent fresh feeding, can be used to create a whale food resource budget for northeastern Bering Sea. A number of assumptions must be made before such a model can be created, and, of course, the value of such a model is thus based on the validity of these assumptions.

The northeastern Bering Sea contains approximately 22,000 km^2 of sea floor that bear evidence of gray whale feeding (Fig. 40). Assuming that a fresh pit is represented by the **0-5.3** m^2 pit size class, then the number of these pits represents a minimum feeding pressure in this area. Since little is known about the modification rates of these pits, great uncertainties exist. If, for example, modification rates were so high that pits only existed a few weeks before enlarging or filling-in, then several generations of pits could conceivably form during the span of one feeding season. Conversely, if modification rates *were* exceedingly slow, pits might last for several seasons before being altered. Both of these scenarios *are* unlikely since the current scour apparently occurs regularly in the fall storm season each year.

Surveys of the same areas at the beginning and at the end of the season could begin to explore this problem. Since the digital 105 kHz side-scan system was only used on the L7-80-BS cruise, no statistics comparing the features observed by the same system can be obtained. In areas of overlap with non-digital systems, some observations can be made. A Type 1 area showed examples of evolution from walrus furrow dominance to whale pit dominance over

a period of one month. In several other cases, Type 1 and Type 2 areas remained more or less constant during that period, again negating ideas of rapid modification.

Type 1 areas are certainly those which show the most profound influence of currents and are the sites at which one would expect to find rapid modification. Unfortunately, low trackline overlap prohibits a detailed assessment of temporal changes of the bottom features. One must assume that since the percentage of disturbance by fresh pits (0-5.3 m^2) is relatively low (0.9 to 11.0%), they represent feeding for the present year only. Conversely, the larger size class pits are probably holdovers from previous feeding seasons. At this point in the research, we cannot determine how long the pits remain unmodified, but we speculate that most features probably are modified in the fall storm season and that fresh features last only one season before being enlarged or infilled.

Since the fresh pitting is probably not cumulative, the fresh pits can be taken as a measure of minimum yearly feeding pressure. Using the distribution of the three feature types (Fig. 40) and the percent area disturbed by fresh whale feeding pits (Table 3, Fig. 42), it is possible to, calculate the total area of fresh pits in the northeastern Bering Sea feeding region. This value is 730 km^2, or an average of 3.4% disturbance due to fresh pits. Since the L7-80-BS data was collected during the second and third weeks of August, and the gray whale feeding season in northeastern Bering Sea lasts from June to late October (Pike, 1962), only 60% of the yearly feeding record was accumulated by the middle of August. Thus, we expect an average percent fresh bottom disturbance of 5.6% by the end of the season and a sum of areas of all

the fresh pits at the end of the feeding season is estimated to be 1200 km^2 in northeastern Bering Sea.

The area of fresh feeding pits, combined with the biomass/unit area of the amphipod population may be used to approximate the total weight of amphipods consumed in one season in northeastern Bering Sea. Nerini (in press) recorded a mean amphipod biomass in the whale foraging area of 161 g/m^2 (161,000 kg/km^2). Mean amphipod biomass in the Nerini study accounted for 34% of the mean total biomass. Stoker (1978, 1981) shows an average total biomass of 533 gin/m^2 (533,000 kg/km^2). Using Nerini's figure of 34% as the amphipod fraction of the total biomass, then Stoker's figures represent a mean amphipod biomass of 181,000 kg/km^2. Using these figures, the consumption of benthic amphipod biomass in northeastern Bering Sea ranges from 117.53 million kg to 132.1 million kg for the season up until the third week of August; it is projected to range from 193.2 million kg to 217.2 million kg for the entire 1980 feeding season.

The amount of food that a mature gray whale consumes each day has been calculated by three groups of workers. Zimushko and Lenskaya (1970) calculated a rate of 1,200 kg/day. Both Rice and Wolman (1971) and Brodie (1975) calculated rates of 1,000 kg/day. Using this range of whale feeding rates and the range of amphipod biomass consumed in northeastern Bering Sea, we can estimate the number of whale feeding days (WFD) in these areas. This range is 97,942 - 132,100 WFD for the partial season and 161,000 - 217,200 WFD for the projected whole season.

The number of whale feeding days/season has significance in determining the relative importance of the northeastern Bering Sea as a gray whale feeding area. In order to do this, the total number of whale feeding days/season in

Alaskan waters must be calculated for the entire gray whale population for the duration of the feeding season. Assuming a population (in 1980) of 17,000 whales (Rugh, 1981) that spends at least 180 days a year feeding in the Bering and Chukchi Seas, this population accrues a total of 3,06,000 WFD/season. Thus, 22,000 km^2 of northeastern Bering Sea accounted for 5.3 - 7.1% (3.2 - 4.3% for the season until late August) of the entire gray whale feeding pressure for the 1980 season.

These estimates can be treated as minima for the following reasons. Only amphipod biomass was used in calculating food resource/unit area. In reality, the whales are utilizing much of the non-amphipod biomass as a food source. Also, side-scan sonar under-represents features that are not parallel to the trackline, and thus all whale feeding pits have not been accounted for in our calculations. Assuming that the whales utilized all of the total biomass (474 gm/m^2 of Nerini or 533 gm/m^2 of Stoker) and that the side-scan sonar missed the maximum possible 50% of the smaller features, then a total of 974,476 to 1,279,000 WFD, or 32 to 42% of the entire whale feeding pressure, would be accrued in the northeastern Bering Sea; this represents the maximum possible food resource utilized in this area. The northeastern Bering Sea region supplies at least 5.3% of the gray whale food resource and probably much less than the 32 to 42% maximum possible because whale stomach contents contain predominantly amphipods and not other biomass.

The summer feeding range of the gray whale occupies 1 million km^2 (Frost and Lowry, 1981). Thus 2% of the range in northeastern Bering Sea supplies a minimum of 5.3% of the food resource and very likely double this because side-scan sonar misses up to 50% of the feeding pits oriented transverse to the trackline. The northeastern Bering Sea therefore must be considered a major

feeding ground for the gray whales. It is not however, the only major feeding ground. The Gulf of Anadyr, the Soviet side of Chirikov Basin, the northern side of the Alaskan Peninsula and all areas in the Chukchi Sea need to be studied to assess their respective contributions for gray whale food sources.

Food farming

Recent investigations show a unique relationship between the gray whales and their prey size. The size distribution of amphipods found in whale stomachs often shows a marked absence of small animals (less than 4-8 mm). Rice and Wolman (1971) examined the stomach of an immature female gray whale and found A. macrocephala ranging in size from less than 6 mm to more than 25 mm. Oliver, Slattery, Silberstein and O'Connor (1983) examined a gray whale fecal specimen and found amphipods as small as 4 mm. Coyle (1981) found no amphipods smaller than 8-10 mm in the stomach of a mature female gray whale. Nerini (1981) measured crab zoea as small as 2 mm in the stomach of a migrating gray whale. Apparently, the baleen separation of the gray whales is of coarse enough mesh size to allow the smaller animals (less than 4 mm) to escape. The size bias for larger amphipods, however, may be an artifact of the whales' stomach acid consuming the smaller organisms first.

If the size separation of prey is real, then it has interesting implications for symbiotic relationships between ampeliscid amphipods and gray whales. Studies of ampeliscid amphipods in Barnstable Harbor on Cape Cod show that they are a tube-building, colonizing amphipod (Mills, 1967). The young thrive in areas of substrate disturbance. In Barnstable Harbor this disturbance exists from tidal scour; in the Bering Sea it is apparently caused by whale feeding disturbance combined with curren-scour modification of

fresh feeding pits. Thus, the whales may be redistributing the young amphipods from mouth effluent feeding plumes into areas of fresh disturbance while at the same time consuming the mature amphipods or essentially "farming" the sea floor.

The possibility that the gray whales might be cultivating the sea floor by creating disturbances for the juvenile amphipods has been discussed previously (Frost and Lowry, 1981). New data presented in this report suggest that the current-scour modification triggered by whale foraging is producing in some areas much greater disturbance than the whales are capable of causing by themselves. For example, station Dog 1 shows 18% total bottom disturbance. Of this figure, only 0.94% is attributable to the smallest size class, the fresh feeding pits. This extreme situation also occurs in the Type 1 features at station Dog 8 (Table 2, Fig. 34). A more common occurrence is for the larger class of pits to constitute approximately half of the total disturbance. Still the increase in the disturbed area by current scour is considerable. This directly increases the area available for colonizing amphipods.

The reworking of the sediment could also be an effective vehicle for the more rapid recycling of nutrients through the system. Thus, the whales also contribute to the primary productivity of the area in two ways, by the addition of their feces as biological sedimentation and by the mixing of the nutrient-rich sediment into the water column and epifaunal environment.

IMPLICATIONS FOR GEOLOGIC PROCESSES

The gray whale feeding habits have a profound effect on the geology of their feeding areas because of the cumulative effect of reworking the sediment. The percentage of sea floor disturbance ranges from 0.9 to 11% for fresh feeding pits each year and the enhanced current scour often more than doubles the reworking by whales. Box cores from central Chirikov Basin show very few primary sedimentary structures. Years of whale feeding must effectively churn through and homogenize the sediment. This action also may lead to a winnowing of the fine particles and a better sorting of the fine sand. Whether the fine sediment suspended by whale feeding remains as part of the suspended sediment load or whether it settles back to the sea floor is a function of the local current regime. Certainly, the majority of sand- and coarse silt-sized particles expelled by the feeding whales will settle almost immediately to the bottom. This rain of expelled particles probably is an active agent in the eventual silting-in of the whale pits.

There is no doubt that the whales are a major force in initiating current scour of the bottom because they eliminate the biological binding of the sediment surface and cause large-scale biologically induced roughness of the sea floor. This is seen most clearly in Type 1 feature areas. The amphipod mat is a binding force that helps hold sediment particles together. When a whale sucks up a patch of the amphipod mat, it roughens the bottom and exposes the fine sand beneath. Current scour becomes active because sediment binding force is reduced and the increased roughness of the bottom greatly lowers threshold velocity required to erode sediment grains (Cacchione and Drake,

1982). In areas where currents are only strong enough to move unbound sediment, the whale activity provides the catalyst for erosion and scour.

The current-scour-enlarged pits can also be used to draw conclusions about current speed and direction. Regional lineation of large current-modified features imply a distinct prevailing current during feature modification.

Finally, the whale pits themselves are a type of megabioturbation and should be recognized as a biologic sedimentary structure. In their genesis they are not dissimilar to feeding pits made by walrus and, in their morphology, to sediment excavations made by rays. Ray pits have been described from modern and Cretaceus sediments (Howard and others, 1974). Whale pits can also provide a modern example of a feature that could be recognized in the rock record to establish the presence of prehistoric benthic-feeding whales. Given the geometry and size of the features, recognition of such large scale features may be difficult at rock outcrop scales.

HAZARDS SUSCEPTIBILITY

The susceptibility of the whale feeding ground to oil spills and oil development is a matter of no small concern. This area is complex due to the presence of sea ice for nearly half the year. All scenarios dealing with potential oil spill trajectories must account for both a winter and a summer situation. The ampeliscid amphipods are highly sensitive to oil spills (Sanders, 1977). Gray whales do not appear to be affected by minor amounts of oil (Braham et al., 1982). During the ice-free season, the current

patterns around Chirikov Basin normally would deflect oil spills from Norton Sound into the Alaskan Coastal Water and around the northeastern margin of Chirikov basin up into the Chukchi Sea (Figs. 9, 10). Whale feeding grounds in the Chukchi Sea therefore might be more affected by an oil spill in Norton Basin than those in the adjacent Chirikov Basin.

During the ice-dominated portion of the year, however, oil spills from Norton Easin would be incorporated in the pack ice, and ice pan movement is highly susceptible to variable wind stress (Ray and Dupre', 1981). As a result, oil-bearing ice may eventually be carried over central Chirikov Basin. Under certain conditions of melting, oil could reach the substrate in this region and impact the amphipod population prior to its summer bloom. With the intense whale feeding in Chirikov Basin and the whales' limitation to a single yearly feeding season in the northeastern Bering Sea, the loss of feeding grounds for even part of a summer season could severely impact the minimum of 5 to 10% of the gray whale population supported by this amphipod stock.

Mining of the substrate in order to produce artificial drilling islands could be harmful to the whale population if portions of the relict inner shelf transgressive sand were utilized. Because the inner shelf sand body is less than 1 meter thick in most of Chirikov Basin and is a relict sediment that will not be replaced by modern processes, the loss of this substrate would permanently impact feeding grounds for a significant proportion of the whale population. More reasonable sand resources exist in other regions of the northeastern Bering Sea in the form of mobile sand bodies that are actively being replenished by Yukon sedimentation (Hess and Nelson, 1982).

POTENTIAL FUTURE STUDIES

The establishment of long-term current meters in the center of Chirikov Basin is essential to model the apparently significant circulation patterns previously considered weak and unimportant compared to the current patterns in the adjacent Bering Strait. Long-term current meter data is necessary to model oil spill trajectories and nutrient plume trajectories. Information should be obtained on the sources of productivity and the possible influence of an oil spill on each region of the whale feeding grounds in the Chirikov Basin. Another benefit from a long-term current study is the ability to quantify periods in which whale feeding features are modified and thus determine relative ages of the features. These data could be used to establish year-to-year fluctuations on the areal extent of the whale feeding grounds and thus determine more accurately the substrate carrying capacity of Chirikov Basin.

The modification rates of whale feeding pits and amphipod regeneration rates are both critical data necessary to understand the implications of gray whale interaction with the sea floor. Site-specific work in the Bering Sea involving the reoccupation of stations at different depths and in different current regimes could begin to quantify these variables.

Another method to approach the problem of feature modification is the sequential timing of side-scan surveys over the same sections of sea floor. It is possible, using shore-based navigational devices, to accurately re-survey an area with side-scan (Erk Reimnitz, USGS, Menlo Park, pers. comm., 1983). The areas of trackline overlap in this study were not adequate to approximate feature change through time because of the accuracy of the

navigation, the use of different side-scan systems, and the temporal spacing of the different surveys. A thorough study should last at least two years and should have a minimum of two surveys a year, one as early as possible and one as late as possible. Ideally, a third survey should be made in the middle of each feeding season. Consistent side-scan techniques should be maintained throughout the study. A digital 500 kHz system would provide the best detail and ease of comparison of records.

A study similar to the present one that combines side-scan sonar surveys, substrate analyses and sediment history could be used to survey whale feeding grounds in the Chukchi Sea, the Beaufort Sea, the southern Gulf of Alaska, and Russian waters including the Gulf of Anadyr. With thorough knowledge of the sediment type and prey distribution throughout the entire feeding range of the gray whale, much more accurate estimates of feeding ground utilization can be obtained. Such a program would require the cooperation of Soviet scientists and should be coordinated with on-going studies of gray whale distribution.

Side-scan data collected on the L7-80-BS cruise was collected on magnetic tape as well as dry paper recorder. These tapes are suitable for computer enhancement. Future work involving enhancement of these data may provide more accurate estimates of figure size and density.

A thorough side-scan and sediment survey of some less remote gray whale summer grounds such as Pachena Bay, Vancouver Island, British Columbia might provide better data on whale feeding behavior and opportunity to correlate the side-scan record with SCUBA diver observations. Pachena Bay is an especially attractive area as the water visibility is very good and the bay supports an ampeliscid amphipod mat community which is actively being utilized by gray whales (Oliver, pers. comm., 1982). In addition, feeding traces on the sea

floor can be accurately mapped by SCUBA divers and marked by side-scan sensitive pingers. Then, when the side-scan survey is conducted over the area, a very accurate determination of how much the features are distorted and how many features are missed can be calculated. These figures could then be extrapolated to the more remote feeding areas such as the Bering Sea that are less conducive to detailed site-specific research.

The question of where the gray whales fed during the Pleistocene might be addressed by deep-water side-scan surveys on the shelf break of the Bering continental shelf. When Beringia was emergent, this area contained the proper habitat depth ranges for the gray whales. Relict sedimentary features from the Pleistocene, namely large sediment waves, have been detected with sub-bottom profilers (Paul Carlson, USGS, Menlo Park, Cal., pers. comm., 1983) and the potential to detect relict whale feeding pits does exist.

The walrus feeding traces discovered in this study deserve further consideration. The walrus feeding furrows show up equally as well on 105 kHz as on the 500 kHz side-scan system but the smaller feeding pits have not yet been recognized on either system. The ability to recognize the smaller feeding pits exists as their size is larger than the minimum resolution claimed by the manufacturers of the 500 kHz system (John Oliver, pers. comm., 1982; Jim Glynn, Klein Assoc., Inc., Salem, New Hampshire, pers. comm., 1983). Also, the discarded bivalve shells around the pits might add to the overall seismic reflectivity of the surficial sediment. With proper diver calibration, it may well be possible to map walrus feeding grounds on side-scan sonar. In addition, the distribution and substrate affinities of the main prey species of the walrus can be mapped to some degree from data already

in existence. Besides delineating the walrus feeding grounds, this type of study would further define the margins of the gray whale feeding areas.

CONCLUSIONS

1. Ampeliscid amphipods, the main prey species of the gray whale, have a high affinity for the widespread homogeneous, relict, inner shelf transgressive sand body that blankets most of Chirikov Basin to a depth of no more than 1.5 meters. The amphipod community occupies nearly 40,000 km^2 in northeastern Bering Sea.

2. Gray whales feed on amphipods from this substrate by means of benthic suction, a process which produces a variety of feeding traces on the sea floor.

3. These traces can be accurately and regionally studied and quantified by means of the side-scan sonar, a planographic sea floor mapping device well suited to regional mapping.

4. Gray whale feeding trace distribution from side-scan sonar matches closely with the distribution of Bering Shelf Water, transgressive fine sand, high concentrations of Ampeliscid amphipods and the summer sighting of feeding gray whales from aerial surveys; this proves the validity of side-scan sonar as a biological mapping tool.

5. 22,000 km² in central Chirikov Basin and the nearshore areas of St. Lawrence Island show evidence of whale feeding as defined by side-scan sonar. Three types of whale feeding areas are recognized. Type 1 regions contain elliptic-shaped, recognizable fresh feeding traces. An older set of pits has been enlarged and regionally oriented by current-scour triggered by the whale feeding itself. Type 2 regions contain high concentrations of elongate (narrow elliptic) pits in areas with the most intense feeding pressure. Type 3 regions contain wide-elliptic-shaped feeding pits and occur in areas of decreasing amphipod density and increasing sediment grain size; they are found in locations with the least intense feeding pressure on the margins of Type 1 and 2 areas.

6. Different morphology of fresh feeding traces in various regions suggests that whale feeding behavior varies with changes in food amount and prey species, substrate type, and local current regimes. In areas of stronger current regimes or where whales are migrating or underway during feeding, original morphology of feeding pits may be more elongate with linear chains of fresh pits. Coarser substrates may result in more oval feeding traces.

7. There is minimal whale feeding pressure in Norton Sound because the Alaskan Coastal Water has low salinity and the substrate is a very fine-grained muddy sand. Both result from the high Yukon discharge and provide poor habitats for potential whale prey species.

8. Walrus feeding furrows can be readily identified on both 105 and 500 kHz side-scan systems and walrus feeding grounds seem to occur in areas of coarser substrate fringing the whale feeding grounds.

9. Total bottom disturbance from whale feeding pits and current scour enlargement of these ranges from 2% to 18% in different feeding areas of northeastern Bering Sea. The smallest size class of bottom pits approximates the size of whale-mouth gape size and is interpreted to represent fresh feeding pits; the larger size classes represent current-scour-enlarged pits with modification occurring mainly during the storm-prone months of the fall. This is substantiated by separate size classes of pits rather than a continual gradation of sizes indicating continual modification.

10. The percent bottom disturbance by the fresh feature size class (0-5.3 m^2) ranges from .9-11% and the average for the northeastern Bering Sea is 3.4%. These figures represent the feeding pressure at the time of data collection. Data for the whole season can be extrapolated from these figures to estimate a total seasonal average of 5.4% fresh disturbance.

11. Utilizing published biomass data, data on whole biomass feeding intake per day and counts of whale feeding days in Alaska, Chirikov Basin is estimated to account for a minimum of 5.3% and a maximum of 32-42% of the entire gray whale summer feeding resource for the Bering Sea and Arctic Ocean in only 2% of the total feeding region. Because side-scan sonar misses up to 50% of feeding traces transverse to the trackline, a minimum food resource estimate of 10% may be reasonable for northeastern Bering Sea.

12. Since the northeastern Bering Sea may provide 10-30% of the gray whale food resource and the amphipod population is susceptible both to oil spills plus any dredging or destruction of their substrate, exploitation affecting Chirikov Basin requires careful planning.

13. The whales may be farming their feeding grounds by (a) selectively capturing adult-sized amphipods, (b) seeding the juvenile amphipods, a pioneer species, into areas of freshly created and current-modified disturbance, and (c) mixing the nutrient-rich sediment into the water column thus boosting productivity.

14. The surficial sediment in Chirikov Basin is essentially devoid of primary sedimentary structures principally because of extensive sediment reworking by feeding whales. The roughening of the sea floor surface and exposure of biologically unbound fine sand caused by feeding, greatly enhances current scour in the central Chirikov Basin. Whale feeding also results in significant resuspension of fine-grained sediment and this combined with northward current advection may be a principal cause of non-deposition of modern sediment in this region.

15. Future studies should include (a) application of similar side-scan sonar reconnaissance in the main gray whale feeding regions of Alaska and the Soviet Union (b) periodic side-scan sonar monitoring of prime feeding grounds in central Chirikov Basis to outline different year classes and fresh feeding pits and refine food resource estimates and (c) utilization of existing USGS

side-scan records to outline areas and importance of walrus feeding habitats in northeastern Bering Sea to ascertain interplay with gray whale feeding grounds.

ACKNOWLEDGEM ENTS

We thank Nary Nerini, John Oliver, Denis Thomson, Larry Martin, Kate Frost, Lloyd Lowry, Sam Stoker, Bud Fay, Ken Coyle, Steve Swartz, Mary Lou Jones, Steve Leatherwood, Jody Derman, Sue Moore, Marilyn Dalheim, Bob Nelson, Dale Rice, Gary Mauseth, Howard Braham, and Nora Foster for their willingness to share their knowledge of whale ecology and benthic biology. Jim Schumacher provided data from long-term current meters in the Bering Sea. Dave Cacchione and George Tate allowed us to use their side-scan data from the California coast. Both Mary Nerini and Denis Thomson were generous with their side-scan data from the Bering Sea. Discussions with Gordy Hess, Erk Reimnitz, Ralph Hunter, Jim Glynn, Chris Sherwood, and Jim Gardner added great depth to our understanding of the abilities and limitations of the side-scan sonar. Lavernne Hutchison helped type the manuscript. Russell Crane and John Barber Jr. aided in the preparation of the figures.

This study was funded by the Bureau of Land Management through interagency agreement with the National Oceanic and Atmospheric Administration as part of the Outer Continental Shelf Environmental Assessment Program.

REFERENCES CITED

Bogoslovskaya, L. S., L.M. Votrogov, and T.N. Semenova, 1981, Feeding habits of the gray whale off Chukotka: Report Int'l. Whaling Comm., vol. 31, p. 507-510, sc/32/ps 20.

Braham, H.W., 1983, Migration and feeding during migration by the Gray Whale (Eschrictius robustus) in: M.L. Jones et al. (eds.), The Gray Whale Eschrictius robustus: Academic Press, New York, 441p., in press.

Braham, H.W., R.D. Everitt, B.D. Krogman, D.J. Rugh, and D.E. Withrow, 1977, Marine Mammals of the Bering Sea: A Preliminary Report on Distribution and Abundance 1975-1976: NOAA-NMFS Northwest and Alaska Fisheries Center Processed Report.

Braham, H.W., G.W. Oliver, C. Fowler, K. Frost, F. Fay, C. Cowles, D. Costa, K. Schneider, D. Calkins, 1982, Marine Mammals, M.J. Hameedi (cd.), Proceedings of the Synthesis Meeting: St. George Environment and Possible Consequences of Planned Offshore Oil and Gas Development, 28-30 April, 1981, Anchorage, Alaska, Chap. 4, pg. 55-81.

Brodie, P. F., 1975, Cetacean energetic, an overview of intraspecific size variation: Ecology, vol. 56, p. 152-161.

Brownell, R. L., 1977, Current status of the gray whale: Report Int'l. Whaling Comm., vol. 27, p. 209-211, se/28/Doe. 33.

Cacchione, D.A. and D.E. Drake, 1979, Sediment Transport in Norton Sound, Alaska, regional patterns and GEOPROBE system measurements: USGS Open-File Report 79-1555, 88 p.

Cacchione, D.A. and D.E. Drake, 1982, Measurements of Storm-Generated Bottom Stresses on the Continental Shelf. Jour. of Geophys. Res., vol. 87, no. C3, p. 1952-1960.

Cacchione, D.A., Drake, D.E., Grant, W.D., and Williams, III, A.J., Large and small scale morphology within the Coastal Ocan Dynamics Experiment (CODE) region, CODE Technical Report No. 17, Woods Hole Oceanographic Institution, in press, 45 p.

Coachman, L. K., K. Aagaard, and R.B. Tripp, 1976, Bering Strait: The regional physical oceanography: Univ. of Washington Press, Seattle.

Coachman, L. K., and R.B. Tripp, 1970, Currents north of Bering Strait in winter: Limnol. and Ocean., vol. 15, p. 625-632.

Consiglieri, L.D., H.W. Braham, L.L. Jones, 1980, Distribution and abundance of marine mammals in the Gulf of Alaska from the platform of opportunity programs, 1978-1979: Outer Continental Shelf Assessment Program Quarterly Report RU-68. 11 p.

Coyle, K. O., 1981, The oceanographic results of the cooperative Soviet and American cruise to the Chukchi and East Siberian seas aboard the Soviet whale hunting ship Razyashchii September-October 1980, Inst. Mar. Sci., Univ. Alaska, Fairbanks, 107 p.

Creager, J. S., M.L. Echols, M.L. Holmes, and D.A. McManus, 1970, Chukchi Sea continental shelf sedimentation (Abstract): American Association of Petroleum Geologists Bulletin, vol. 54, no. 12, p. 2475.

Drake, D.E., D.A. Cacchione, R.D. Muench, C.H. Nelson, 1980, Sediment Transport in Norton Sound, Alaska: Mar. Geol., 36: 97-126.

Dupre, W.R., 1982, Depositional environments of the Yukon Delta, northeastern Bering Sea, in: Geologie en Mijnbouw, vol. 61, p. 63-71.

EG & G Environmental Equipment, SMS 960 Seafloor Mapping System, Technical presentation, 151 Bear Hill Road, Waltham, Mass. 02154.

Fathauer, T. F., 1975, The great Bering Sea storms of 9-12 November, 1974: Weatherwise Magazine of the American Meteorological Society, vol. 18, p. 76-83.

Fay, F.H., 1982, Ecology and Biology of the Pacific Walrus, Odobenus rosmarus divergens Illiger, Fish and Wildlife Service series, North American Fauna, no. 74.

Feder, H. M. and S.C. Jewett, 1981, Feeding interactions in the eastern Bering Sea with emphasis on the benthos, in: The eastern Bering Sea shelf: Oceanography and Resources, vol. 2, D. W. Hood and J. A. Calder, eds., Off. Marine Pollution Assessment, NOAA. Distrib. by Univ. Washington Press, Seattle.

Filatova, Z. A., and N.G. Barsanova, 1964, Communities of benthic fauna in the western Bering Sea: Trudy Inst. Okeanologiya, vol. 69, p. 6-97.

Fleming, R. H., and D. Heggarty, 1966, Oceanography of the southeastern Chukchi Sea, in: N. J, Wilimovsky and J. N. Wolfe, eds., Environment of the Cape Thompson region, Alaska, U.S. Atomic Energy Comm., p. 607-754.

Flemming, B.W., 1976, Side scan sonar: a practical guide. Technical report no. 7, Univ. of Capetown or Int. Hyd. Rev., vol. LIII #l.

Frost, K. J. and L.F. Lowry, 1981, Foods and trophic relationships of cetaceans in the Bering Sea, in: The eastern Bering Sea shelf: oceanography and resources, vol. 2, D. W. Hood and J. A. Calder, eds., Off. Marine Pollution Assessment, NOAA. Distrib. by Univ. Washington Press, Seattle.

Gilmore, R. M., 1955, The return of the Gray Whale, Sci. Amer. , vol. 192, no. 1.

Harrison, C. S., 1979, The association of marine birds and feeding gray whales: Condor, vol. 81, p. 93-95.

Herzing, D. L. and B.R. Mate, 1981, California gray whale migration along the Oregon coast, in: 4th Biennial Conf. Biol. Mar. Mammals, 14-18 December 1981, San Francisco, p. 54.

Hess, G.R. and C.H. Nelson, 1982, Geology Report for Proposed Norton Sound OCS Sand and Gravel Lease Sale: USGS Open-File report no. 82-997.

Hess, G.R., B.R. Larsen, D. Klingman, and D. Moore, 1981, Marine Geologic Hazards in the Nortern Bering Sea, Final Report on data collected in FY 1980, RU429, Annual Report.

Hickey, L.J., 1973, Classification of the architecture of dicotyledonous leaves. Am. Jour. Bot. 60 (l): 17-33.

Holmes, M.L. and D.R. Thor, 1982, Distribution of gas-charged sediment in Norton Sound and Chirikov Basin, Geologie en Mijnbouw, vol. 61, p. 79-91.

Howard, J.D., T.V. Mayon, and R.W. Heard, 1977, Biogenic sedimentary structures formed by Rays: J. Seal. Pet., vol. 47, no. 1, p. 339-346.

Howell, A. B. and L.M. Huey, 1930, Food of the California gray and other whales: J. Mammal., vol. 2, p. 321-322.

Hudnall, J., 1981, Population estimate, feeding behavior and food source of the gray whales, Eschrichtius robustus, occupying the Strait of Juan de Fuca, British Columbia, in: 4th Biennial Conf. Biol. Mar. Mammals, 14-18 December, 1981, San Francisco, p. 58.

Husby, D. M., 1969, Report Oceanographic Cruise USCG Northwind, Northern Bering Sea-Bering Strait-Chukchi Sea, 1967: U. S. Coast Guard Oceanogr. Rep. 24, Washington, D. C., 75 p.

Husby, D. M. and G.L. Hufford, 1971, Oceanographic investigations in the northern Bering Sea and Bering Strait, 8-21 June, 1969: U.S. Coast Guard Oceanogr. Rep. No. 42.

Kasuya, T. and D.W. Rice, 1970, Notes on baleen plates and on arrangement of parasitic barnacles of gray whale: Sci. Report Whales Res. Inst., vol. 22, p. 39-43.

Klein Associates, Inc., 1982, Hydroscan, Klein Side Scan Sonar and Sub-bottom Profiling Systems, 47p.

Kuznetsov, A. A., 1964, Distribution of benthic fauna in western Bering Sea by trophic zone and some general problems of trophic zonation: Trudy Inst. Okean, vol. 69, p. 98-117 (Transl. Office of Naval Intelligence).

Larsen, M.L., C.H. Nelson, and D.R. Thor, 1979, Geologic implications and potential hazards of scour depression on Bering shelf, Alaska: Environ- . mental Geology, vol. 3, p. 49-47.

Larsen, M.L., C.H. Nelson, and D.R. Thor, 1981, Sedimentary Processes and Potential Geologic Hazards on the Seafloor of the Northern Bering Sea, p" 247-267 in: The eastern Bering Sea Shelf: oceanography and resources, D.W. Hodd and J.A. Calder (eds.), OMPA, NOAA, Univ. of Wash. Press.

Inst. Okeanol. Akad. Nauk USSR, (Transl. by Israel Program for Scientific Translations), available from U.S. Dept. Commerce, Clearinghouse for Fed. Sci. and Tech. Infer., 1969, 614 p.

Lowry, L. F. and K.J. Frost, 1981, Feeding and trophic relationships of phocid seals and walruses in the eastern Bering Sea, in: The eastern Bering Sea shelf: oceanography and resources, D. W. Hood and J. A. Calder, eds., Office Marine Pollution Assessment, NOAA. Distrib. by Univ. Washington Press, Seattle, p. 813-824.

Lowry, L. F., K.J. Frost, and J.J. Burns, 1980, Feeding of bearded seals in the Bering and Chukchi seas and trophic interaction with Pacific walruses: Arctic, vol. 33, p. 330-342.

McManus, D. A., J.C. Kellery, and J.S. Creager, 1969, Continental shelf sedimentation in an arctic environment: Geological Society of America Bulletin, vol., 80, p. 1961-1984.

McManus, D.A. and C.S. Smyth, 1970, Turbid bottom water on the continental shelf of nothern Bering Sea: J. Seal. Pet., vol. 40, p. 869-877.

McManus, D. A., K. Venkataratham, D.M. Hopkins, and C.H. Nelson, 1977, Distribution of bottom sediments on the continental shelf, northern Bering Sea: U.S. Geol. Surv. Prof. Pap. 759-C.

Mead, J. G. and E.D. Mitchell, in press, The Atlantic Gray Whale in: The Gray Whale: Eschrichtius robustus, M.L. Jones et al. eds., 'Academic Press, 441p, in press.

Miller, M. C., I.N. McCave, and P.D. Komar, 1977, Threshold of sediment motion under unidirectional currents, Sedimentology, vol. 24, p. 507-527.

Mills, E. L., 1967, The biology of an Ampeliscid Amphipod Crustacean sibling species pair: Jour. Fish. Res. Bd. Canada, vol. 24, no. 2, p. 305-355.

Moore, S. and D. Ljungblad, 1983, The Gray Whale (Eschrichtius robustus) in the Bering, Beaufort and Chukchi Seas: Distribution and Sound production, in: M.L. Jones et al., eds., The Gray Whale: Eschrichtius robustus, Academic Press, N. Y., 441 p., in press.

Neiman, A. A., 1961, Nekotorye zakonomernosti kolishestvennogo raspredeleniya bentosa v Beringovom more (Certain regularities in the quantitative distribution of the benthos in the Bering Sea): Okeanologiya, vol. 1, p. 294-304.

Nelson, C. H., 1982, Holocene transgression in deltaic and non-deltaic areas of the Bering epicontinental shelf, in: The Northeastern Bering Shelf: New Perspectives of Epicontinental Shelf Processes and Depositional Products, Geologie en Mijnbouw, C. H. Nelson and S. D. Nio, eds., Geologie en Mijnbouw, vol. 61, p. 37-48.

Nelson, C. H. and J.S. Creager, 1977, Displacement of Yukon derived sediment from Bering Sea to Chukchi Sea during the Holocene: Geology, vol. 5, p. 141-146.

Nelson, C. H., W.R. Dupre, M.E. Field, and J.D. Howard, 1982, Linear sand bodies on the Bering epicontinental shelf, in: Nelson, C. H., and Nio, S. D., (eds.), 'I'he Northeastern Bering Shelf: New Perspectives of Epicontinental Shelf Processes and Depositional Products, Geologie en Mijnbouw, vol. 61, p. 37-48.

Nelson, C. H. and D. M. Hopkins, 1972, Sedimentary processes and distribution of particulate gold in northern Bering Sea: U.S. Geol. Surv. Prof. Pap. 689.

Nelson, C. H., D.M. Hopkins, and D.W. Scholl, 1974, Cenozoic sedimentary and tectonic history of the Bering Sea, in: Oceanography of the Bering Sea, D.W. Hood and E.J. Kelley, (Eds.), Univ. of Alaska, IMS, Occasional pub. 2, p. 485-512.

Nelson, C.H., K.A. Kvenvolden, and E.C. Clukey, 1978, Thermogenic gas in sediment of Norton Sound, Alaska, Proceedings Offshore Technical Conference, Houston, Texas, Paper No. 3354, p. 1612-1633.

Nelson, C.H., R.W. Roland, S. Stoker, and B.R. Larsen, 1981, Interplay of physical and biological sedimentary structures of the Bering Sea epicontinental shelf, in: The eastern Bering Sea shelf: oceanography and Resources, D.W. Hood and J.A. Calder, eds. Office Marine Pollution Assessment, NOAA. Distrib. by Univ. Washington Press, Seattle.

Nelson, C.H., D.R. Thor, M.W. Sandstrom, and K.A. Kvenvolden, 1980, Modern biogenic gas-generated craters (sea floor "pockmarks") on the Bering shelf, Alaska: Geol. Sot. Amer. Bull., vol. 90, p. 1144-1152.

Nemoto, T., 1970, Feeding pattern of baleen whales in the ocean, in: Marine Food chains, J. H. Steele, cd., Univ. California Press, Berkeley, p. 241-252.

Nerini, M., 1981, Gray whales and the structure of the Bering Sea community, in: 4th Biennial Conf. Biol. Mar. Mammals, 14-18 December, San Francisco, p. 84.

Nerini, M., in press, The Feeding Ecology of the Gray Whale: A Review, in: The Gray Whale: Eschrichtius robustus, M.L. Jones et al., (eds.), Academic Press, N. Y., 441 p.

Nerini, M. K., L. Jones, and H.W. Braham, 1980, Gray whale feeding ecology. First Year Final Report, Mar.-Dec., 1980, OCSEAP, RU593, contract no. R7120828.

Nerini, M.K. and J.S. Oliver, in press, Gray whales and the structure of the Bering Sea benthos: Oecologia.

Norris, K.S. and B. Wursig, 1979, Gray whale lagoon entrance aggregations. pg. 44 in: Abstr. 3rd Biennnial Conf. Biol. Mar. Mammals, 7-11 October, 1979, Seattle.

Oliver, J.S., P.N. Slattery, M.A. Silberstein, E.F. O'Connor, 1983, A comparison of gray whale feeding in the Bering Sea and Baja California: Fish. Bull., vol. 81, in press.

Oliver, J.S., P.N. Slattery, E.F. O'Connor, and L.F. Lowry, 1983, Walrus Feeding in the Bering Sea: a benthic perspective: Fish. Bull., vol. 81, in press.

Oliver, J.S., P.N. Slattery, M.A. Silberstein, and E.F. O'Connor, in press, Gray Whale Feeding on Dense Ampeliscid amphipod communities near Bamfield, British Columbia: Can. Jour. of Zool.

Pike, G.C., 1962, Migration and feeding of the gray whale: J. Fish. Res. Board Can., vol. 19(5), p. 815-838.

Ray, G. C. and W.E. Schevill, 1974, Feeding of a captive gray whale: Mar. Fish. Rev., vol. 36, p. 31-37.

Ray, V. M. and W.R. Dupre, 1981, The Ice-Dominated Regimen of Norton Sound and Adjacent Areas of the Bering Sea. in: The eastern Bering Sea shelf: oceanography and resources, D.W. Hood and J.A. Calder, eds., OMPA, NOAA, Univ. of Wash. press.

Reilly, S., D. Rice, and A.A. Wolman, 1980, Preliminary population estimate for the California Gray Whale based upon Monterey shore censuses, 1967/68 to 1978/79: Report Int'l. Whaling Comm., vol. 30, p. 359-368.

Rice, D. W. and A.A. Wolman, 1971, The life history and ecology of the gray whale (Eschrichtius robustus): Am. Sot. Mammal. Spec. Publ. No. 3, 142 p.

Rowland, R. W., 1972, Ecology of the benthic fauna of the northern Bering Sea: Geological Society of America, Abstracts with Programs, vol. 4, p. 646.

Rugh, D., 1981, Fall gray whale census at Unimak Pass, Alaska 1977-79, in: 4th Biennial Conf. Biol. Mar. Mammals, 14-18 December 1981, San Francisco, p. 100.

Rugh, D. J. and M.A. Fraker, 1981, Gray whale (Eschrichtius robustus) sightings in the eastern Beaufort Sea: Arctic, vol. 34, p. 186-187.

Russell-Cargill, W.G,A., (cd.), 1982, Recent developments-in side-scan sonar techniques, Cape Town, South Africa, 141P.

Sanders, H. L., 1977, The West Falmouth spill, Florida, 1969: Oceanus, vol. 20, no. 4, p. 15-24.

Scammon, C.M., 1874. The marine mammals of the northwestern coast of North America, Dover Publ., Inc., N.Y. 319 p.

Schumacher, J. D. and R.B. Tripp, 1979, Response of northeast Bering Sea shelf waters to storms: EOS, Trans. Amer. Geophys. Union, vol. 60, p. 856.

Sharma, G. D., 1970, Recent sedimentation on southern Bering shelf (Abstract): American Association of Petroleum Geologists Bulletin, vol. 54, no. 12, p. 2503.

Stoker, S. W., 1973, Winter studies of under-ice benthos on the continental shelf of the northeastern Bering Sea, Master's Thesis, Univ. of Alaska, unpublished.

Stoker, S.W., 1978, Benthic invertebrate macrofauna of the eastern continental shelf of the Bering and Chukchi Seas, Ph.D. Thesis, Univ. of Alaska, unpublished. 259 p.

Stoker, S.W., 1981, Benthic invertebrate microfauna of the eastern Bering/Chukchi continental shelf, in: The eastern Bering Sea shelf: oceanography and resources, vol. 1, D.W. Hood and J.A. Calder, eds., Off. Marine Pollution Assessment, NOAA. Distrib. by Univ. Washington Press, Seattle.

Sund, P.N., 1975, Evidence of feeding during migration and of an early birth of the California Gray Whale (Eschrichtius robustus): J. Mammal, vol. 56, p. 265-266.

Thomson, D.H., cd., 1983, Feeding Ecology of Gray Whales in the Chirikov Basin: in press, final report to OCSEAP-NOAA.

Thor, D.R. and C.H. Nelson, 1981, Sea ice as a geologic agent on the subarctic Bering shelf, in: The eastern Bering Sea shelf: oceanography and resources, vol. 1, D.W. Hood and J.A. Calder, eds., Off. Marine Pollution Assessment, NOAA, Distrib. by Univ. Washington Press, Seattle, p. 279-291.

Votrogov, L.M. and L.S. Bogoslovskaya, 1980, Gray whales off the Chukotka Peninsula: Report Int'l. Whaling Comm., vol. 30, p. 435-437, sc/31/Doc. 55.

Walker, T.J., 1971, The California Gray Whale comes back: Nat'l. Geogr., vol. 139, no. 3, p. 394-415.

Wellington, G.M. and S. Anderson, 1978, Surface feeding by a juvenile gray whale, Eschrichtius robustus: Fish. Bull., vol. 76, p. 290-293.

Zenkovich, B.A., 1934, (Research data on cetacea of far eastern seas): Bull. Far East Acad. Sci., USSR, No..10. In Russian (Transl. by F. Essapian, Miami, Fl., 34 p.).

Zenkovich, B.A., 1937 [More on the gray California whale (Rhachianectes glaucus Cope, 18641: Bull. Far East Acad. Sci. USSR 23. In Russian (Transl. by Bur. Commer. Fish., Off. Foreign Fish. Transl., Washington, D. C., 19 p.).

Zenkovich, B.A., 1955, 0 migratsiiakh kitov, promyslove raiony v dal'-nevostochnyk vodakh (The migration of whales, whale fishing in the waters of the Soviet Far East), in: Kitoiony Promysel Sovetskogo Soyuza, VNIRO, Part I, S. E. Kleinenberg and T. I. Makarova, eds. In Russian (Transl. by Israel Program Sci. Transl. for U.S. Dept. Interior and Nat'l. Sci. Found., 1968, 14 p.)

Zimushko, V.V. and M.V. Ivashin, 1980, Some results of Soviet investigations and whaling of gray whales (Eschrichtius robustus Lilljeborg, 1961): Report Int'l Whaling Comm., vol. 30, p. 237, sc/31/Doc. 19.

Zimushko, V.V. and S.A. Lenskaya, 1970, [Feeding of the gray whale (Eschrichtius gibbosus Erx.) at foraging grounds]: Ekologiya, vol. 1, p. 26-35. In Russian (Transl. by Consultant's Bur., Plenum Publ. Corp., NY, 1971, 8 p.).

APPENDIX A

SOURCES FOR THE DATA BASE

APPENDIX A-1 Sources for the Data Base.

DATA TYPE	DATE	COLLECTED BY	CRUISE NO.	LOCATION	MISC.
105 kHz digitized side-scan	1980	USGS-Nelson	L7-80-BS	Norton Sound Chirikov Basin'	Rolls 1-49
105 kHz side-scan	1980	USGS-Nelson NMML-Nerini	S01-80-BS	Chirikov Basin	Rolls 1-21
105 kHz side-scan	1977	USGS-Nelson	S5-77-B5	Chirikov Basin	Rolls 30-59
105 kHz side-scan	1978	USGS-Nelson	S9-78-BS	Chirikov Basin	Rolls 34-38
105 kHz side-scan	6/2 3/8 0	NMML-Nerini	-----	Chirikov Basin	Rolls 1-21
500 kHz side-scan	7/1 7/80	NMML-Nerini	-----	St. Lawrence Is.	Rolls 1-21
500 kHz side-scan	7/82	L.G.L. Ltd.-Thomson	Leg 1	Chirikov Island St. Lawrence Is.	Transects 2-44
100 kHz side-scan	9/82	L.G.L. Ltd.-Thomson	Leg 2	Chirikov Basin	Transects 103-134
500 kHz side-scan	"	"	"	St. Lawrence Is.	
105 kHz digitized side-scan	1982	USGS-Cacchione Code Geology Rept.	S1-82-NC	No. Calif. Coast	
Vibracore radiographs and logs	1980	USGS-Nelson	L7-80-BS	Chirikov Basin Norton Sound	
Box cores	1968	USGS-Nelson	68-ANC-BS	"	
Box cores	1969	"	69-ANC-BS	"	
Box cores	1970	"	70-ANC-BS	"	
Underwater video	1980	"	L7-80-BS	"	
Underwater video	1978	"	S5-77-BS	"	
Underwater video	1977	"	S9-78-BS	"	

APPENDIX A-1 continued

Underwater still photos	1980	USGS-Nelson	L7-80-BS	Chirikov Basin and Norton Sound
Underwater still photos	1977	"	S5-77-BS	"
Box core radiographs	1976	"	S5-76-BS	"
Box core radiographs	1977	"	S5-77-BS	"
Box core radiographs	1978	"	S9-78-BS	"
Vibracore logs	1960	"	68-ANC-BS	"
Vibracore logs	1969	"	69-ANC-BS	"
Vibracore logs	1970	"	70-ANC-BS	"
Vibracore loge	1976	"	S5-76-BS	"
Vibracore logs	1977	"	S5-77-BS	"
Vibracore logs	1978	"	S9-78-BS	"
Grab samples	1978	S. Stoker, U. of Alaska	---	Bering and Chukchi Seas
Grab samples	1980	NMML-Nerini	SU1-80-BS	Chirikov Basin
Grab samples	1982	L.G.L. ltd.-Thomson	Legs 1&2	Chirikov Basin and St. Law. Is.
SCUBA diver observations	1980	NMML-Nerini	---	"
SCUBA diver observations	1980	J. Oliver, Moss Landing Marine Lab	---	"
SCUBA diver observations	1982	L.G.L. ltd.-Thomson	Legs 1&2	"
SCUBA diver observations	1982	J. Oliver	---	Pachena Bay, Vancouver Island. British Columbia
Current speed data current meters	1982	J. Schumacher	---	Bering Sea
Current speed data spot checks	1960-80	NOAA-PM EL USGS, Univ. of Wash.	all cruises	N. Bering Sea

APPENDIX B

RESULTS OF THE QUANTIFICATION OF 105 kHz DIGITAL SIDE-SCAN MONOGRAPHS

SIDE-SCAN QUANTIFICATION STATIONS:

Dog 1 through Dog 16

Tate 1

length

middle of interval	number of observations	
0*00	0	
1.00	0	
2*00	15	********$******
3*00	8	********
4.00	4	****
5.00	4	****
6*00	3	***
7.00	11	****n'******
B*00	3	***
9*00	1	*
10.00	9	*********
11.00	1	*
12.00	0	
13.00	2	**
14*00	1	*
15.00	0	
16.00	1	*
17*00	0	
18.00	0	
19.00	0	
20.00	1	*

length in meters

width

middle of interval	number of observations	
0.000	0	
0.500	0	
1.000	17	******************
1.500	4	****
2.000	8	********
2.500	0	
3.000	16	*****************
3.500	2	**
4.000	10	**********
4.500	0	
5.000	7	*******

width in meters

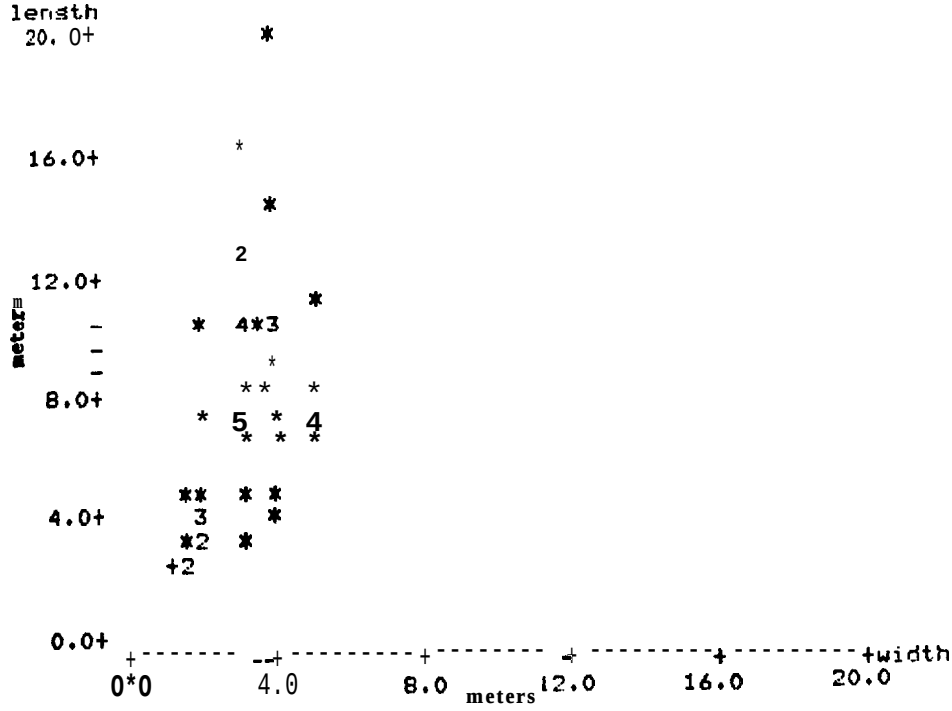

•rea

area in square meters: middle of interval	number of observations	
0.00	19	******************
5*00	9	********$
10.00	4	****
15.00	9	*********
20.00	7	*******
25.00	12	***$********
30.00	1	*
35.00	2	**
40.00	0	
45.00	0	
50.00	0	
55.00	1	*

orient.

degrees: middle of interval	number of observations	
0.0	12	************
10.0	9	*********
20,0	4	****
30.0	5	*****
40.0	17	*****************
50.0	5	*****
60.0	0	
70*0	0	
80.0	0	
90.0	0	
100*0	0	
110,0	0	
12040	0	
130.0	0	
140.0	0	
150.0	0	
160.0	0	
170.0	0	
180.0	0	
190.0	0	
200 .0	0	
210*0	0	
220.0	0	
230,0	0	
240.0	0	
250.0	0	
260.0	0	
270.0	1	*
280 * 0	0	
290.0	0	
300 .0	0	
310.0	0	
320.0	1	*
330.0	0	
.340.0	1	*
350.0	7	*******
360 * 0	2	* *

lenstth

middle of interval	number of observations	
0,000	0	
0.500	0	
1.000	0	
1.500	0	
2.000	13	**********
2.500	5	*****
3.000	17	**********
3.500	2	**
4.000	8	********
4.500	2	**
5.000	2	**
5.500	0	
6.000	1	*

length in meters

width

middle of interval	number of observations	
0*000	0	
0.500	0	
1.000	4	****
1.500	9	*********
2?000	26	**************************
2.500	3	***
3.000	7	*******
3.500	0	
4.000	1	*

width in meter

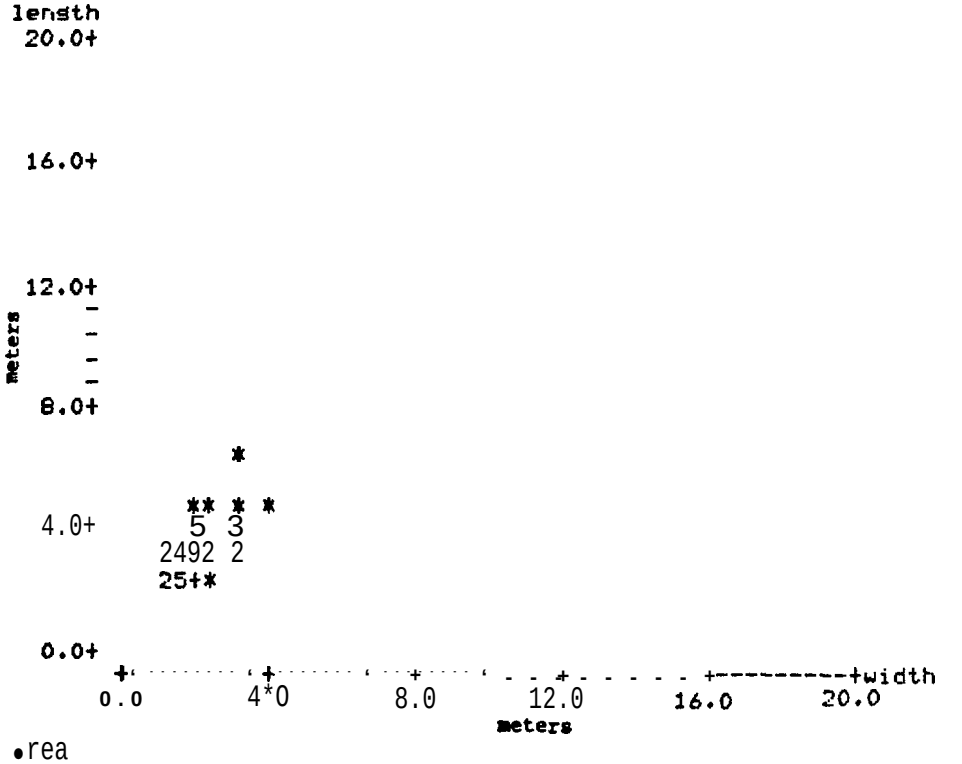

•rea

middle of interval	number of observations	
0.00	0	
1.00	2	**
2*00	6	******
3.00	15	***************
4.00	9	*********
S*00	8	********
6.00	1	*
7.00	2	**
B*00	4	****
9*00	0	
10.00	1	*
11,00	0	
12*00	2	**

area in square meters

length

middle of interval	number of observations	
0.000	0	
0.500	0	
1.000	0	
1.500	0	
2.000	8	********
2.500	4	****
3.000	14	********$*****
3.500	3	***
4.000	5	*****
4.500	1	*
5.000	13	*************
5.500	0	
6.000	6	******
6.500	1	*
7.000	4	****
7.500	0	
8.000	6	******
8.500	0	
9.000	1	*.
9.500	0	
10.000	1	*
10.500	0	
11.000	0	
11.500	0	
12.000	0	
12.500	0	
13.000	0	
13.500	0	
14.000	1	*

length in meters

width

middle of interval	number of observations	
0.000	0	
0.500	0	
1.000	20	***************$****
1.500	14	**************
2.000	30	************$.******************
2.500	2	**
3.000	1	*
3.500	0	
4.000	1	*

width in meters

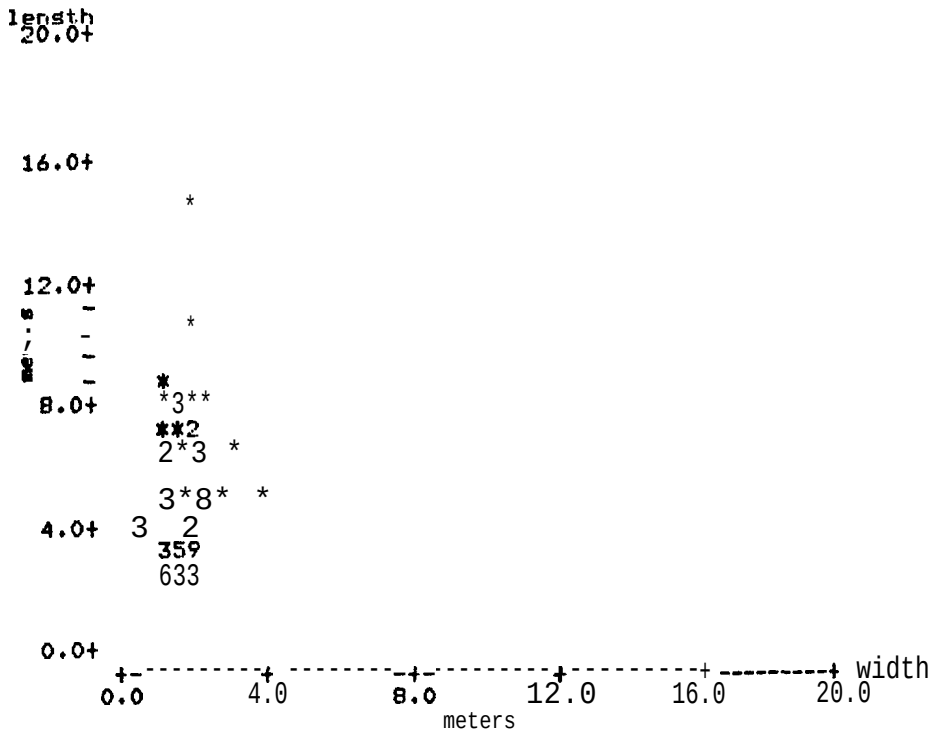

● rea

middle of interval	number of observations	
0*00	0	
1.00	4	****
2.00	7	*******
3*00	14	**************
4.00	9	*********
5.00	8	********
6.00	2	**
7.00	9	*********
E*00	7	*******
9.00	2	**
10.00	0	
11.00	1	*
12*00	1	*
13.00	3	***
14.00	0	
15*00	0	
16.00	0	
17.00	0	
18.00	0	
19*00	1	*

area in square meters

orient.

middle of interval	number of observations	
O*O	2	* *
10*0	0	
20.0	0	
30.0	0	
40.0	0	
50.0	0	
60.0	0	
70*0	0	
80*0	0	
90.0	0	
100*O	0	
110.0	0	
120.0	0	
130.0	0	
140.0	0	
150.0	0	
160.0	0	
170.0	0	
180.0	2	* *
190.0	2	* *
200 * 0	3	* * *
210 . 0	5	*****
220 . 0	18	**********$***
230.0	19	**********
240.0	4	****
250.0	7	*******
260.0	3	$**
270.0	2	**
280.0	1	*

degree.

lenstth

middle Of interval	number of observations	
0*000	0	
0.500	0	
1 * 000	0	
1.500	0	
2.000	6	******
2.500	7	******$
3.000	10	**********
3 * 500	3	***
4.000	5	*****
4.500	0	
5 .000	11	*******$***
5,500	0	
6 .000	7	*******
6.500	1	*
7,000	5	*****
7.500	0	
8.000	2	**
8* 500	1	*
9 .000	1	*
9.500	0	
10.000	1	*
10*500	0	
11.000	1	*
11.500	0	
12.000	0	
12.500	0	
13.000	1	*
13.500	0	
14.000	1	*
14.500	0	
15.000	1	*

length in meters

width

middle of interval	number Of observations	
0.000	0	
0.500	0	
1.000	24	***********$**********
1,500	9	*********
2.000	23	**$*********************
2 .500	5	*****
3,000	3	***

width in meters

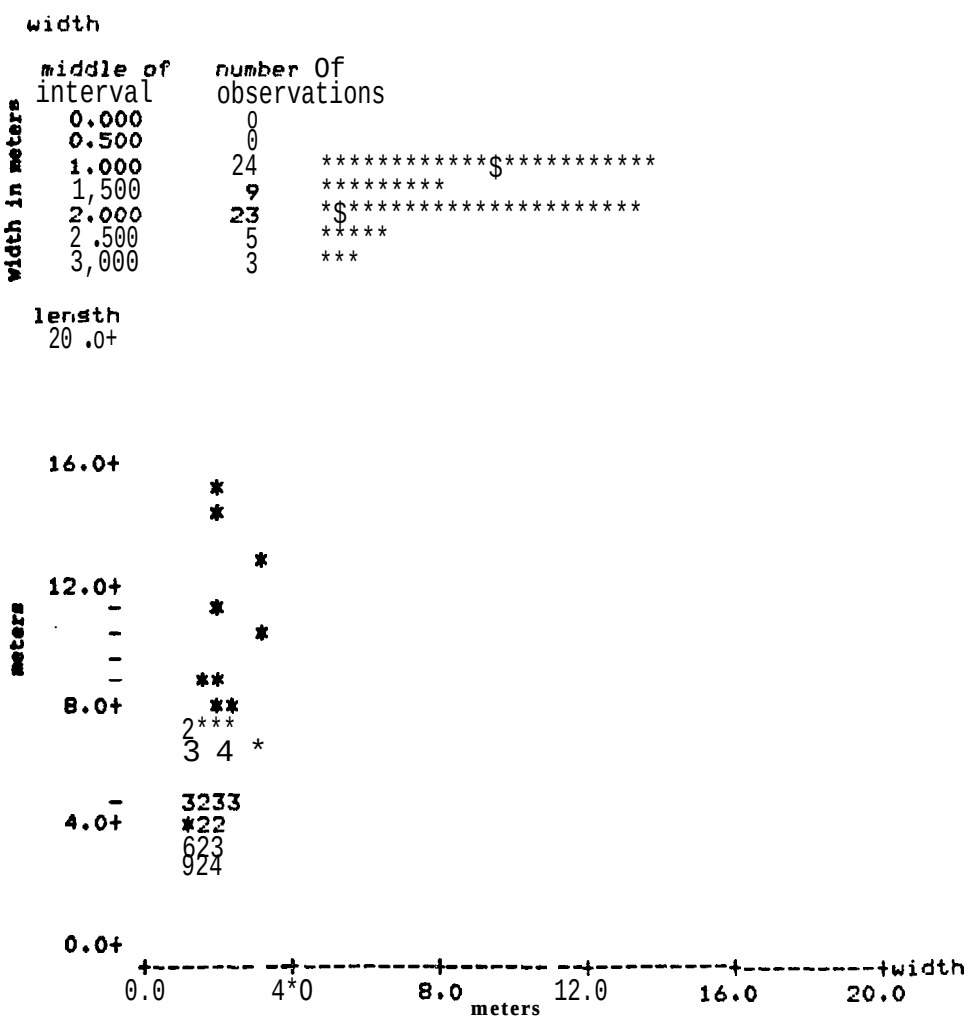

area

area in square meters: middle of interval	number of observations	
0*00	0	
1400	2	**
2.00	14	**********
3*00	9	*********
4*00	10	**********
5.00	5	*****
6*00	1	*
7*00	4	$***
8.00	7	*******
9*00	2	**
10*00	0	
11.00	2	**
12.00	2	**
13.00	1	*
14*00	0	
15*00	1	*
16.00	0	
17.00	0	
19*00	0	
19.00	1	*
20.00	2	**
21.00	0	
22.00	0	
23.00	0	
24.00	0	
25.00	0	
26.00	1	*

orient.

degrees: middle of interval	number of observations	
0*0	1	*
10.0	0	
20.0	0	
30.0	0	
40.0	0	
50.0	0	
60.0	0	
70.0	0	
80.0	0	
?0.0	0	
100.0	0	
110.0	0	
120.0	0	
130.0	0	
140.0	0	
150.0	0	
160.0	0	
170.0	0	
18000	1	*
190.0	5	*****
200.0	16	**********
210*0	13	**********
220.0	11	**********
230.0	10	**********
240.0	3	***
250.0	1	*
260.0	3	***

lenstth

middle of interval	number o? observations	
0 .000	0	
0.500	0	
1 .000	S	*****
1.500	11	**********
2.000	27	**************************
2.500	10	**********
3.000	7	*******
3.500	1	*
4.000	0	
4.s00	1	*
5.000	5	*****
5.500	0	
6.000	0	
6.500	0	
7 * 000	0	
7.500	0	
8,000	1	*

length in meters

width
each *represents 2 observations

middle of interval	number of observations	
0.000	0	
0.500	3	**
1.000	55	*****************************
1,500	6	***
2.000	4	**

width in meters

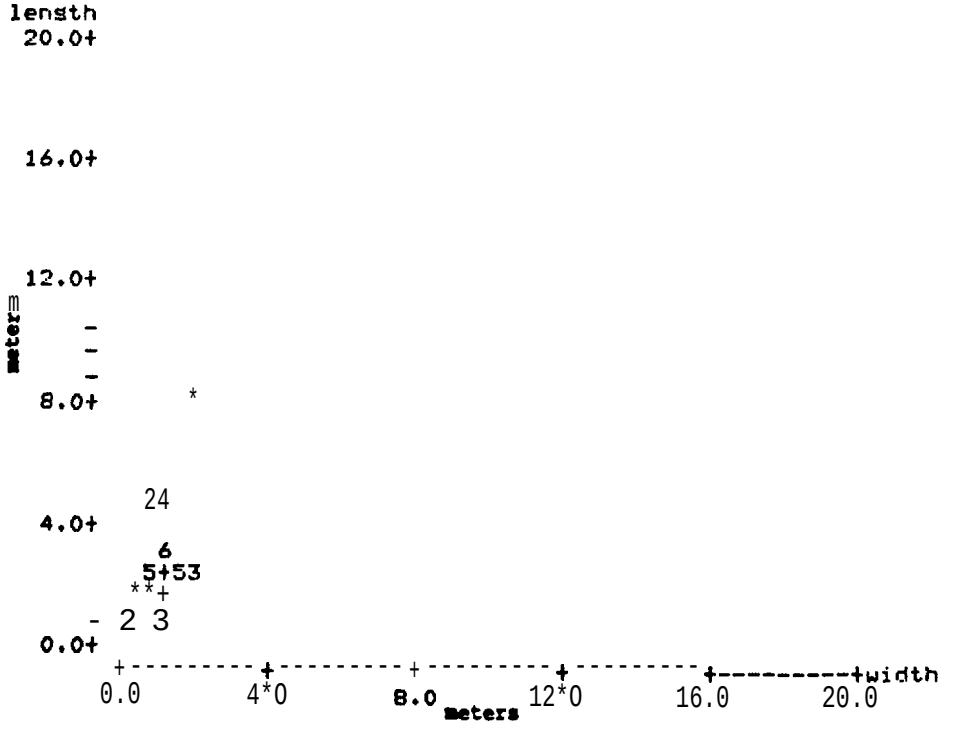

•rea

area in square meters

middle of interval	number of observations	
0.00	2	**
1*00	35	**********
2.00	17	**********
3*00	10	**********
4.00	3	***
5.00	0	
6.00	0	
7.00	0	
0.00	0	
9.00	0	
10*00	0	
11.00	1	*

orint.

degrees

middle of interval	number of observations	
0.0	4	****
10*0	0	
20*0	0	
30.0	1	*
40.0	7	*******
50.0	14	**********
60,0	14	**********
70.0	15	**********$**********
80.0	10	**********
90.0	2	**
100*0	1	*

length

middle of interval	number of observations	
0.000	0	
0.500	0	
1.000	3	***
1.500	3	***
2.000	9	*********
2.500	6	******
3.000	15	***/##########
3.500	1	*
4.000	8	********
4.500	2	**
5.000	5	*****
5.500	1	*
6.000	5	*****
6.500	1	*
7.000	3	***
7.500	0	
8.000	1	*
8.500	0	
9.000	2	**
9.500	0	
10.000	0	
10.500	0	
11.000	1	*

length in meters

width
each * represents 2 observations

middle of interval	number of observations	
0.000	0	
0.500	1	*
1.000	54	*********$**********
1.500	8	****
2.000	3	**

width in meters

length
20.0+

16.0+

12.0+
*

meters
-
-
**
*
8.0+
2*
5*
*
*6
4.0+ 6$*
* +*
2+2
4
2*

0.0+
+---------+---------+---------+---------+---------+width
0*0 4*O 8.0 12.0 16,0 20.0
meters

area

area in square meters: middle of interval	number of observations	
0.000	0	
0.500	3	***
1.000	5	*****
1.500	12	************
2.000	12	************
2.500	9	*********
3.000	5	*****
3.500	4	****
4.000	4	****
4.500	2	**
5.000	2	**
5.500	1	*
6.000	1	*
6.500	0	
7.000	1	*
7.500	1	*
8.000	1	*
8.500	1	*
9.000	1	*
9.500	1	*

orient.

degrees: middle of interval	number of observations	
0.0	3	***
10.0	1	*
20.0	2	**
30.0	0	
40.0	5	*****
50.0	12	************
60.0	12	************
70.0	9	*********
80.0	9	*********
90.0	9	*********
100.0	2	**
110.0	0	
120.0	0	
130.0	1	*
140.0	1	*

length

middle of interval	number of observations	
0.000	0	
0.500	0	
1.000	8	********
1.500	3	***
2.000	17	*****************
2.500	7	*******
3.000	17	*****************
3.500	0	
4.000	2	**
4.500	2	**
5.000	4	****
5.500	0	
6.000	1	*
6.500	0	
7.000	2	**
7.500	1	*

length in meters

width
each * represents 2 observations

middle of interval	number of observations	
0.000	0	
0.500	3	**
1.000	53	***************************
1.500	6	***
2.000	2	*

width in meters

30 points out of bounds

-- plot c1 o 20 c2 o 20

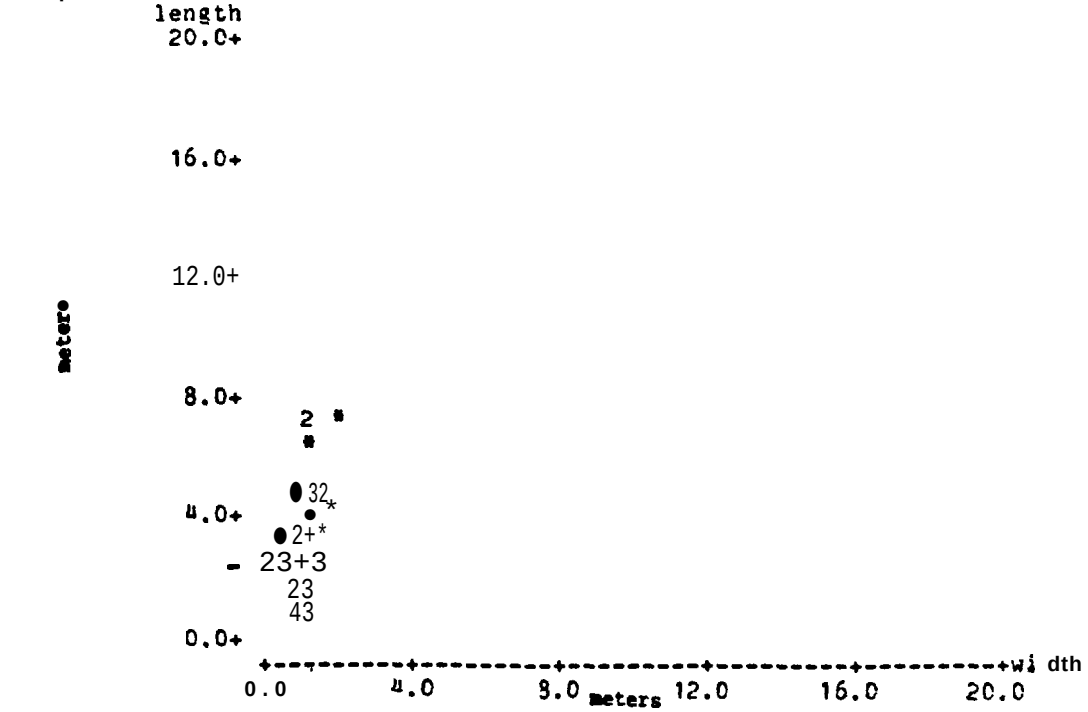

area

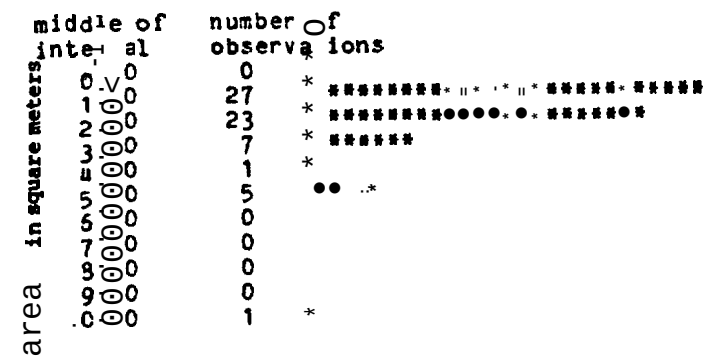
area
in square meters
middle of interval
number of observations

orient.

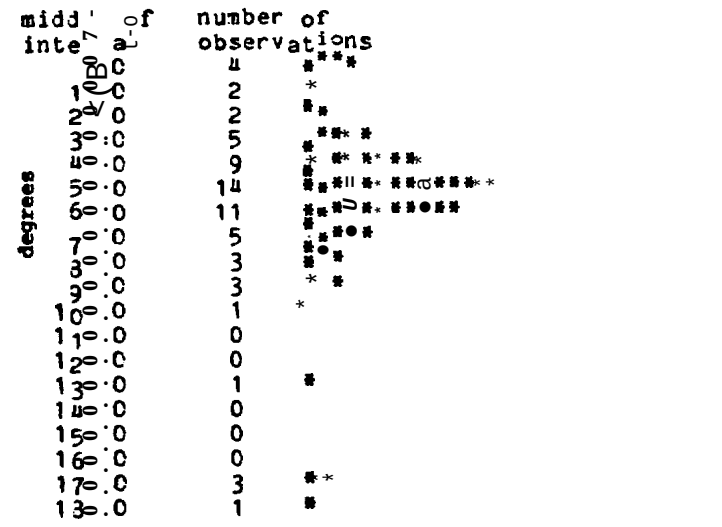
degrees
middle of interval
number of observations

lensth

middle of interval	number 0? observations	
0.00	o	
1*OO	8	********
2.00	5	*****
3*OO	14	**************
4.00	9	*********
5.00	8	********
6.00	3	***
7.00	3	***
8*OO	o	
9.00	1	*
10.00	5	*****
11.00	3	***
12*00	2	**
13*00	i	*
14.00	1	*
15.00	2	**
16*00	0	
17.00	1	*
18.00	0	
19.00	2	**

length in meters

width

middle of interval	number 01' observations	
0.00	0	
1.00	28	**********$***
2*00	15	**********
3.00	8	********
4.00	5	*****
5.00	7	*******
6.00	3	$**
7.00	1	*
8.00	0	
9.00	0	
10*00	1	*

width in meters

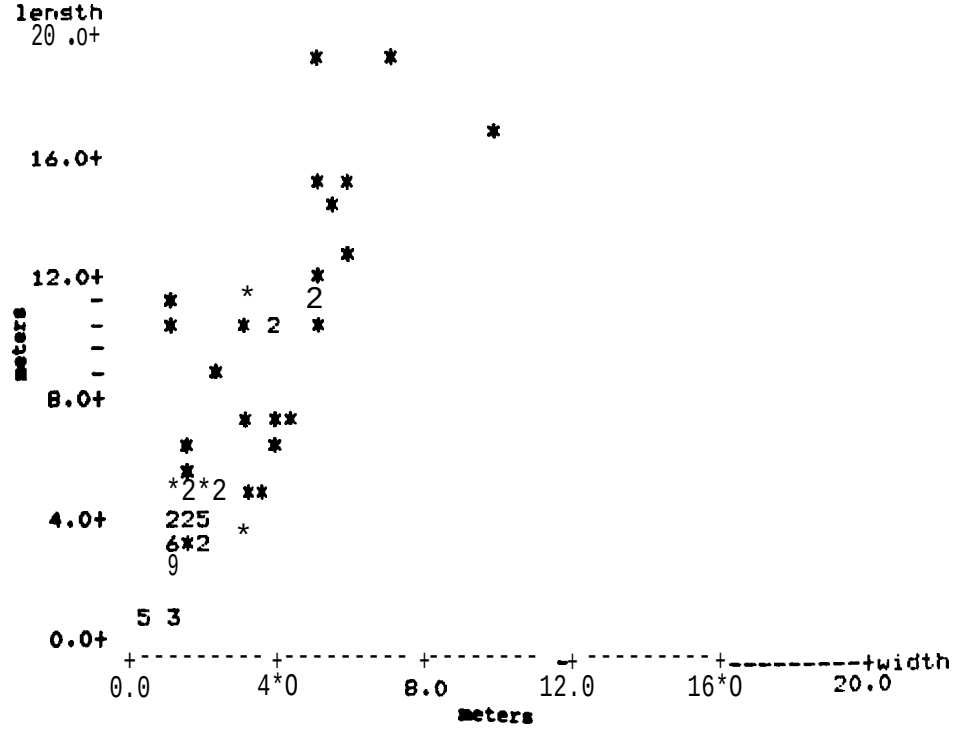

•rea

area in square meters: middle of interval	number of observations	
0.0	31	******************************
10.0	18	******************
20.0	6	******
30.0	3	***
40.0	3	***
50.0	3	***
60.0	2	**
70.0	0	
80.0	0	
90.0	1	*
100.0	0	
110.0	1	$

orient.

degrees: middle of interval	number of observations	
0*0	11	***********
10*0	9	*********
20.0	9	********* "
30.0	9	*********
40.0	13	*************
50.0	2	**
60.0	1	*
70.0	0	
80.0	0	
90.0	0	
100*0	0	
110*0	0	
120*0	0	
130.0	1	*
140.0	0	
150.0	0	
160.0	2	**
170.0	9	*********
180.0	2	**

lenstth

length in meters: middle of interval	number of observations	
0.000	0	
0,500	0	
1.000	5	*****
1.500	0	
2.000	17	*****************
2.500	7	*******
3.000	23	**********************
3.500	6	******
4.000	5	*****
4.500	0	
5.000	1	*

width

width in meters: middle of interval	number of observations	
0.000	0	
0.500	0	
1.000	27	**********$
1.500	18	******************
2.000	15	***************
2.500	1	*
3.000	2	**
3.500	0	
4.000	1	*

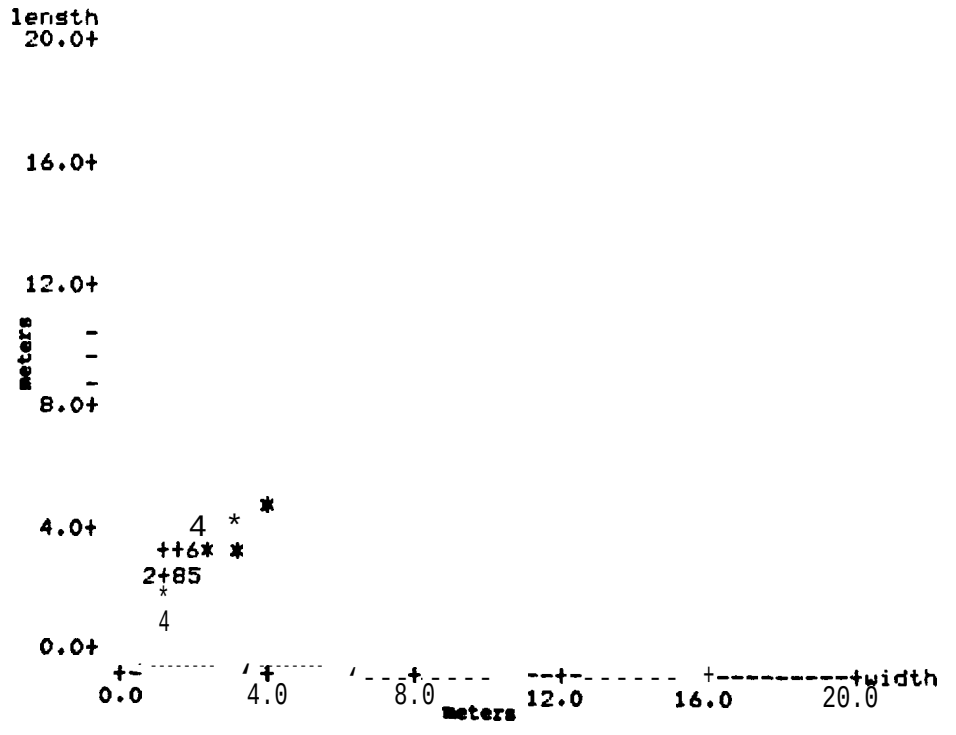

area

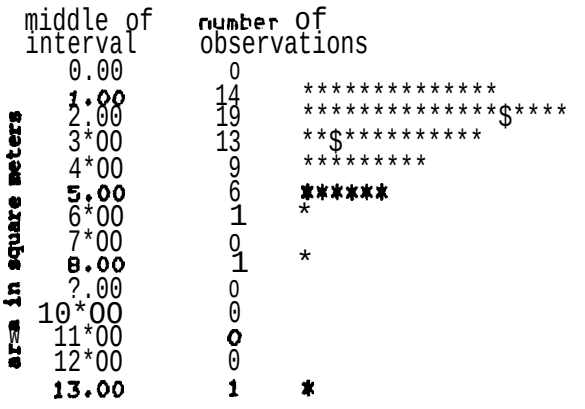
middle of interval
number of observations
area in square meters
0.00 0
1.00 14 **********
2.00 19 **********$****
3*00 13 **$**********
4*00 9 *********
5.00 6 ******
6*00 1 *
7*00 0
8.00 1 *
?.00 0
10*00 0
11*00 0
12*00 0
13.00 1 *

length

middle of interval	number of observations	
0.000	0	
0.500	5	*****
1.000	6	******
1.500	4	****
2.000	18	******************
2.500	7	*******
30000	8	S*******
3.500	6	******
4.000	5	*****
4.500	1	*
5.000	2	**
5.300	0	
6.000	1	*
6.500	0	
7.000	0	
7.500	0	
8,000	0	
8.500	0	
9.000	0	
9.500	1	*

length in meters

width

middle of interval	number of observations	
0.000	0	
0.500	6	******
1.000	25	**********%**********
1.500	18	******************
2.000	14	*******M*****
2.500	1	*

width in meters

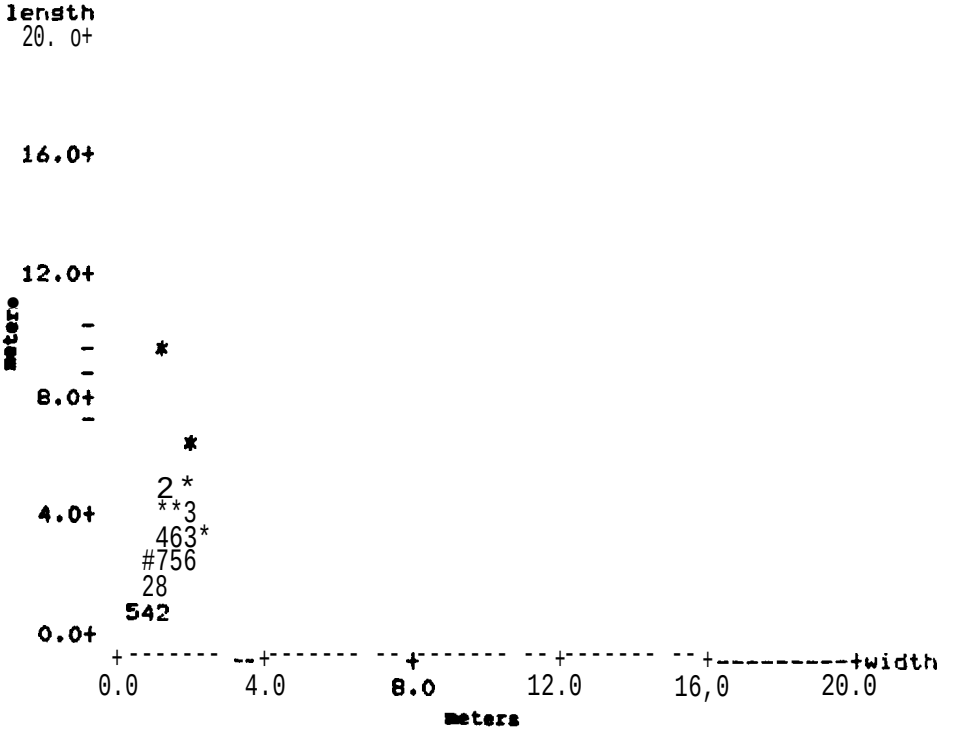

area

area in square meters

middle of interval	number of observations	
0*00	6	******
1*00	16	****************
2.00	13	*************
3.00	14	******$*******
4.00	8	********
5.00	3	$**
6.00	2	**
7.00	0	
8.00	2	**

length

middle of interval	number of observations	
0.000	0	
0.500	0	
1.000	31	**********$**********
1.500	8	********
2.000	18	**********
2.500	2	**
3.000	3	***
3.500	1	*
4.000	1	*

length in meters

width

middle of interval	number of observations	
0.000	0	
0.500	11	**********
1.000	46	**********
1.500	4	****
2.000	1	*

width in meters

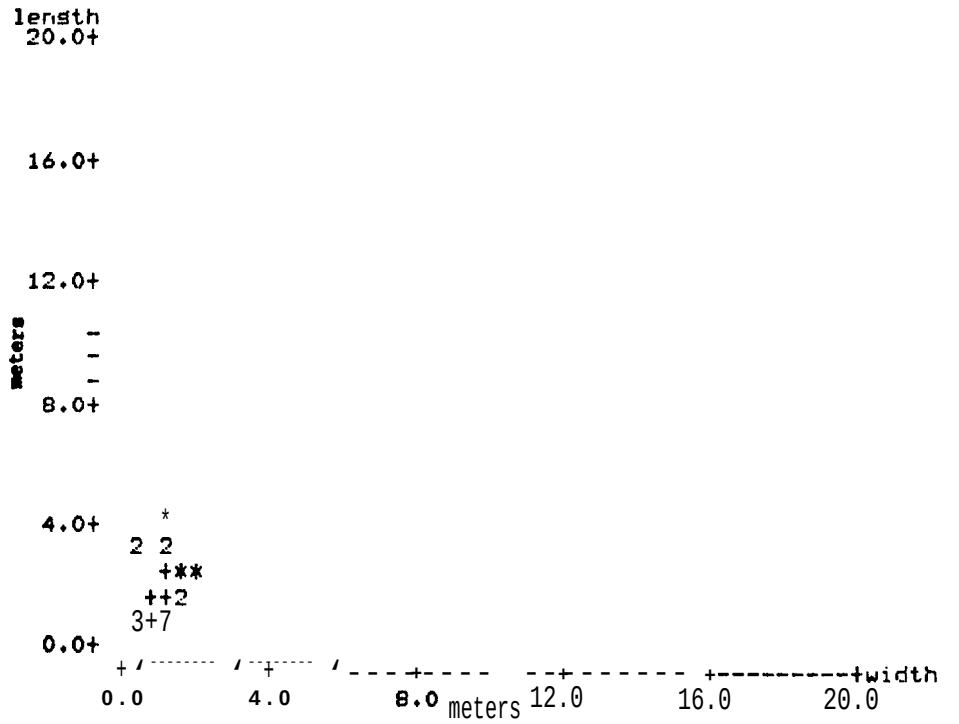

•rea

middle of interval	number of observations	
0.000	1	*
0.500	30	**********
1.000	12	**********
1.500	15	**********
2.000	2	**
2.500	2	**
3.000	2	**

area in square meters

length

middle of interval	number of observations	
0*000	o	
0.500	0	
1.000	7	*******
1 .500	7	*******
2.000	16	****************
2.500	8	********
3,000	8	$*******
3.500	2	**
4.000	3	***
4.500	0	
5.000	6	*$****
5.500	0	
6,000	0	
6.500	0	
7.000	4	****
7.500	1	$
B ,000	0	
e .500	0	
9.000	1	*
9.500	0	
10.000	1	*

length in meters

width

middle of interval	number of observations	
0.000	0	
0.500	15	***************
1.000	36	************************************
1.500	8	********
2.000	4	****
2.500	1	*

width in meters

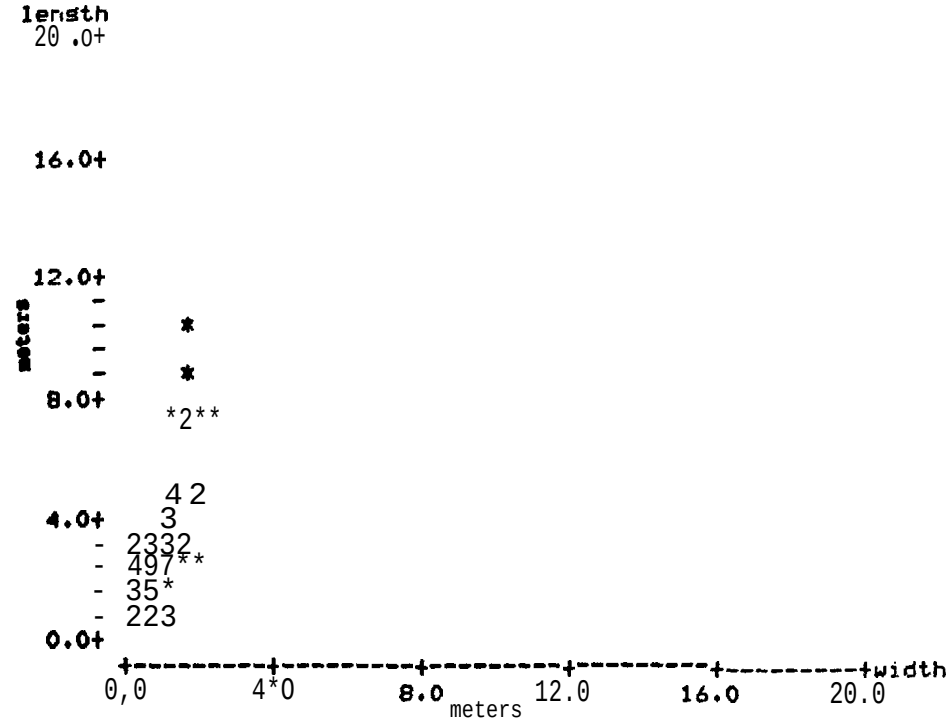

area

area in square meters: middle of interval	number of observations	
0.00	3	***
1.00	30	****$**********
2.00	12	**********
3.00	9	*$*******
4*00	1	*
5.00	1	*
6.00	0	
7*00	3	***
8*00	1	*
9.00	1	*
10*00	2	**
11*00	0	
12.00	1	*.

length

middle of interval	number of observations	
0*00	0	
1.00	14	**********
2.00	9	*********
3.00	14	**********
4.00	7	*******
5.00	4	****
6.00	6	******
7.00	2	**
8*00	3	***
9.00	1	*
10*00	0	
11.00	1	*
12*00	0	
13.00	0	
14*00	0	
15.00	1	*
16.00	0	
17*00	0	
18.00	0	
19,00	0	
20.00	1	*

length in meters

width

middle of interval	number of observations	
0 .000	0	
0.500	22	**********
1.000	20	**********
1.500	7	*********
2.000	9	*********
2.500	2	**
3.000	0	
3.500	1	*

width in meters

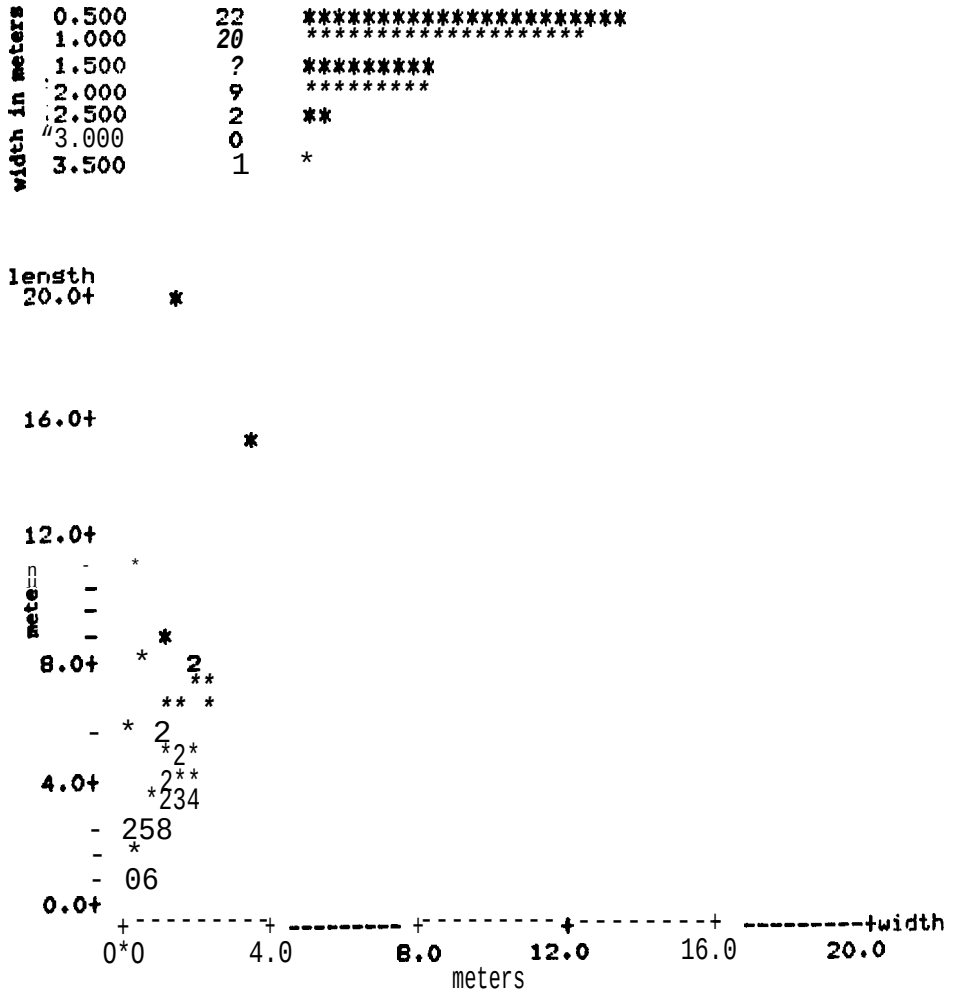

area

area in square meters

middle of interval	number 01' observations	
0.00	19	*******************
2.00	17	*****************
4*00	14	**********$**
6.00	6	******
8.00	0	
10.00	4	****
12.00	1	*
14.00	0	
16.00	0	
18.00	0	
20.00	1	*
22.00	0	
24*00	0	
26.00	0	
28 .00	0	
30.00	0	
32.00	0	
34.00	0	
36.00	1	*

lensth

length in meters: middle of interval	number of observations	
1.	9	*********
2.	22	********$**************
3.	10	**********
4.	7	*******
5.	6	******
6.	4	****
7.	4	****
8.	3	***
9.	1	*
10.	0	
11.	0	
12.	0	
13*	0	
14.	1	*

width

width n meters: middle of interval	number of observations	
0*5	15	***************
1.0	24	****$********************
1*5	7	*******
2.0	10	**********
2.5	2	**
3.0	6	******
3.5	0	
4.0	1	*
4.5	2	**

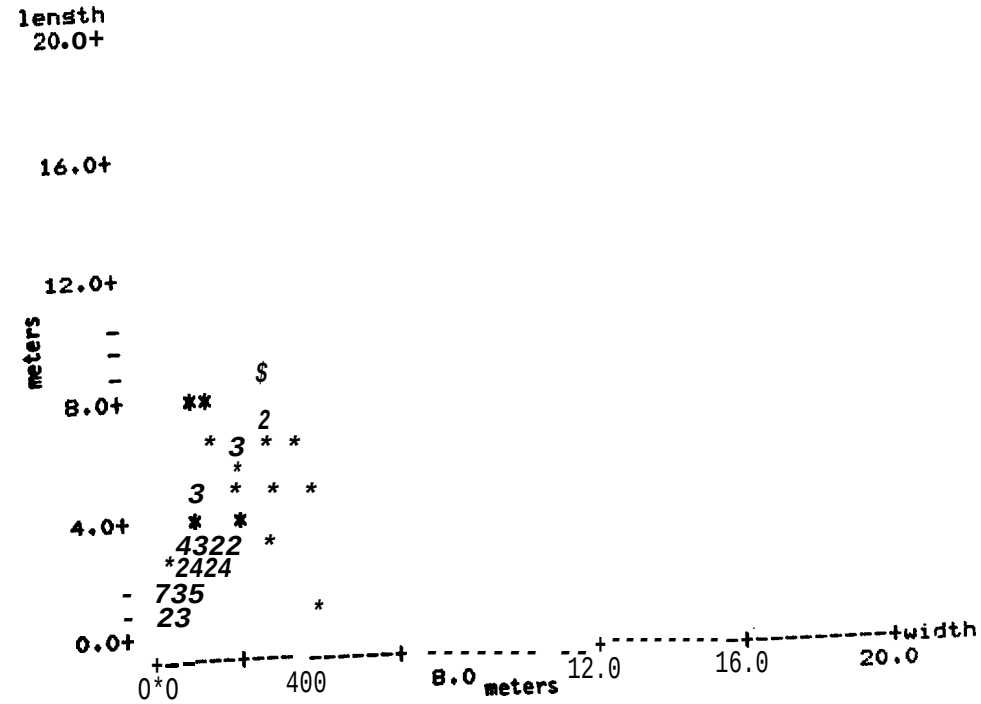

area

middle of interval	number of observations	
0*	16	***************
2.	24	***************%*$******
4.	9	*********
6.	4	****
8.	6	******
10.	1	*
12.	0	
14.	2	**
16.	3	$**
18.	2	**

area in square meters

length

length in meters: middle of interval	number of observations	
1*0	4	****
1.5	10	*$********
2.0	31	*********************************
2.5	7	*******
3.0	4	****
3.5	2	**
4.0	4	$***
4.5	0	
5.0	1	$
5.5	0	
6.0	0	
6.5	1	*

width

width in meters: middle of interval	number of observations	
0.8	3	***
0.9	1	*
1.0	33	*******$*************************
1.1	4	****
1.2	4	$***
1.3	2	**
1.4	3	***
1.5	6	******
1.6	1	*
1.7	0	
1.8	4	****
1.9	0	
2.0	2	**
2.1	1	*

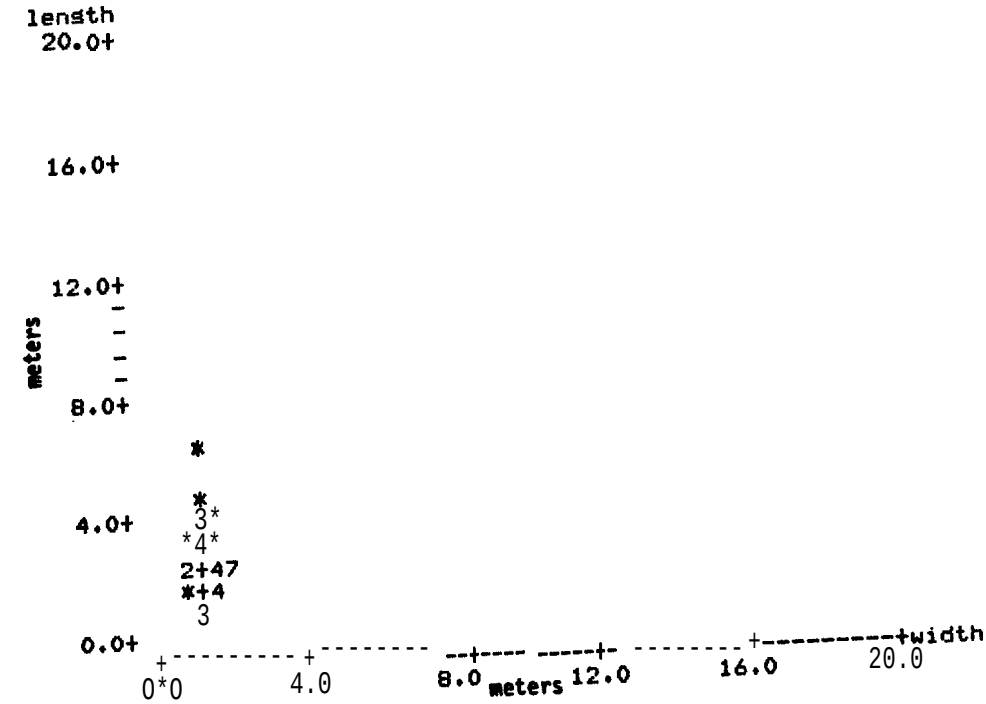

area

area in square meters

middle of interval	number of observations	
0.5	2	**
1.0	13	**********
1.5	23	**********
2.0	7	*******
2*5	10	IF*********
3*0	5	*****
3.5	3	***
4.0	0	
4.5	1	*

lensth

length in meters: middle of interval	number of observations	
0.000	0	
0.500	2	**
1.000	15	***************
14500	9	*********
2.000	27	***************************
2.500	4	**$*
3*000	7	*******
3.500	1	*

width

width in meters: middle of interval	number of observations	
0.000	0	
0.500	10	**********
1.000	48	**
1.500	3	***
2.000	4	****

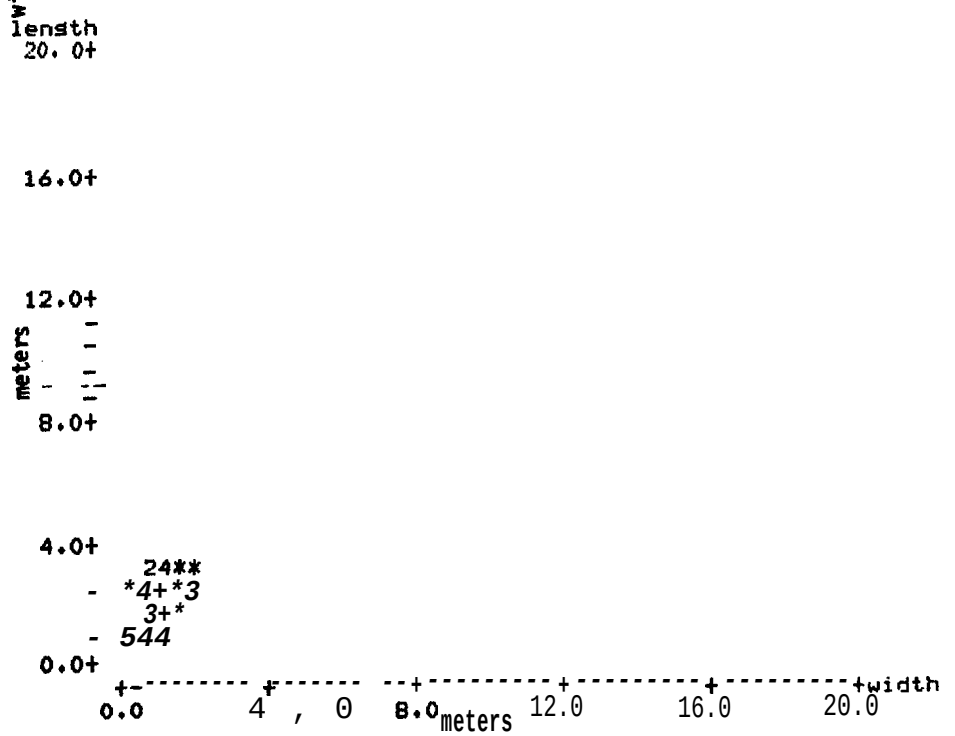

a rea

area in square meters: middle of interval	number of observations	
0.0	1	*
0*5	13	************
1.0	21	************$*******
1.5	18	******************
2.0	4	****
2.5	5	*****
3*0	2	**
3*5	0	
4.0	0	
4.5	1	*

length

length in meters — middle of interval	number of observations	
0.000	0	
0 .500	0	
1 .000	0	
1.500	0	
2.000	5	*****
2. 500	9	***$*****
3 .000	13	*************
3 .500	8	********
4. 000	30	-$******************************
4 . 500	5	*****
5.000	18	******************
5.500	2	**
6.000	11	**********
6*500	3	***
7 .000	10	**********
7.500	2	**
8,000	2	*%
8.500	1	*
9 .000	0	
9.500	0	
10*000	2	**

width

width in meters — middle of interval	number of observations	
2*	5	*****
3.	23	**********
4.	37	**************************************
5.	24	****$**********%****
6.	12	**********
7.	13	S**********
8.	4	****
9.	1	*
10.	2	**

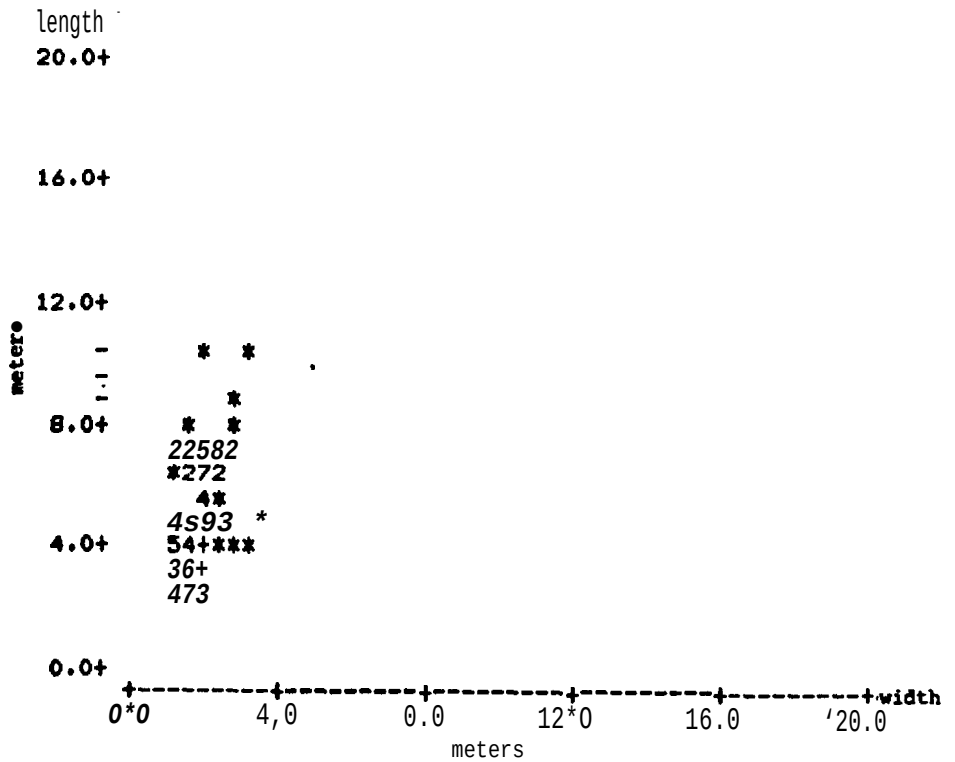

Orient.

middle of interval	number of observations	
0*0	0	
10.0	0	
20.0	0	
30.0	0	
40,0	0	
50.0	0	
6000	7	*******
70,0	4	****
80.0	0	
90,0	0	
100*0	2	**
110*0	2	**
120,0	11	**********
130.0	20	**********$*******
140,0	20	********************
150.0	33	*********************************
160.0	15	***************
170.0	7	*******

degree